RE-67-084-CRE-42
Copy No 12

AIRCO

Research and Engineering Department

AIR REDUCTION COMPANY, INC.

GPO PRICE $ _____

CFSTI PRICE(S) $ _____

Hard copy (HC) 3.00

Microfiche (MF) .65

ff 653 July 65

CR # 61843
RE-67-084-CRE-42

SATURN MANUFACTURING TECHNOLOGY FOR WELDING METHODS AND TECHNIQUES

Final Report

Contract No. NAS8-20338

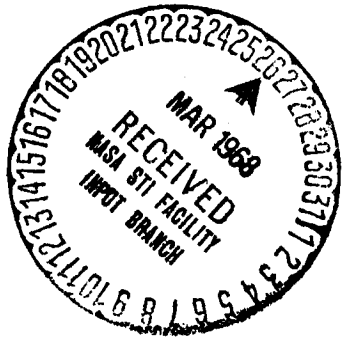

AIRCO RESEARCH and ENGINEERING DEPARTMENT

SQ 7-50289K

AIR REDUCTION COMPANY
INCORPORATED
RESEARCH AND ENGINEERING DEPARTMENT
MURRAY HILL, NEW JERSEY

RE-67-084-CRE-42

Saturn Manufacturing Technology for Welding Methods and Techniques

Final Report

to

National Aeronautics and Space Administration
George C. Marshall Space Flight Center
Huntsville, Alabama 35812
Attention: Purchasing Office
PR-SC

Contract No. NAS8-20338
Control No. DCN 1-6-30-32619 (IF)

E.H. Cushman

June 29, 1967

Report Period:
June 1966 - June 1967

Number of Pages:
vii + 149

ABSTRACT

The purpose of this program was to assess the relative merits of new types of power supplies for gas tungsten-arc welding of 2014-T6 aluminum. The new power supplies can vary the asymmetry and frequency of alternating current, and provide pulsed direct current. Varying the current wave form in one of these ways might yield benefits such as to increase the depth-to-width ratio of the weld, stir the weld pool to refine the grain structure, or to alter the mode of solidification of the weld to minimize segregation within the weld metal.

Early in the program, the a-c supplies were found to be suitable for welding as-received aluminum plate. However, under certain conditions, arc instability resulted when welding on plate which was freshly scraped prior to welding. This cleaning technique is used by NASA to achieve good fusion of the joint when welding with d-c straight polarity, and was recommended for use in this program. In conventional a-c welding, cathode sputtering removes surface oxides from the plate, and scraping is not necessary. However, it seems that as-received plate surfaces contain residual quantities of emissive compounds which stabilize the arc. Scraping the plate removes these compounds and instability results. Deliberate application of an emissive agent to scraped plate surfaces stabilized the arc, but this practice had a surprisingly strong effect on reducing the weld penetration. Numerous modifications were made in the power supplies to achieve stability on freshly scraped plate, but at a reduction in maximum allowable current and frequency.

In the first phase of the program, exploratory tests were made to determine the welding conditions required of each power supply to achieve full penetration welds in 1/4 in. plate and to determine their soundness and properties. The second phase involved an evaluation of the influence and interaction of the welding parameters on weld shape and properties for each of the power supplies. Finally, fully penetrated welds were made with each power supply adjusted for its best mode of operation, and the welds were compared with others made with conventional a-c and d-c power supplies. In the final comparison none of the new power supplies was found to have a significant advantage over the conventional power supplies. With proper welding current and travel speed, sound welds with good mechanical properties could be obtained when welding with each of the power supplies tested. Using the optimum conditions of welding, the conventional direct-current welds produced the highest average yield and tensile strengths of all the welds tested. It should be pointed out, however, that excessive travel speed and current did significantly reduce the tensile strength of the conventional d-c welds even though the yield strength of the joints was maintained at a high level. The reduction in tensile strength may have been caused by a loss of adequate shielding at the excessive travel speed, thereby causing premature tensile failures due to weld embrittlement.

TABLE OF CONTENTS

TABLES

TABLES (contd.)

ILLUSTRATIONS

ILLUSTRATIONS (contd.)

ILLUSTRATIONS (contd.)

ILLUSTRATIONS (contd.)

1. INTRODUCTION

The gas tungsten-arc process is used almost exclusively for fabricating space-launch vehicles because of its simplicity and reliability. Moreover, the process is easy to mechanize, and the parameters can be controlled precisely. In spite of its effectiveness, however, some problems exist. One of the primary problems with the resultant weldments is porosity, and considerable care in cleaning the surfaces prior to welding is required to prevent its occurrence. Even a completely sound weld may not have achieved the greatest possible strength or ductility with existing equipment and techniques. The 2014-T6 aluminum alloy derives its maximum strength by precipitation hardening, and overheating of the plate in the vicinity of the weld will cause it to overage and weaken. Equally important, segregation in the weld metal may cause internal planes of weakness which would impair the performance of the weldment, and in extreme cases, initiate microfissures or visible cracks in the weld. The problems associated with overaging could possibly be minimized by making changes which increase the depth-to-width ratio of the weld in order to reduce the power needed to produce a weld. Changes in welding parameters also may affect the mode of solidification of the weld to minimize segregation within the weld metal, increase its soundness and improve its mechanical properties.

Recent developments in new power supplies prior to this contract offered potential for improving the welds in aluminum plate. For example, an alternating-current power supply was developed in which the wave form could be made asymmetrical. With this power supply, the reverse-polarity and straight-polarity components can be varied. It was thought that such a wave form could allow a sufficient but reduced reverse-polarity component for sufficient weld cleaning action without imparing the current-carrying capacity of the electrode. Thus, it was postulated that deeper penetrating welds could be made because smaller-diameter electrodes could be used. Further, other evidence suggested that a frequency greater than 60 cycles per second might allow greater stirring of the weld pool thereby possibly refining the weld microstructure and minimizing segregation. The Air Reduction Company had developed an alternating-current power supply with which both of the parameters (frequency and asymmetry) could be evaluated. In the case of direct-current welding, improvements were anticipated by pulsing the current. Pulsing was expected to stir the weld pool, refine the grain structure and minimize the segregation as in the case of the higher-frequency alternating-current power. In addition, increases in penetration using pulsed power had been noted in other applications. A power supply for pulsed direct-current welding also had been developed at the Air Reduction Company prior to the contract.

The general purpose of this study has been to establish the merits of using new types of power supplies for gas tungsten-arc welding 2014 aluminum alloy components in the Saturn space-launch

vehicles. Evaluated were asymmetric a-c, high-frequency a-c, and pulsed d-c power supplies to establish with reasonable confidence those conditions which produce the most optimum welds. The study was designed statistically.

The program was divided into two broad phases. In the first phase, exploratory tests were made to determine the welding conditions required of each power supply to achieve full penetration in 1/4 in. 2014-T6 aluminum alloy plate and to determine the soundness and properties of the resultant weldments. The second phase of the work involved a thorough evaluation of the influence and interaction of the welding parameters on weld shape and properties for each of these power supplies. In the first portion of this second phase (Phase IIA) the experiments were designed to establish optimum conditions for producing deep-penetrating narrow welds or those having superior metallurgical structures. Later in this phase of work (Phase IIB), the optimum conditions for each power supply were to be used to make fully penetrated welds in 1/4 in. plate and evaluate their mechanical properties to compare them with those obtained with older types of welding power.

The special power supplies heeded were designed and built at the Air Reduction Central Research Laboratories prior to the inception of this program. They were found to provide stable arcs for welding as-received aluminum plate. In the early stages of this contract work, however, NASA personnel indicated a preference for making all of the welds on plate which was freshly scraped prior to welding. Under certain conditions, with freshly scraped plate, the asymmetric and variable-frequence a-c power supplies caused arc instability. The instability apparently was caused by lack of thermionic electrons from the plate to sustain an arc as the current crossed zero into the reverse polarity portion of each a-c cycle. When this problem was detected in the early stages of the program, preliminary experimentation indicated that the skin on as-received plate is emissive presumably as the result of the caustic cleaning. Welding was continued on as-received plate. However, parallel efforts were made to modify the power supplies to develop the higher voltages needed to weld on scraped plate. At the time, it was believed that the trends in penetration would not be affected by some minor changes in the character of the plate surface, and the first phase of the work was completed using as-received plate as well as plate with cesium compounds intentionally added to insure acceptable arc stability. As the first phase of the work was completed, electrical changes in the power supply were finished and enabled the welding to be done on scraped plate. Moreover, toward the conclusion of the first phase of work, it was found that the emissive characteristics of the plate surface had a significant effect on the weld dimensions under some conditions. Thus, the first phase of the work with alternating current needed to be repeated using scraped plate. All of the original and repeat runs for the first phase are reported herein for purpose of documentation. Moreover, additional work was performed in the second phase of the program to illustrate the changes which could occur in practice when plate with variable surface conditions is welded.

All of the significant results, interpretation and conclusions are presented herein in this final report for the work conducted on NAS8-20338.

2. DESCRIPTION OF POWER SUPPLIES

The power sources consisted of laboratory-constructed equipment utilizing solid state switches and circuitry. Transistors were used in the timing and control circuits, and silicon-controlled rectifiers (SCR) were used as power switches.

To achieve stability during current reversals, the alternating-current supplies incorporated circuits to produce a synchronized high voltage pulse at the time when the arc current decayed to zero or an adjustable instant of time slightly after. This discharge was necessary to reignite the arc and was more suitable for the purpose than the more conventional spark-gap oscillator which produces a continuous, high-frequency, high-voltage discharge.

2.1 ASYMMETRICAL AND VARIABLE-FREQUENCY ALTERNATING-CURRENT POWER SUPPLY

These two sources were incorporated in a common unit which consists of an SCR bridge inverter. Although the main source of power delivered direct current, the inverter periodically switched the polarity to provide alternating current to the arc. Fig. 1 shows a block diagram of this system as arranged in the early part of the program. In this representation, a comparison is made to an equivalent electromechanical device. For asymmetric operation, the trigger pulse repetition rate was held fixed while the timing between SCR 1-3 trigger pulses and SCR 2-4 trigger pulses was varied. Conversely, variable frequency operation was obtained by maintaining an equal time interval between SCR 1-3 and SCR 2-4 trigger pulses and varying the pulse rate.

The operating ranges and current ratings of the alternating-current equipment in the initial stages of the program were as follows:

1) Asymmetric Alternating Current

Duty cycle (ratio of time duration of either polarity to time of 1 cycle)	10 - 90% (1.2 milliseconds minimum time duration of either polarity)
Current	25 - 400 amp. rms

2) Variable-Frequency Alternating Current

Frequency	5 - 300 cycles per second
Current	25 - 300 amp. rms

The early stages of the program were conducted with the equipment described above. As the program progressed, the need for modifications to the power supplies became apparent. It proved extremely difficult to obtain a stable alternating current (a-c)

arc when welding on a freshly scraped aluminum surface, because the arc frequently failed to reignite during the reverse-polarity portion of the cycle. The diagram shown in Fig. 2 indicates the additions made in the circuitry to achieve a-c stability. They include:

1) A second d-c power supply in series with the first to obtain higher open-circuit voltage.

2) A large capacitor bank (0.156 farad) across the machine terminals to hasten current reversal.

3) A water-cooled inductor to limit the peaks of current in the solid state switches of the inverter.

4) A series resistance to force higher inverter operating voltage for stable power arc follow-up after current reversal.

5) A resistance-diode combination for improved current balance to compensate for the partial rectification caused by the tungsten-aluminum arc.

6) An auxiliary capacitor discharge circuit to aid reverse polarity arc reignition.

After incorporating these components in the circuit, stable a-c arcs could be maintained on freshly scraped plate, but the upper limit of frequency had to be reduced to 200 cycles per second to avoid excessive rms currents in the inverter solid state switches.

2.2 PULSED DIRECT-CURRENT POWER SUPPLY

This source was designed to superimpose high-current pulses of controlled amplitude and duration on a "base" arc current of lower magnitude. This is accomplished with an SCR switch as shown in the block diagram of Fig. 3. The pulse current is turned on when gate trigger signal G1 is applied to the main switch and is turned off when capacitor C1 is discharged through SCR 2. The pulse duration is determined by the time delay between application of gate pulses G1 and G2. During the off period, the "base" supply maintains a conductive plasma and, since it can be varied, also is used to provide variations in arc power at constant levels of pulse amplitude.

1)	Duty cycle (ratio of on to off time of pulse)	10 - 90%
2)	Pulse frequency	10 - 120 pulses per second
3)	Peak current	1200 amp.max. at 10% duty cycle
4)	Base Current	400 amp.max.

3. EQUIPMENT AND INSTRUMENTATION

The equipment and some of the instruments that were used in the program are shown in Fig. 4. The side beam carriage is on the left. The operator's station for the speed control is mounted on the carriage. An in-line, digital-type dial is used to set the travel speed directly in inches per minute. The travel speed can be varied from zero to 99.9 i.p.m. The travel speed control unit is insensitive to line voltage fluctuation and was calibrated to be accurate within 1% of the setting. The electrode holder is supported by the carriage, and a rack and pinion allows manual adjustment of the holder, and consequently of arc length.

The work fixture is constructed of non-magnetic materials to minimize the possibility of magnetic arc blow. Stainless steel clamps press the workpiece firmly on two transite strips which insulate the workpiece from the aluminum base of the fixture. The purpose of the insulation is to reduce the effects of an irregular heat sink. The backing groove between the transite strips is supplied with inert gas to shield the underside of the weld bead. To the right of the side beam carriage is the asymmetric a-c and variable frequency a-c power supply. The primary d-c source and the pulsed d-c power supply are not shown in the picture.

The recording oscillograph in the background has channels for measuring travel speed, average and instantaneous are voltage, and average and instantaneous arc current. Recording a-c ammeters were available which were accurate for measuring conventional sine wave alternating current, but the asymmetry of the current wave form in this program would have seriously affected the accuracy of these instruments. Therefore, the rms value of arc current was read on a tong-test ammeter. Although this meter lacks a high degree of accuracy (2% on a.c., 5% on d.c.) it does indicate rms values directly. Not shown in the figure, but installed later are potentiometric type instruments for recording travel speed and rectified average arc voltage and current. The oscilloscope on the right was used for checking variables such as frequency, asymmetry, duty cycle, and pulse peak.

4. PHASE I

In Phase I of this study, as initially conceived, full penetration welds were to be made using freshly-scraped 1/4 in. 2014-T6 aluminum-alloy plate with each of the special power supplies. Three levels of welding current, three travel speeds, and one arc length (0.010 in.) were to be used. These welds were to be made to ascertain the levels of the variables to be used in Phase II and, also, to screen the significance of the unique features of each power supply which was expected to be of value.

Preliminary test welds were made without difficulty on as-received plate using the asymmetric a-c power supply for the Phase I study. However, when subsequent test welds were attempted on freshly-scraped plate, the arc became erratic. An examination of the problem showed that the arc did not always reignite at the instant the clean aluminum plate became the cathode; the wave form displayed on the oscilloscope showed that the current was rectified. Reasonable arc stability could be obtained only by:

1) Using the plate without scraping it, or

2) Painting the plate surface with a dilute solution of cesium nitrate or some other thermionic compound.

Evidently, the unscraped plate contains a residue of some thermionic material which aids in reigniting the arc when the aluminum plate is the cathode. The same effect is achieved on scraped plate by the intentional addition of a thermionic material such as the cesium nitrate. Since the welds made in unscraped plate were sound and uniform, the decision was made to use unscraped plate for making the a-c welds. A set of weld specimens was made on unscraped plate using the asymmetric a-c power supply, and attention was turned to testing variable frequency a-c. With this power, however, the arc was not always stable on unscraped plate. With the combination of low welding current, high frequency and low travel speed a useful arc could not be maintained. Consequently, after evaluating a number of thermionic materials, a set of weld specimens was made with the variable frequency supply on plate surfaces that were scraped and then treated with a solution of cesium carbonate.

A rerun of Phase I tests was found to be necessary when some Phase II work showed that the presence of cesium on the plate surface might have a stronger effect on weld penetration than the welding parameters under study. Efforts were then concentrated on modifications of the power supplies to make it possible to maintain stable a-c arcs on freshly scraped plate with all of the conditions to be studied. This goal was partially accomplished. The upper limit of frequency had to be reduced from the 300 cycles per second orginally planned to about 200 cycles per second, and the usable arc length for a-c welds was limited to 1/8 in. for reasons which will be detailed later.

The following sections of this report, under Phase I, give details of the earlier welds made on emissive plate surfaces and the later welds made on freshly scraped plate.

4.1 ASYMMETRIC A-C WELDS (ON EMISSIVE PLATE SURFACE)

With 10% reverse polarity asymmetry (and 90% straight polarity), at 60 cycles per second, the current carrying capacity of various electrodes was determined by increasing the current in increments of 25 amp. until the electrode failed. Each of the electrodes that failed did so by melting at a point approximately halfway between the tip of the electrode and the collet. This electrode behavior is characteristic when D.C.S.P. power is used. With a somewhat greater component of D.C.R.P. for each cycle, failure would be expected by melting and loss of the electrode tip. The 1/8 in.diam. electrodes were not tested above 400 amp. because that is the nominal rating of the power supply. The test conditions and results are listed in Table 1.

An Airco M50A electrode holder with a 5/16 in. ID gas nozzle was used in all tests. The electrode was adjusted to protrude 1/4 in. from the nozzle. The arc gap was set initially at 0.024 in., using a feeler gage. A calculation based on earlier electrode thermal measurements indicated that the thermal expansion of the electrode would amount to 0.014 in., leaving an actual arc length of 0.010 in. Bead-on-plate rather than butt welds were made to eliminate inconsistencies due to variations in fit-up. The test plan of welding conditions for Phase I was as follows.

1) With the current set at the maximum rating of the machine, determine the travel speed to provide full penetration.

2) Using 1/3 of the travel speed determined in Condition 1, adjust the current for full penetration.

3) Using 2/3 of the travel speed of Condition 1, adust the current for full penetration.

4) Use current of Condition 2 and travel speed of Condition 1.

5) Use current of Condition 3 and travel speed of Condition 1.

6) Use current of Condition 2 and travel speed of Condition 3.

7-12) Make replicates of Conditions 1 - 6.

Each weld was made along the center line of 1/4 in. plate which was 8 in. wide and 24 in. long. The plate surface was wiped with clean paper toweling prior to welding. The data in Table 2 describe the conditions used. Note that some arc outages were observed. These "outages" were caused by failure of the arc to reignite during the reverse-polarity portion of the cycle. However, since the asymmetry of the supply had been adjusted so that reverse polarity current could flow only 10% of the time, the loss of a small percentage of reverse-polarity current was expected to have only a minor effect.

After welding, the test plates were radiographed and sectioned for metallographic specimens and tensile bars as shown in Fig. 5. The tensile bars were finish-machined as shown in Fig. 6. No porosity was detected in either the radiographs or on surfaces of the metallographic sections. Some of the full-penetration welds were undercut as expected since no filler metal had been used to compensate for the volume of metal that formed the underbead.

The depth and width measurements of the weld beads were made at a magnification of 10 × and the results are listed in Table 3. The mean values of the data in Table 3 also are displayed graphically in Figs. 7 - 12, which show the influence of current and travel speed on the weld dimensions. As expected, both current and speed had highly significant effects on the bead width and no significant interaction appears to exist between them. However, interaction on the bead depth does exist between current and speed; the graph of Fig. 8 indicates that at the slower speed the effect of increasing the current is greater on bead depth than it is at the higher speed. Figs. 9 and 11 show that both the bead width and depth appear to be exponentially related to travel speed. However, the width and depth appear to vary linearly with current. Empirical equations were derived from the above data which allow approximations of bead widths and depths over a current range of 250 - 330 amp. and a speed range of 10.50 - 15.75 i.p.m. The equations are:

$$W = 0.001138\ I - 0.012\ S + 0.1365$$

$$D = 0.003251\ I + 0.092091\ S - 0.001476\ IS - 0.1956$$

where:

W = Bead width (in.),

D = Bead depth (in.),

I = Welding current (amp.), and

S = Travel speed (i.p.m.).

These equations can be compared later on with similar equations derived from tests of the other power supplies.

All of the tensile tests incorporated an extensometer set for a 2 in. gage length to determine the yield strength based on a 0.2% offset. Elongations were calculated for both 1/2 in. and 1 in. gage lengths. The mechanical properties obtained are listed in Table 4 and the mean values are plotted in Fig. 13. Calculated values for Least Significant Differences (L.S.D.) at the 95% probability level have been included in Table 4. When two values differ by an amount that is greater than the L.S.D., the difference is considered to be statistically significant. As seen in Fig. 13, the yield strength increases as the current and travel speed are simultaneously increased, and the increase is statistically significant. The tensile strength first increases significantly with increasing current and travel speed, and then levels off with further increases in current and speed. There was considerable scatter in the elongation data, resulting in rather large L.S.D.'s; the indicate increases in elongation with increasing current and speed are not significant.

4.2 ASYMMETRIC A-C WELDS (SCRAPED PLATE)

After the power supply had been modified, as described earlier in Fig. 2, considerable difficulty was encountered when attempts were made to remake the full-penentration welds on freshly scraped plate for Phase I. The arc action was erratic. In some tests the arc was stable. In others, however, the arc frequently failed to reignite when the aluminum plate became cathodic. The instability was traced to:

1) Sensitivity to arc length, and
2) The electrode condition.

The unusual effect of arc length was first noticed while making full-penetration welds at short arc length (0.015 in.) with the asymmetric a-c supply. It might be expected that decreasing the arc gap would facilitate arc reignition, but the reverse effect was found to be the case. When welding conditions were such that erratic reignition was occurring, arc stability was restored by increasing the arc length, and instability resumed when the arc length was shortened. Because of this behavior, a brief study of arc length effects on arc stability was made so that realistic values of arc length could be chosen for the rest of the program.

A series of tests was made to determine the minimum length at which the arc would be stable under all operating conditions. It was found that a length of 1/8 in. would allow welds to be made at the high and low limits of current, frequency, asymmetry, and speed. Operation at shorter arc length was troublesome. Consequently, it was decided to eliminate arc length as one of the variables in the test program, and to make all welds with a standard 1/8 in. arc length.

While experimenting with arc length effects, another inconsistency arose. Under some welding conditions, a stable arc could be maintained if the electrode was dressed before the test, but in a repeat run, under the same conditions with the same

electrode, the arc would be unstable unless the electrode was redressed. Microscopic examination of the electrode tip following a test run usually revealed a small hole leading to a more or less spherical cavity within the previously-molten tip. A possible mechanism for the formation of these voids is thought to be the sublimation of some tungsten oxide trapped within the electrode. The vapor thus formed might form a small bubble in the molten tungsten, and then escape through the surface, leaving an irregularity on the tip. The thermionic properties of such irregularities might differ from the surrounding tungsten, and cause erratic electrode behavior. The formation of voids in tungsten electrodes is not unique to welding with these special power supplies. On another program, previously conducted in our laboratory, voids were observed in the shanks of electrodes that were tested for their their capacity to carry direct current. Voids probably form also in the tips of electrodes used in conventional a-c TIG welding; however, their formation goes unnoticed when they do not cause rectification. The conventional a-c power supply inherently provides a high reignition voltage at the instant it is needed and, furthermore, cathodic sputtering normally provides cleaning action. Scraping the plate prior to welding with alternating current is not the usual practice and residual thermionic material is present to aid reignition.

Using the procedure of dressing the electrode prior to each weld, and setting the arc length at 1/8 in., the Phase I full-penetration welds were made on freshly-scraped 1/4 in. plate. In another departure from the initial procedure, a value of 300 amp. rms was chosen as the maximum current to be used with each of the power supplies, rather than using the power supplies at their individual ratings which varied. This change in procedure was made to simplify comparison of the power supplies. Partial penetration welds on scraped plate were not made under Phase I since a plan was evolved for Phase II to test the effect on bead dimensions of as-received vs. scraped plate.

After welding, the test plates were radiographed and machined into metallographic specimens and tensile bars in accordance with the original specifications in Figs. 5 and 6. Again, no porosity was detected in either the radiographs or on surfaces of the metallographic specimens.

After aging a minimum of 14 days, tensile tests of the specimens were made. The mechanical properties are listed in Table 5, which includes calculated average values, 95% confidence intervals, and the values of least significant difference [L.S.D. ($P = 0.05$)]. The strength values are plotted in Fig. 14. As was the case with the welds made on emissive plate surfaces, the yield strength of these welds increased significantly with increasing welding current and speed, and the tensile strength at first increased and then leveled off with increasing current and speed. The elongation results were not plotted since the fracture paths varied in the specimens tested, and the value of such results is questionable. The large L.S.D. values indicate that the difference in average elongation are not statistically significant.

4.3 HIGHER FREQUENCY A-C WELDS ON EMISSIVE PLATE SURFACES

With the variable frequency a-c power supply set at 300 cycles per second, using symmetrical wave shape (50% reverse polarity, 50% straight polarity), the current carrying capacity of pure tungsten electrodes of varying diameter was determined. These tests were conducted in order that the smallest electrode capable of carrying a particular current could be selected in future tests with this power supply. Using three electrode diameters (3/32, 1/8 and 3/16 in.), the current was increased in increments of 25 amp. until they failed. Two conditions were considered. In the extreme case, formation of a bulbous molten zone at the electrode tip constituted failure or "excessive current". More conservatively, the maximum safe current was that current at which the electrode tip, though molten, maintained its hemispherical shape, with the same diameter as the electrode. The results of these tests are listed in Table 6. Note that the current capacities shown, which are for 50% reverse polarity current, are much lower than the capacities for 10% reverse polarity current given in Table 1. In this respect asymmetric a.c. has an advantage over balanced a.c., that is, to increase capacity and still maintain cathodic cleaning action at low values of reverse polarity component.

The test plan of welding conditions was to follow that of the asymmetric a-c power supply and also to weld on plates that were not scraped, but were cleaned by wiping. During the first such test, made at 300 amp. and 300 cycles per second, the arc was stable. At lower currents, however, the arc was not stable at this frequency. Again, erratic reignition of the arc was the problem. Stability could be achieved by wiping the plate with a dilute solution of cesium nitrate to make it a more thermionic cathode and, in the interest of time, it was decided to continue the tests using cesium nitrate-treated plate. The welding conditions for this series of tests are listed in Table 7. The effects of travel speed and current on bead width and depth are listed in Table 8, and the mean values are plotted in Figs. 15 - 20. The trends are similar to those obtained on unscraped plate with the asymmetric a-c power supply, although the actual values of depth and width differed. The bead width and depth increase with current (Figs. 15, 16, 18, 20). No significant interaction seems to be evident between the influence of travel speed and current on bead width (Fig. 15), but interaction does exist when bead depth is considered (Fig. 16). The bead depth is increased more at the lower travel speed than at the higher speed (Fig. 16). At constant current the bead width and depth decrease with increasing travel speed as shown in Figs. 17 and 19.

Empirical equations derived from these data allow approximations of bead widths and depths over a current range of 225 - 270 amp., and a speed range of 5.83 - 8.75 i.p.m.

$$W = 0.003867\ I - 0.0274\ S - 0.4980$$

$$D = 0.010670\ I + 0.224333\ S - 0.001039\ IS - 2.317682$$

where:

W = Bead width (in.),

I = Welding current (amp.),

D = Bead depth (in.), and

S = Travel speed (i.p.m.)

Comparison of these equations with those derived for the 10% asymmetric a-c welds on unscraped plate shows a similar response to changes in welding parameters, but the degree of response varies considerably. The width and depth of the 300 cycle per second welds were much more strongly affected by changes in welding current and speed than were the welds made with 10% asymmetric a-c power. However, precise comparisons would be difficult since the welds were made at different currents and travel speeds, in addition to the differences in frequency and degree of asymmetry.

After aging a minimum of 14 days, the welds were tested in tension. The mechanical properties are listed in Table 9, which includes calculated average values, 95% confidence interval, and L.S.D. (P = 0.05). The average values are plotted in Fig. 21. As was the case with both sets of asymmetric a-c welds, the yield strength increased significantly with increasing welding current and speed, and the tensile strength at first increased and then leveled off with increasing current and speed. Changes in elongation with changes in current and speed were not statistically significant except for the elongation in 1/2 in. gage length for the welds made at low values of current and speed.

4.4 HIGHER FREQUENCY A-C WELDS ON SCRAPED PLATE

The variable frequency a-c power supply (with modifications shown in Fig. 2) was adjusted to produce 300 amp. (rms) at a frequency of 200 cycles per second with a balanced wave (50% R.P., 50% S.P.). The arc length was fixed at 1/8 in. and a newly-dressed tungsten electrode was used to produce each weld on freshly-scraped 1/4 in. thick 2014-T6 aluminum plate shielded with pure argon. Full penetration welds were made using three combinations of welding current and travel speed. The welding conditions are listed in Table 10. In addition, the mechanical properties of individual specimens, average values, 95% confidence interval, and L.S.D. are tabulated. All of the welds were radiographed, and showed no porosity. The average values of yield and tensile strength are plotted as functions of current and speed in Fig. 22. The indicated increase in tensile strength with increasing current and speed is smaller, numerically, than the L.S.D. and would not be considered statistically significant in an isolated case. However, in previous tests, there also was a tendency for tensile

strength to increase with increasing current and speed over approximately the same range. Therefore, the increasing trend in tensile strength in Fig. 22 probably is valid. In the case of yield strength the indicated initial increase is statistically significant, and the subsequent decrease is not significant.

Comparison of the higher frequency a-c welds made on scraped plate with those made on cesium-treated plate would indicate that the presence of cesium had no effect on either yield strength or tensile strength. The strength values for welds made at similar currents and speeds were practically identical. The cesium did have an effect on welding speed, however. For instance, with 300 amp. welding current, full-penetration welds were made in cesium-treated plate at 8.95 i.p.m. At the same current, full-penetration welds were made in scraped plate at 10.5 i.p.m., an increase in speed of over 15%. The cesium probably lowered the cathode voltage drop at the surface of the aluminum plate and caused a reduction in heat input to the plate.

4.5 PULSED D-C WELDS (FIRST GROUP OF TESTS)

Early in the program, the maximum current to be used for making the welds with any of the power supplies was selected according to the current rating of the applicable equipment. In the case of the pulsed d-c power supply the current rating was 400 amp. (rms.). With this power supply, however, care had to be taken that the peak pulse current did not exceed values that would cause air to be aspirated into the inert-gas shield. Then, the base current had to be adjusted to produce the desired 400 amp. (rms.) level. Preliminary tests indicated this condition to be satisfied with a peak current of 475 amp. and a base current of 310 amp. (giving a peak current-base current ratio of about 1.5). The flow rate of helium shielding gas was set at the high value of 125 c.f.h. to provide effective gas coverage.

Because the maximum current-carrying capacities of electrodes of various diameters were established with asymmetric a-c power at 90% straight polarity, the experiment was not repeated for the pulsed d-c welds, which were made with 100% straight polarity and, therefore, would generate less energy in the electrode. The minimum diameter electrode for each selected current level was used according to the electrode studies conducted using asymmetric a-c power. Thoriated-tungsten electrodes were used. With continuous straight-polarity direct current, arc reignition was not involved, and scraped plate could be used throughout the pulsed d-c tests without an emissive agent since the plate was always anodic.

The plan for establishing the welding conditions for the pulsed d-c welds was the same as that followed for the initial asymmetric and higher-frequency a-c welds on emissive plate surfaces. The number of weldments and the radiographing, sectioning, machining, and testing followed the same procedure.

The effects of travel speed and current on bead width and depth are shown in Table 11 and the mean values are plotted in Figs. 23 - 28. As indicated in Figs. 23, 24, 26 and 28 the bead width and depth increased with increasing current. Moreover, a definite interaction existed between the effects of current and travel speed on bead depth and width. The bead depth and width increase by greater proportions at lower travel speeds for proportional increases in current. As shown in Figs. 25 and 27, both bead width and depth decreased with increasing current and speed.

Empirical equations derived from these data allow approximations of bead widths and depths over a current range of 240 - 340 amp. and a speed range of 33 - 49.5 i.p.m.:

$$W = 0.00052\ I - 0.001333\ S + 0.2242$$

$$D = 0.00334\ I + 0.012151\ S - 0.000056\ IS - 0.6656$$

where:

W = Bead width (in.),

D = Bead depth (in.),

I = Welding current (amp.), and

S = Travel speed (i.p.m.).

Comparison of these equations with the earlier equations for asymmetric a-c and variable frequency a-c welds indicates that the width of the pulsed d-c welds was affected less by changes in current and speed than were the a-c welds, while the effect on bead depth was about the same as it was in the asymmetric a-c welds.

The mechanical properties of the pulsed d-c welds are listed in Table 12. Average values, 95% confidence interval, and L.S.D. are included. Fig. 29 shows that the yield strength increased significantly with increases in current and speed. The same trend was noted in the welds made with the other power supplies. However, as the current and travel speed increased the tensile strength and elongation first decreased rapidly, and then leveled off with further increases in current and speed. This behavior was not clearly understood, and was noted in later phases of the work with both pulsed d-c and conventional d-c power supplies. The high welding speeds made possible by the use of helium shielding gas might provide an explanation. Conceivably, in welds made at high speed the weld metal might remain molten after leaving the protected zone near the nozzle and might be weakened by atmospheric contamination. Note that the lowest speed (16.5 i.p.m.) d-c welds were fully as strong as the a-c welds made at comparable speed.

4.6 PULSED D-C WELDS (SECOND GROUP OF TESTS)

Pulsed d-c welds that were made earlier in the test program were made on freshly-scraped plate and did not have to be repeated to eliminate the troublesome side effects of cesium treatment. However, the welds were made with an arc length and a maximum welding current that differed from the standards that were adopted after modifications of the power supplies were made to allow stable a-c operation on scraped plate. Consequently, full penetration pulsed d-c welds were made at the same 1/8 in. arc length and the same maximum current (300 amp.) used for the a-c welds on scraped plate. The shielding gas was helium at a flow of 125 c.f.h. The electrode was 1/8 in.diam. 2% thoriated tungsten, ground to the standard hemispherical tip.

The mechanical properties of the welds are listed in Table 13, with average values, 95% confidence interval, and L.S.D. The strength values are plotted in Fig. 30. As in the earlier pulsed d-c welds, the tensile strength of welds made at high speed was significantly lower than that of welds made at moderate speed. Although none of the welds had any detectable porosity, and no difference in microstructure could be detected, the loss in tensile strength was attributed to atmospheric contamination of the weld metal due to a partial loss of shielding at the higher welding speeds. The photomicrographs of Fig. 31 illustrate the similarity in microstructure of "strong" and "weak" welds. The tensile strengths of the individual specimens were 47,600 p.s.i. and 43,600 p.s.i., respectively.

5. PHASE II

When work on this phase of the study was started, the alternating current power supply had not yet been modified to maintain a stable a-c arc on scraped plate. Consequently, an initial series of welds was made on cesium-treated plate, with the asymmetric a-c supply circuit shown in Fig. 1. A factorial design (2^4) was used, with high and low values of welding current, travel speed, degree of asymmetry, and arc length. The test plates were radiographed, and sent to the machine shop for sectioning. In the meantime some progress had been made in finding an electrical solution to the problem of arc reignition. A circuit involving high open-circuit voltage made it possible to maintain a stable a-c arc on scraped plate when welding at 60 cycles per second. Using this circuit welds were made on scraped plate with the asymmetry of the supply set at various levels of reverse polarity. These welds were compared with others that had been made earlier on cesium-treated plate. A large difference in penetration was noted; the presence of the cesium compound on the plate had a much greater effect on penetration than had been anticipated. Table 14 lists the welding conditions and gives results of depth and width measurements taken from cross-sections of the welds. Welds 16-1 and 19-1 were made under the same conditions except for cesium treatment of the plate. The bead dimensions were practically the same, the cesium treatment reducing the amount of melting only slightly. With the current unbalanced to 10% reverse polarity the aluminum plate serves as an anode for 90% of the time and, since emissive agents are effective only on cathodes, little effect of the cesium could be expected. When comparing Welds 16-10 and 19-3 a significant difference in the fused zone was noted; the cesium-treated plate was the cathode 30% of the time and the cesium was more effective in reducing the heat input to the plate. The greatest effect of the cesium was noted in Weld 16-15, where the aluminum was the cathode 50% of the time and the effect of the cesium was most pronounced. Note that there was no measurable penetration in Weld 16-15. In addition, note that Weld 16-5, although welded at the same current and speed, and with the same cesium treatment as Weld 16-15, was cathodic only 10% of the time. Therefore, the effects of the cesium treatment were not as pronounced.

The above-mentioned welds (with and without cesium treatment) were made 2 months apart, during which time there was a remote possibility that some undetected change had taken place in the equipment or instrumentation which could account for the observed differences. Consequently, a series of welds was made, all on the same day, with the same power supply circuit, welding equipment, and instrumentation. They were made with the same current and travel speed (250 amp., 5 i.p.m.) at 3 levels of reverse polarity (10, 30, 50%). One set of 3 welds was made on freshly scraped plate. Another set was made on plate that had been scraped and then treated with a dilute solution of cesium carbonate. (25 g./liter). The test plates were machined into metallographic specimens, and the previously molten areas of the weld bead cross-sections were measured with the aid of a shadowgraph and a planimeter. The test

results are plotted in Fig. 32 which shows, quite dramatically, that deliberately-applied emissive agents may have a stronger effect on weld penetration than the welding parameters under study. For the scraped plate, the increase in melted area with increase in reverse polarity might be expected because the cathode voltage drop of an aluminum electrode is higher than the anode voltage drop, as noted in the previous paragraph. For the cesium treated plate, the marked decrease in melted area with increasing percentage of reverse polarity suggests that the presence of cesium on the aluminum surface may have reduced the cathode voltage drop of the composite aluminum cathode to a value considerably lower than the anode voltage drop of aluminum. Oscillographic data recorded during these tests indicated that the presence of cesium lowered the total arc voltage by as much as 4.5 v. when welding at 50% reverse polarity (a drop from 19.5 v. to 15 v., at 1/8 in. arc. length). No satisfactory method has been developed for determining how the total arc voltage is shared by its 3 components (cathode, plasma, and anode voltage drops), but the data enumerated above suggest that inconsistencies in weld penetration when welding with conventional a-c TIG techniques may be due to random quantities of emissive contaminants on the plate surface, even though the contaminants may not be as potent as cesium. In any event, the need for an electrical (power supply design) solution for the reignition problem became imperative, and experimentation was continued along this line, culminating in the circuit described earlier in the schematic diagram of Fig. 2. This circuit imposed some limitations in the original scope of the program. Frequencies above 200 cycles per second caused overheating of circuit components; operation at arc lengths of less than 1/8 in., and repeated use of the same electrode without redressing caused periods of arc instability. Despite these limitations, tests were continued with confidence that meaningful data still could be gathered to compare the merits of the power supplies.

5.1 PHASE IIA

The purpose of the Phase IIA tests was to determine the optimum combination of welding conditions for producing deeply penetrating narrow welds having superior metallurgical structures by determining the effects of welding parameters on bead shape. Arc length was not varied as originally planned because arc instability was encountered when welding at short arc lengths with alternating current. Consequently, all the welds were made at a constant arc length of 1/8 in. on 1/2 in. thick 2014-T6 aluminum-alloy plate. A set of test welds was made on freshly-scraped plate with both the a-c and d-c power supplies. Then a set of test welds was made on as-received plate with the a-c supplies to see whether or not residual quantities of some unknown emissive agent affected weld penetration.

For the study of each power supply, a 2^3 factorial experimental design was used. Two levels of each of 3 welding variables were selected based on experience gained in Phase I. In addition, replicate welds were made using median values of the

variables. The test results for the scraped plate are summarized in Table 15, and plotted in Figs. 33 - 41. The results for the as-received plate are summarized in Table 16, and plotted in Figs. 42 - 49.

5.1.1 Asymmetric A-C Welds (scraped plate)

Varying the percentage of reverse polarity (R.P.) had a decided effect on the bead widths of asymmetric a-c welds, as shown in Fig. 33. Increasing the percentage of R.P. from 10 to 50 caused the bead width to increase in each speed-current combination. Such an increase could be expected because the aluminum plate becomes cathodic for a greater percentage of the time when the R.P. percentage is increased. Since the cathode voltage drop for aluminum is higher than the anode voltage drop, more heat is generated at the plate surface. Data listed in Table 15 indicate that the increase in bead width is not statistically significant in two of the current-speed combinations. However, for reasons just cited, the upward trend is believed to be valid.

Only small differences in bead depth were observed for most combinations of current and travel speed when the R.P. was increased from 10 - 50%. Only the combination of the highest current and lowest travel speed produced a sizable increase in depth with an increase in R.P., as shown in Fig. 34.

The change in depth-width ratio was variable as shown in Fig. 35. Each of the indicated changes was considered significant with the exception of the lowest speed-current combination.

Empirical equations were derived from the above data for ranges of 220 - 300 amp., 3 - 9 i.p.m., and 10 - 50% R.P. The equations are more complex than those given earlier because there was more interaction among the variables in these tests.

$$D = 0.0941 + 0.0476\left(\frac{I-260}{40}\right) - 0.0434\left(\frac{S-6}{3}\right) - 0.0204\left(\frac{I-260}{40}\right)\left(\frac{S-6}{3}\right) + 0.0147\left(\frac{S-6}{3}\right)\left(\frac{P-30}{20}\right) + 0.0157\left(\frac{P-30}{20}\right)$$

$$W = 0.3617 + 0.0766\left(\frac{I-260}{40}\right) - 0.0734\left(\frac{S-6}{3}\right) + 0.0473\left(\frac{P-30}{20}\right)$$

$$\frac{D}{W} = 0.2308 + 0.0761\left(\frac{I-260}{40}\right) - 0.0640\left(\frac{S-6}{3}\right) - 0.0251\left(\frac{I-260}{40}\right)\left(\frac{S-6}{3}\right) - 0.0317\left(\frac{S-6}{3}\right)\left(\frac{P-30}{20}\right)$$

where:

D = Bead depth (in.),

I = Welding current (amp.),

S = Travel speed (i.p.m.),

P = Percentage R.P., and

W = Bead width (in.).

The equations were left in the above form to simplify checking of special points. When maximum values of the variables are used in the equations, each of the bracketed terms becomes +1. When the median values are used, the bracketed terms become zero, and for minimum values, the bracketed terms become -1.

5.1.2 Variable Frequency A-C Welds (scraped plate)

In the variable frequency a-c welds the effect of varying the frequency on the bead width was not straightforward. Fig. 36 shows that an increase in frequency caused the bead width to increase with the combination of high speed and low current, but an increase in frequency decreased the bead width with the combination of low speed and high current. Statistical data in Table 15 indicate that each change was significant. Using the other combinations of speed and current, an increase in frequency also caused a decrease in bead width although the decrease was not significant with the high-speed, high-current combination. Fig. 37 shows that changing the frequency resulted in some changes in bead depth, none of which was considered significant. The changes in depth-width ratio shown in Fig. 38 also were insignificant.

Empirical equations were derived from the above data for the ranges of 205 - 300 amp., 3.5 - 10.5 i.p.m., 60 - 200 cycles per second.

$$D = 0.0813 + 0.457\ I - 0.0457\left(\frac{I - 252}{47.5}\right) - 0.0346\left(\frac{S-7}{3.5}\right) -$$

$$0.0191\left(\frac{I-252}{47.5}\right)\left(\frac{S-7}{3.5}\right) + 0.0076\left(\frac{S-7}{3.5}\right)\left(\frac{F-130}{70}\right)$$

$$W = 0.3415 + 0.1095\left(\frac{I-252}{47.5}\right) - 0.0784\left(\frac{S-7}{3.5}\right) - 0.0216\left(\frac{F-130}{70}\right) +$$

$$0.0240\left(\frac{S-7}{3.5}\right)\left(\frac{F-130}{70}\right)$$

$$\frac{D}{W} = 0.2074 + 0.0621\left(\frac{I-252}{47.5}\right) - 0.0456\left(\frac{S-7}{3.5}\right) - 0.0179\left(\frac{I-252}{47.5}\right)\left(\frac{S-7}{3.5}\right)$$

where:

I = Welding current (amp.),

D = Bead depth (in.),

S = Travel speed (i.p.m.),

W = Bead width (in.), and

F = Frequency (cycles per second).

As in the previous set of equations the bracketed terms become (+1), (0), or (-1) when using maximum, median, or minimum values of the variables respectively.

5.1.3 Pulsed D-C Welds

Fig. 39 shows that the bead width of the pulsed d-c welds decreased only slightly with an increase in the peak-base current ratio. However, the statistical data of Table 15 indicate that these decreases are significant in all cases except for that using high speed in combination with high current. Also, as shown in Fig. 40, slight changes in bead depth were observed when the peak-base ratio was changed, and the changes were significant in the cases involving high current. Fig. 41 shows that significant changes in depth-width ratio also occur, at the high current level, with changes in the peak-base ratio.

Empirical equations were derived from the pulsed d-c data in the ranges of 180 - 300 amp., 8 - 24 i.p.m., 1.5 - 2.5 peak-base ratio.

$$D = 0.1586 + 0.0778\left(\frac{I-240}{60}\right) - 0.0622\left(\frac{S-16}{8}\right) - 0.0336\left(\frac{I-240}{60}\right)\left(\frac{S-16}{8}\right)$$

$$W = 0.4219 + 0.1200\left(\frac{I-240}{60}\right) - 0.0863\left(\frac{S-16}{8}\right) - 0.0384\left(\frac{I-240}{60}\right)\left(\frac{S-16}{8}\right) - 0.0070\left(\frac{R-2}{0.5}\right)$$

$$\frac{D}{W} = 0.3394 + 0.0781\left(\frac{I-240}{60}\right) - 0.0661\left(\frac{S-16}{8}\right) - 0.0144\left(\frac{I-240}{60}\right)\left(\frac{S-16}{8}\right) - 0.0080\left(\frac{I-240}{60}\right)\left(\frac{S-16}{8}\right)\left(\frac{R-20}{0.5}\right)$$

where:

D = Bead depth (in.),

I = Welding current (amp.),

S = Travel speed (i.p.m.),

W = Bead width (in.), and

R = Peak current - base current ratio.

5.1.4 A-C Welds on As-Received Plate

During Phase I the use of cesium compounds to stabilize a-c arcs was discontinued when it was learned that the application of cesium to scraped plate surfaces had a strong effect on the penetration pattern. There was some evidence that as-received plate might contain random quantities of some unknown emissive agent, but no tests were made to determine if the unknown agent had any effect on penetration pattern. Consequently, Phase IIA welds were repeated, using the same welding conditions except that the plate surfaces were not scraped. They were cleaned by merely wiping with clean paper towels. A summary of the results including the statistical calculations, 95% confidence intervals and the least significant differences (L.S.D.) is shown in Table 16. The data are plotted in Figs. 42 - 44 and 46 - 48.

Fig. 42 shows the effect of reverse polarity percentage on bead width of the asymmetric a-c welds (as-received plate). An (S) or (N) is used to indicate whether the dimension change from 10 - 50% reverse polarity is or is not statistically significant. The data indicate that an increase in reverse polarity from 10 - 50% causes a significant increase in bead width when welding at low speed (3 i.p.m.) and either high or low current (300, 220 amp.) but does not cause a significant change when welding at high speed (9 i.p.m.) at either value of current. These results do not differ substantially from those obtained when welding on scraped plate. Any residual emissive agent on the as-received plate does not appear to have much effect on the bead width.

As shown in Fig. 43, an increase in reverse polarity component also causes a significant increase in bead depth when welding at slow speed (3 i.p.m.) and either high or low current (300, 220 amp.) but does not cause a significant change when welding at high speed (9 i.p.m.) and either value of current. These test results are almost identical with the scraped plate results. Evidently, any emissive agent that may have been on the as-received plate did not affect the bead depth.

The depth-to-width ratio increased significantly with increasing reverse polarity percentage when welding with the combination of low speed and high current (3 i.p.m., 300 amp.) as shown in Fig. 44. No significant change occurred when using any of the other three combinations of speed and current.

In fig. 45, the depth-to-width ratios of asymmetric a-c welds made on scraped and as-received plates are compared. Welds made at the low speed of 3 i.p.m. show a slightly greater depth-to-width ratio at 50% reverse polarity for scraped plate compared to as-received plate. The differences, however, are not great. The welds made at the high speed of 9 i.p.m. on scraped plate had an apparent decrease in depth-width ratio with increasing reverse polarity percentage.

Changing the frequency from 60 to 200 cycles per second caused a significant decrease in bead width for most of the variable frequency a-c welds made on as-received plate. The data are plotted in Fig. 46. Similar trends were noted when welding on scraped plate except for the welds made at high speed and low current (10.5 i.p.m., 205 amp.) which showed a significant increase in bead width caused by an increase in frequency.

The graphs in Fig. 47 indicate that increasing frequency causes a decrease in bead depth of the variable frequency a-c welds on as-received plate. Although the differences in bead depth were not large, they were considered to be statistically significant. The dead depths of the earlier welds made on scraped plate differed slightly from the depths of the welds made on as-received plate; however, changes in bead depth with changes in frequency were not significant except for the welds made at low speed and high current (3.5 i.p.m., 300 amp.).

The graphs in Fig. 48 indicate that increasing frequency causes a significant decrease in depth-width ratios of the asymmetric a-c welds on as-received plate in all tests except for the low speed - low current combination (3.5 i.p.m., 205 amp.) in which case there was a significant increase in depth-width ratio. When earlier, comparable welds were made on scraped plate, the differences in depth-width ratios were not statistically significant.

In Fig. 49, the depth-to-width ratio results for as-received plate are compared with those previously obtained for scraped plate. At the fast travel speed (10.5 i.p.m.), the depth-to-width ratio increased significantly for the welds made on scraped plate compared to as-received plate at 50% reverse polarity. Further, the ratio was greater for as-received plate at 10% reverse polarity when the welds were deposited at 300 amp. and 10.5 i.p.m. At the slower travel speed (3.5 i.p.m.), differences were noted between scraped and as-received plate results, but the differences were not as great as some found at the higher travel speed. In general, the greatest depth-to-width ratios were obtained using combinations of high current and low travel speed levels for scraped and as-received plate.

In reviewing the results of tests made on plates that were either scraped or as-received, some inconsistencies are apparent. The tests indicate that the as-received plate surfaces contained a variable quantity of some residual emissive agent; and, apparently at times, the emissive agent was present in sufficient quantity to cause a change in the penetration pattern. To ensure uniformity of penetration, residual emissive agents on the plate surfaces should be removed completely before welding.

Empirical equations for the welds on as-received plate were derived as follows:

For asymmetric a.c. in ranges of 220 - 300 amp., 3 - 9 i.p.m., 10 - 50% R.P.:

$$D = 0.0943 + 0.0482\left(\frac{I-260}{40}\right) - 0.0442\left(\frac{S-6}{3}\right) - 0.0289\left(\frac{I-260}{40}\right)\left(\frac{S-6}{3}\right) + 0.0159\left(\frac{P-30}{20}\right) - 0.0163\left(\frac{S-6}{3}\right)\left(\frac{P-30}{20}\right)$$

$$W = 0.03482 + 0.0843\left(\frac{I-260}{40}\right) - 0.0842\left(\frac{S-6}{3}\right) - 0.0267\left(\frac{I-260}{40}\right)\left(\frac{S-6}{3}\right) + 0.0343\left(\frac{P-30}{20}\right) - 0.0361\left(\frac{S-6}{3}\right)\left(\frac{P-30}{20}\right)$$

$$\frac{D}{W} = 0.2355 + 0.0662\left(\frac{I-260}{40}\right) - 0.0537\left(\frac{S-6}{3}\right) - 0.0327\left(\frac{I-260}{40}\right)\left(\frac{S-6}{3}\right)$$

For variable frequency a.c. in ranges of 205 - 300 amp., 3.5 - 10.5 i.p.m., 60 - 200 cycles per second:

$$D = 0.0867 + 0.0578\left(\frac{I-252}{47.5}\right) - 0.0456\left(\frac{S-7}{3.5}\right) - 0.0235\left(\frac{I-252}{47.5}\right)\left(\frac{S-7}{3.5}\right) - 0.0088\left(\frac{F-130}{70}\right)$$

$$W = 0.3455 + 0.1182\left(\frac{I-252}{47.5}\right) - 0.1057\left(\frac{S-7}{3.5}\right) - 0.0295\left(\frac{F-130}{70}\right)$$

$$\frac{D}{W} = 0.1972 + 0.0951\left(\frac{I-252}{47.5}\right) - 0.0668\left(\frac{S-7}{3.5}\right)$$

where:

D = Bead depth (in.),

I = Welding current (amp.),

S = Travel speed (i.p.m.),

P = Percentage of R.P.,

W = Bead width (in.), and

F = Frequency (cycles per second).

In comparing these equations with those derived for the a-c welds on scraped plate, very little difference can be found. In some isolated tests a residual emissive agent appeared to affect weld penetration. However, the similarity of the equations indicates that the overall effect on penetration of any such agent was negligible. Some agent on unscraped plate aids arc reignition, but whatever the agent may be, it does not have nearly as strong an effect on penetration as do deliberately applied agents such as cesium compounds.

5.2 PHASE IIB

In this phase of the program full penetration welds were made in 1/4 in. 2014-T6 aluminum plate using conditions for each power supply which appeared optimum based on experience gained in Phases I and IIA. The purpose of these welds is to compare those made with the specialty supplies and those produced with standard a-c and d-c power supplies. Unfortunately, many of the results of the Phase IIA study are either ambiguous or of small aid in choosing optimum conditions. For instance in Fig. 35 the greatest depth-width ratio in the asymmetric a-c welds was obtained with 50% R.P., 300 amp., and 3 i.p.m., but this combination of variables would cause burn-through of 1/4 in. plate. Reducing the current or R.P.%, or increasing the speed are shown to cause the depth-width ratio to decrease. For making the Phase IIB asymmetric a-c welds, the values 300 amp., 8 i.p.m., and 15% R.P. were chosen for the practical reasons that this combination of values produced uniform, fully-penetrated welds in 1/4 in. plate at a reverse polarity duty cycle sufficiently different from that of a conventional a-c machine to reveal changes that might be due to asymmetry. In like manner, Fig. 38 indicates that frequency does not have a statistically significant effect on depth-width ratio. The practicable values chosen for the higher frequency a-c welds were 300 amp., 10 i.p.m., and 200 cycles per second. Fig. 41 shows that the greatest depth-width ratio for pulsed d-c welds was obtained at 300 amp., 8 i.p.m., and 1.5 peak-base ratio. However, welds made in Phase I at 300 amp. suffered a loss in tensile strength. The values chosen for the Phase IIB pulsed d-c welds were: 240 amp., 16 i.p.m., 1.7 peak-base ratio since strong welds had been made with this combination.

For comparison with the welds made with the special power supplies, welds also were made with conventional a-c and d-c supplies. An available standard commercial power supply with a nominal open-circuit voltage of 80 v. was found to be unsuitable for welding on freshly-scraped aluminum plate because of frequent periods of rectification of the welding current. Consequently, two standard a-c power supplies were connected in series to produce the high open-circuit voltage of a commercial "conventional" power supply which is on the market, but which was not immediately available. Rectification did not occur when using the high open-circuit voltage (150 v.), but the arc was rather erratic. Although the arc reignited on every cycle, the reverse polarity component of the current varied and, furthermore, the 3/16 in.diam. tungsten electrode could no longer carry 300 amp. (rms) without the loss of some tungsten. Instantaneous values of welding current over 500 amp. were noted on the oscillograph, which probably accounts for the "spitting" of tungsten. The equipment was modified to accommodate a 1/4 in.diam. electrode and tests were made at 300 and 325 amp. There was no loss of tungsten, but the arc was erratic, and penetration varied. Finally, the "conventional" a-c welds were made with a 3/16 in. tungsten electrode at a reduced current of 275 amp. The conventional d-c welds were made using a motor-generator set for the power supply. Two sets of welds (4 welds per set) were made: one at 240 amp. to compare with the pulsed d-c welds, and another at 300 amp. for comparison with the a-c welds.

The photographs in Fig. 50 are of typical welds made with the asymmetric a-c power supply at 15% R.P., the variable frequency a-c power supply at 200 cycles per second, and the conventional 60 cycle a-c power supply. Note that the area affected by cathode sputtering action is practically the same in each case even though the aluminum plate for the asymmetric a-c welds was cathodic only 15% of the time.

The photographs of Fig. 51 are top and bottom views of welds made with the pulsed d-c, and conventional d-c supplies. The underbead of the conventional d-c weld made at 300 amp. was surprisingly irregular, even though the top of the bead was uniform. The irregularity was present in all of the conventional d-c welds made at 300 amp. The waviness might have been caused by the high travel speed. However pulsed d-c welds that were made at still higher speeds early in Phase I were uniform though lacking in tensile strength.

All the welds were radiographed and machined into metallographic and tensile specimens. No porosity was detectable. The results of tensile tests are summarized in Table 17. Each listed value is the average for 8 specimens. Calculated values for 95% confidence intervals and least significant differences (L.S.D.) are listed in Table 18. As a visual aid in testing significance, least significant confidence intervals (L.S.C.I.) are displayed in Figs. 52 - 54 ($L.S.C.I. = \text{mean} \pm \frac{L.S.D.}{2}$). When such intervals

overlap, any indicated differences in mean values are not considered statistically significant; when they do not overlap the differences are significant. For instance, for the yield strength of asymmetric a-c welds made at 300 amp. and 8.i.p.m., L.S.C.I. = mean $\pm \frac{L.S.D.}{2} = 27706 \pm \frac{620}{2}$ giving an interval from 27,396 p.s.i. to 28,016 p.s.i., represented by the double-headed arrow in the lower left section of Fig. 52. This interval overlaps that for the conventional a-c welds made at 275 amp. and 6 i.p.m., indicating that the difference in the means of yield strength is not statistically significant. Note that the yield strengths of the conventional d-c welds, at both levels of current and speed, were significantly greater than the yield strengths of all the others, including the pulsed d-c welds. The large L.S.C.I. for the conventional d-c welds made at 300 amp. and 24 i.p.m. is a reflection of considerable scatter in the strength data for these welds. The scatter was probably due to the fact that all of these welds had irregular underbeads. The data in Fig. 53 show that there was no significant difference in tensile strength of welds made with the asymmetric, variable frequency, or conventional a-c power supplies. With the d-c supplies, however, there was a difference. The pulsed d-c welds, made at 240 amp. and 16 i.p.m., had significantly lower tensile strength than the conventional d-c welds made at the same levels of current and speed. The low value for tensile strength of the conventional d-c welds made at 300 amp. and 24 i.p.m. also was statistically significant.

In the conventional d-c welds the drop in tensile strength at high welding current and travel speed was similar to that which occurred in the Phase I welds made with the pulsed d-c power supply. Again, metallographic examination of the weld specimens did not reveal any significant difference in microstructure. However, poor shielding still is thought to be a possible reason for the drop in tensile strength. Welding at high speed might expose the weld pool to the atmosphere before it has solidified. Conceivably, a compound could form which, though undetectable under the microscope, might serve to both strengthen and embrittle the weld metal. Embrittled areas might trigger premature failure of the weld even though the yield strength is higher. In production welding the use of a trailing gas shield probably would eliminate the drop in tensile strength.

Least significant confidence intervals for elongation of the welds are plotted in Fig. 54. The data show that the elongation in 1/2 in. was significantly greater than the elongation in 1 in. The difference in elongation values undoubtedly is due partially to the fact that gage lengths included both weld metal and base metal, and the 1/2 in. gage length contained the larger percentage of weld metal. No statistically significant difference in elongation appears to exist due to the choice of power supplies, with one exception. In elongation in 1 in., there is no overlap in the L.S.C.I.'s for the asymmetric a-c welds and the conventional d-c welds made at 300 amp. The differences in elongation values of the conventional d-c welds made at different currents and speeds, though not significant, are consistent with the concept that the welds made at the higher speed were embrittled by atmospheric contamination.

6. CONCLUSIONS

1) Conventional alternating current power supplies are effective only for welding plate that has been cleaned superficially. When the surface of 2014-T6 aluminum plate is scraped prior to welding with alternating current, the arc becomes unstable unless a high open circuit voltage is available to reignite the arc. For this reason, the original design for Airco's asymmetric and variable frequency power supply was not effective for reigniting the arc at those instants when the aluminum plate became the cathode. The same problem occurred with conventional a-c power supplies designed for TIG welding. Radio-frequency stabilization was not helpful nor sufficient to insure consistent reignition.

2) This problem appears to be aggravated at higher frequencies. For example, arc stability could not be achieved on as-received plate when the frequency was increased to 300 cycles per second. The plate surface evidently contained a residual quantity of some emissive agent that aided arc reignition, but the amount of emissive agent was insufficient to promote arc stability under all conditions in the test program.

3) For all test conditions, the arc could be stabilized on scraped plate by washing it with dilute solutions of compounds containing cesium. However, this practice was found to reduce weld penetration significantly.

4) Stable alternating current arcs were achieved finally with changes in the inverter circuit of the power supply to raise the open circuit voltage to 135 v. Even with this improvement, however, stable arcs could not be achieved with frequencies in excess of 200 cycles per second. Short arc lengths were also shown to be unstable. As a result, arc length was eliminated as a variable in the test program, and all test welds were made at 1/8 in. arc length. No explanation has been found for the erratic performance at short arc lengths.

5) With the modified inverter circuit, welding on freshly scraped plate, changing the percentage of reverse polarity caused a variable change in the depth-to-width ratio of the weld. The combination of low speed and high current caused the depth-to-width ratio to increase with increasing reverse polarity percentage. With the combination of high speed and low current, however, the depth-to-width ratio decreased.

6) Changing the frequency of the welding current did not cause a significant change in the depth-to-width ratio of the weld.

7) When welding with the pulsed d-c supply, changing the ratio of peak current-to-base current did not affect the depth-to-width ratio at low current, but did affect it at high current. The effect varied with travel speed; at high speed the depth-to-width ratio increased with increasing peak-to-base ratio, while at low speed, it decreased.

8) Full penetration welds made in 1/4 in. plate using 15% reverse polarity asymmetry had mechanical properties essentially the same as welds made with conventional a-c (50% reverse polarity), at similar currents and travel speeds.

9) Full penetration welds made in 1/4 in. plate using a frequency of 200 cycles per second also had mechanical properties similar to welds made with conventional a-c (60 cycles per second) at similar currents and travel speeds.

10) Full penetration welds made in 1/4 in. plate with pulsed direct current at a peak current-to-base current ratio of 1.7 had significantly lower values of mechanical properties than welds made with conventional direct current at the same current (rms) and travel speed.

11) Metallographic examination of weld specimens did not reveal any differences in microstructure that were attributed to differences in either frequency or asymmetry of alternating current, or in pulsed direct current. None of the welds had any porosity.

12) Welds with good mechanical properties could be obtained when welding with each of the power supplies tested. The strongest welds were made with a conventional d-c power supply, using helium shielding gas.

13) Setting the asymmetry of alternating current at low values of reverse polarity component increases the current-carrying capacity of the electrode, and still provides adequate cathodic cleaning action of the aluminum plate surface.

14) Under some conditions of current and speed the pulsed d-c welds were more uniform than their counterparts made with conventional d.c.

E.H. Cushman

Approved:

K.E. Dorschu

cb,mb

Table 1. CURRENT-CARRYING CAPACITY of ELECTRODES (90% D.C.S.P.; 10% D.C.R.P.)

Electrode Type	Diam. (in.)	Maximum Safe Current (amp.)	Failure Current (amp.)
Tungsten	1/16	175	200
Tungsten (2% Th)	1/16	150	175
Tungsten	3/32	350	375
Tungsten (2% Th)	3/32	350	375
Tungsten	1/8	400	
Tungsten (2% Th)	1/8	400	

Constant Conditions

Electrode holder:	Airco Model M50A
Gas nozzle:	5/8 in. ID
Shielding gas (at nozzle):	Argon, 20 c.f.h.
Shielding gas (underbead):	Argon, 10 c.f.h.
Electrode extension:	1 in. (from collet to electrode tip)
Electrode tip shape:	Hemispherical
Frequency:	60 cycles per second

Table 2. CURRENTS and TRAVEL SPEEDS USED for ASYMMETRIC A-C WELDS (on emissive plate): PHASE I

Spec. No.	Travel Speed (i.p.m.)	Current (amp.)	Generator Setting (Tap No.)	Open Circuit Voltage (v.)	Electrode Diameter (in.)	Remarks
2083-3-1	15-3/4	420	8	80	1/8	Full penetration, occasional arc outage.
-2	5-1/4	250	6	73	3/32	Full penetration, frequent arc outage.
-3	10-1/2	330	6	83	3/32	Full penetration, occasional arc outage.
-4	15-3/4	250	6	73	3/32	Very few arc outages.
-5	15-3/4	330	6	85	3/32	Very few arc outages.
-6	10-1/2	250	6	73	3/32	Very few arc outages.
-7	15-3/4	420	8	80	1/8	Full penetration, occasional outage.
-8	5-1/4	250	6	73	3/32	Full penetration, occasional outage.
-9	10-1/2	330	6	83	3/32	Full penetration, occasional outage.
-10	15-3/4	250	6	73	3/32	Very few arc outages.
-11	15-3/4	330	6	85	3/32	Very few arc outages.
-12	10-1/2	250	6	73	3/32	Very few arc outages.

Table 5. DEPTH and WIDTH MEASUREMENTS of ASYMMETRIC A-C WELDS (on emissive plate)

Spec. No.	Speed (i.p.m.)	Current (amp.)	Depth (in.)	Width (in.)
2083-3-1B	15.75	420	0.250	0.394
1E	15.75	420	0.250	0.402
1G	15.75	420	0.250	0.392
2B	5.25	250	0.250	0.414
2E	5.25	250	0.250	0.400
2G	5.25	250	0.250	0.424
3B	10.50	330	0.250	0.380
3E	10.50	330	0.250	0.390
3G	10.50	330	0.250	0.379
4B	15.75	250	0.082	0.246
4E	15.75	250	0.082	0.234
4G	15.75	250	0.080	0.232
5B	15.75	330	0.163	0.324
5E	15.75	330	0.162	0.324
5G	15.75	330	0.157	0.325
6B	10.50	250	0.111	0.285
6E	10.50	250	0.110	0.282
6G	10.50	250	0.113	0.285
7B	15.75	420	0.250	0.399
7E	15.75	420	0.250	0.400
7G	15.75	420	0.250	0.411
8B	5.25	250	0.250	0.406
8E	5.25	250	0.250	0.410
8G	5.25	250	0.250	0.416
9B	10.50	330	0.250	0.390
9E	10.50	330	0.250	0.392
9G	10.50	330	0.250	0.403
10B	15.75	250	0.078	0.230
10E	15.75	250	0.078	0.230
10G	15.75	250	0.083	0.239
11B	15.75	330	0.156	0.314
11E	15.75	330	0.144	0.317
11G	15.75	330	0.147	0.314
12B	10.50	250	0.115	0.296
12E	10.50	250	0.114	0.305
12G	10.50	250	0.118	0.301

Table 4. MECHANICAL PROPERTIES of ASYMMETRIC A-C WELDS (on emissive plate)

Spec. No.	Speed (i.p.m.)	Current (amp.)	Yield Strength 0.2% Offset (p.s.i.)	Tensile Strength (p.s.i.)	Elong. in 1/2 in. (%)	Elong. in 1 in. (%)	Location of Failure
3-1C	15.75	420	32,900	45,700	11.4	8.0	Weld
1F	15.75	420	32,400	46,100	11.3	7.3	Weld
7A	15.75	420	32,900	44,900	11.1	7.9	Weld
7H	15.75	420	32,450	44,900	11.2	6.9	Weld
Average	15.75	420	32,700	45,400	11.25	7.53	
3-2C	5.25	250	29,400	43,850	11.0	6.6	Weld
2F	5.25	250	28,800	44,850	11.2	7.0	Weld
8C	5.25	250	28,700	43,600	11.0	6.4	Weld
8F	5.25	250	29,750	44,850	11.0	7.2	Weld
Average	5.25	250	29,200	44,300	11.05	6.8	
3-3C	10.50	330	31,900	44,900	11.4	8.0	Weld
3F	10.50	330	31,000	46,500	11.0	6.7	Fusion line
9C	10.50	330	31,000	45,900	11.1	7.0	Weld
9F	10.50	330	31.400	46,300	11.4	8.0	Fusion line
Average	10.50	330	31,325	45,900	11.2	7.43	
95% Confidence Interval			±412	±758	±0.15	±0.62	
L.S.D. (p = 0.05)			580	930	0.21	0.88	

Table 5. MECHANICAL PROPERTIES of ASYMMETRIC A-C WELDS* on SCRAPED PLATE

Spec. No.	Speed (i.p.m.)	Current (amp.)	Yield Strength 0.2% Offset (p.s.i.)	Tensile Strength (p.s.i.)	Elong. in 1/2 in. (%)	Elong. in 1 in. (%)	Location of Failure
31-1C	9	300	32,600	48,700	8.0	8.0	Fusion line
1F	9	300	31,250	50,400	8.0	8.0	Fusion line
4C	9	300	29,750	46,00	6.0	8.0	Fusion line
4F	9	300	30,000	47,350	10.0	8.0	Fusion line
Average	9	300	30,900	48,113	8.0	8.0	
31-2C	3	220	24,400	43,500	8.0	8.0	Weld
2F	3	220	24,400	45,300	8.0	8.0	Fusion line
5C	3	220	25,200	45,800	4.0	11.0	Base metal
5F	3	220	25,750	45,600	4.0	11.0	Base metal
Average	3	220	24,938	45,050	6.0	9.5	
31-3C	6	260	28,400	49,100	8.0	8.0	Fusion line
3F	6	260	27,500	46,900	8.0	8.0	Fusion line
6C	6	260	27,500	48,000	12.0	9.0	Edge of weld
6F	6	260	28,100	48,900	12.0	8.0	Edge of weld
Average	6	260	27,875	48,225	10.0	8.2	
95% Confidence Interval L.S.D. (P = 0.05)			±1,340 1,890	±1,840 2,600	±3.3 4.6	±1.7 2.5	

* The following conditions were constant: 1/8 in.diam. tungsten electrode, 1/8 in. arc length, argon shielding gas (25 c.f.h.).

Table 6. CURRENT-CARRYING CAPACITY of PURE TUNGSTEN ELECTRODES
(50% D.C.S.P.; 50% D.C.R.P.)

Diam. (in.)	Maximum Safe Current (amp.)	Excessive Current (amp.)
3/32	125	150
1/8	200	225
3/16	300	-

Constant Conditions

Electrode holder:	Airco Model M50A
Gas nozzle:	5/8 in. ID
Shielding gas (at nozzle):	Argon, 20 c.f.h.
Shielding gas (underbead):	Argon, 10 c.f.h.
Electrode extension:	1 in. (from collet to electrode tip)
Electrode tip shape:	Hemispherical
Frequency:	300 cycles per second

Table 7. CURRENTS and TRAVEL SPEEDS USED for 300 CYCLE PER SECOND WELDS: PHASE I

Spec. No.	Travel Speed (i.p.m.)	Current (amp.)	Generator Setting (Tap No.)	Open Circuit Voltage (v.)	Electrode Diameter (in.)	Remarks*
2083-8-1	8.75	300	6	80	3/16	Full penetration (no $CsNO_3$).
-2	2.92	225	6	75	3/16	Full penetration.
-3	5.83	270	6	80	3/16	Full penetration.
-4	8.75	225	6	75	3/16	Partial penetration.
-5	8.75	270	6	80	3/16	Partial penetration.
-6	5.83	225	6	75	3/16	Partial penetration.
-7	8.75	300	6	80	3/16	Full penetration. (no $CsNO_3$).
-8	2.92	225	6	75	3/16	Full penetration.
-9	5.83	270	6	80	3/16	Full penetration.
-10	8.75	225	6	80	3/16	Partial penetration.
-11	8.75	270	6	80	3/16	Partial penetration.
-12	5.83	225	6	75	3/16	Partial penetration.

*Unless noted otherwise all plates were treated with $CsNO_3$.

RE-67-084-CRE-42

Table 8. DEPTH and WIDTH MEASUREMENTS of 300 CYCLE PER SECOND WELDS (on emissive plate)

Spec. No.	Speed (i.p.m.)	Current (amp.)	Depth (in.)	Width (in.)
2083-8-1B	8.75	300	0.250	0.373
-1E	8.75	300	0.250	0.378
-1G	8.75	300	0.250	0.374
-2B	2.92	225	0.250	0.426
-2E	2.92	225	0.250	0.406
-2G	2.92	225	0.250	0.410
-3B	5.83	270	0.250	0.380
-3E	5.83	270	0.250	0.397
-3G	5.83	270	0.250	0.379
-4B	8.75	225	0.009	0.131
-4E	8.75	225	0.020	0.126
-4G	8.75	225	0.020	0.125
-5B	8.75	270	0.086	0.284
-5E	8.75	270	0.083	0.280
-5G	8.75	270	0.094	0.289
-6B	5.83	225	0.025	0.162
-6E	5.83	225	0.047	0.210
-6G	5.83	225	0.030	0.164
-7B	8.75	300	0.250	0.406
-7E	8.75	300	0.250	0.400
-7G	8.75	300	0.250	0.382
-8B	2.92	225	0.250	0.445
-8E	2.92	225	0.250	0.424
-8G	2.92	225	0.250	0.422
-9B	5.83	270	0.250	0.404
-9E	5.83	270	0.250	0.365
-9G	5.83	270	0.250	0.396
-10B	8.75	225	0.024	0.152
-10E	8.75	225	0.020	0.120
-10G	8.75	225	0.018	0.137
-11B	8.75	225	0.084	0.267
-11E	8.75	225	0.110	0.321
-11G	8.75	225	0.097	0.324
-12B	5.83	225	0.039	0.204
-12E	5.83	225	0.050	0.239
-12G	5.83	225	0.054	0.233

Table 9. MECHANICAL PROPERTIES of 300 CYCLE PER SECOND WELDS* on CESIUM-TREATED PLATE

Spec. No.	Speed (i.p.m.)	Current (amp.)	Yield Strength 0.2% Offset (p.s.i.)	Tensile Strength (p.s.i.)	Elong. in 1/2 in. (%)	Elong. in 1 in. (%)	Location of Failure
8-1C	8.95	300	29,600	47,550	14	7	Fusion line
1F	8.95	300	31,500	48,200	14	7	Fusion line
7C	8.95	300	31,700	47,100	12	7	Weld
7F	8.95	300	32,400	48,550	14	7	Weld
Average	8.95	300	31,300	47,850	13.5	7	
8-2C	2.92	225	26,800	44,500	10	9	Weld
2F	2.92	225	26,700	45,200	12	9	Weld
8C	2.92	225	27,050	45,000	12	7	Weld
8F	2.92	225	26,650	44,650	8	7	Weld
Average	2.92	225	26,800	44,900	10.5	8	
8-3C	5.83	270	30,050	46,750	12	8	Weld
3F	5.83	270	30,200	48,050	12	8	Fusion line
9C	5.83	270	30,000	48,650	14	7	Fusion line
9F	5.83	270	30,000	48,000	14	7	Weld
Average	5.83	270	30,063	47,625	13	7.5	
95% Confidence Interval			± 700	± 622	± 1.40	± 0.88	
L.S.D. (P = 0.05)			990	880	2.0	1.24	

* The following conditions were constant: 3/16 in.diam. tungsten electrode, 0.010 in. arc length, argon shielding gas (25 cfh).

Table 10. MECHANICAL PROPERTIES of 200 CYCLE PER SECOND A-C WELDS* on SCRAPED PLATE

Spec. No.	Speed (i.p.m.)	Current (amp.)	Yield Strength 0.2% Offset (p.s.i.)	Tensile Strength (p.s.i.)	Elong. in. 1/2 in. (%)	Elong. in. 1 in. (%)	Location of Failure
31-7C	10.5	300	30,900	48,550	16	11	Weld
7F	10.5	300	28,250	45,850	16	11	Weld
10C	10.5	300	32,400	48,450	18	12	Weld
10F	10.5	300	32,400	46,950	18	11	Fusion line
Average	10.5	300	30,988	47,450	17	11.2	
31-8C	3.5	205	28,600	50,400	10	11	Weld
8F	3.5	205	25,500	46,800	10	11	Fusion line
11C	3.5	205	24,750	43,300	16	11	Weld
11F	3.5	205	25,800	44,000	16	10	Weld
Average	3.5	205	26,175	46,125	13	10.8	
31-9C	7.0	250	30,650	46,300	10	9	Fusion line
9F	7.0	250	31,500	47,700	14	10	Weld
12C	7.0	250	28,900	49,450	16	10	Fusion line
12F	7.0	250	36,200	46,100	16	10	Weld
Average	7.0	250	31,813	47,388	14	9.8	
95% Confidence Interval			±2,330	±2,910	±4.2	±0.8	
L.S.D. (P = 0.05)			3,300	4,120	6.2	1.2	

* The following conditions were constant: 3/16 in.diam. tungsten electrode, 1/8 in. arc length, argon shielding gas (25 c.f.h.), 200 cycles per second.

Table 11. DEPTH and WIDTH MEASUREMENTS of PULSED D-C WELDS

Spec. No.	Speed (i.p.m.)	Current (amp.)	Depth (in.)	Width (in.)
2083-10-1-B	49.5	400	0.250	0.332
-1-E	49.5	400	0.250	0.336
-1-G	49.5	400	0.250	0.326
2083-11-2-B	16.5	240	0.250	0.433
-2-E	16.5	240	0.250	0.427
-2-G	16.5	240	0.250	0.401
-3-B	33.0	340	0.250	0.369
-3-E	33.0	340	0.250	0.371
-3-G	33.0	340	0.250	0.377
-4-B	49.5	240	0.077	0.261
-4-E	49.5	240	0.081	0.256
-4-G	49.5	240	0.080	0.258
-5-B	49.5	340	0.141	0.335
-5-E	49.5	340	0.143	0.333
-5-G	49.5	340	0.140	0.337
-6-B	33.0	240	0.103	0.293
-6-E	33.0	240	0.091	0.301
-6-G	33.0	240	0.102	0.307
2083-10-7-B	49.5	400	0.250	0.321
-7-E	49.5	400	0.250	0.333
-7-G	49.5	400	0.250	0.321
2083-11-8-B	16.5	240	0.250	0.419
-8-E	16.5	240	0.250	0.415
-8-G	16.5	240	0.250	0.418
-9-B	33.0	340	0.250	0.362
-9-E	33.0	340	0.250	0.358
-9-G	33.0	340	0.250	0.355
-10-B	49.5	260	0.085	0.318
-10-E	49.5	260	0.083	0.321
-10-G	49.5	260	0.083	0.324
-11-B	49.5	340	0.137	0.318
-11-E	49.5	340	0.137	0.321
-11-G	49.5	340	0.144	0.324
-12-B	33.0	240	0.105	0.294
-12-E	33.0	240	0.104	0.293
-12-G	33.0	240	0.102	0.300

Table 12. MECHANICAL PROPERTIES of PULSED D-C WELDS (first set)

Spec. No.	Speed (i.p.m.)	Current (amp.)	Yield Strength 0.2% Offset (p.s.i.)	Tensile Strength (p.s.i.)	Elong. in 1/2 in. (%)	Elong. in 1 in. (%)	Location of Failure
10-1C	49.5	400	37,250	43,500	12	6	Weld
1F	49.5	400	37,250	41,100	12	6	Weld
7C	49.5	400	37,200	39,750	10	5	Fusion line
7F	49.5	400	36,400	41,200	12	5	Fusion line
Average	49.5	400	37,025	41,388	11.5	5.5	
11-2C	16.5	240	35,300	49,600	14	9	Weld
2F	16.5	240	33,150	49,500	14	8	Weld
8C	16.5	240	33,350	48,500	16	8	Weld
8F	16.5	240	34,850	49,700	16	8	Weld
Average	16.5	240	34,162	49,325	15	8.25	
11-3C	33.0	340	36,200	46,100	12	7	Fusion line
3F	33.0	340	34,400	40,600	12	6	Fusion line
9C	33.0	340	34,850	39,650	10	5	Fusion line
9F	33.0	340	34,750	41,200	10	5	Weld
Average	33.0	340	35,050	41,888	11	5.75	
95% Confidence Interval			± 806	± 606	± 1.74	± 1.08	
(L.S.D. (P = 0.05)			1,140	856	2.46	1.52	

Table 13. MECHANICAL PROPERTIES of PULSED D-C WELDS* (second set)

Spec. No.	Speed (i.p.m.)	Current (amp.)	Yield Strength 0.2% Offset (p.s.i.)	Tensile Strength (p.s.i.)	Elong. in 1/2 in. (%)	Elong. in 1 in. (%)	Location of Failure
34-1C	24	300	30,900	43,600	14	9	Weld
1F	24	300	29,300	45,400	14	9	Weld
6C	24	300	28,200	46,100	18	9	Weld
6F	24	300	28,400	43,900	14	8	Weld
Average	24	300	29,200	44,750	15	8.8	
34-3C	8	180	29,200	47,600	18	10	Weld
3F	8	180	30,200	47,850	18	9	Weld
4C	88	180	28,100	48,800	16	9	Weld
4F	8	180	28,500	47,750	16	9	Weld
Average	8	180	29,000	47,988	17	9.3	
34-2C	16	240	30,300	48,300	18	10	Weld
2F	16	240	29,500	48,750	18	10	Weld
5C	16	240	29,000	48,600	10	9	Weld
5F	16	240	29,350	48,600	20	9	Weld
Average	16	240	29,538	48,563	19	9.5	
95% Confidence Interval			± 1,380	± 890	± 2.0	± 0.8	
L.S.D. (P = 0.05)			1,950	1,256	2.8	1.2	

* The following conditions were constant: 1/8 in.diam. 2% Th. electrode, 1/8 in. arc length helium shielding gas (125 c.f.h.)

Table 14. THE EFFECT of CESIUM TREATMENT on WELD DEPTH and WIDTH

Weld No.	Welding Current (amp.)	Welding Speed (i.p.m.)	Reverse Polarity (%)	Cesium Used	Fused Zone		Decrease in Dimension	
					Depth (in.)	Width (in.)	Depth (%)	Width (%)
19-1	400	5.25	10	No	0.1882	0.5086		
16-1	400	5.25	10	Yes	0.1818	0.4607	3.4	9.4
19-3	325	10.5	30	No	0.0761	0.3277		
16-10	325	10.5	30	Yes	0.0413	0.1945	46	41
19-2	250	5.25	50	No	0.0740	0.4295		
16-5	250	5.25	10	Yes	0.0687	0.2448	7.2	43
16-15	250	5.25	50	Yes	0.0	0.0	100	100

Table 15. SUMMARY of BEAD DIMENSION RESULTS for PHASE IIA WELDS DEPOSITED on SCRAPED PLATE

Power Supply	Current (amp.)	Speed (i.p.m.)	R.P. (%)	Frequency (c.p.s.)	Peak-Base Current (ratio)	Av. Depth (in.)	Av. Width (in.)	Depth-Width (ratio)
Asymmetric A-C	220	3.0	10	60		0.0556 (S)*	0.2979 (S)	0.1866 (N)
	220	3.0	50	60		0.0834	0.4158	0.2006
	220	9.0	10	60		0.0251 (N)	0.1710 (N)	0.1468 (S)
	220	9.0	50	60		0.0217	0.2560	0.0848
	260	6.0	30	60		0.0620	0.3380	0.1831
	300	3.0	10	60		0.1585 (S)	0.4806 (N)	0.3298 (S)
	300	3.0	50	60		0.2524	0.5462	0.4621
	300	9.0	10	60		0.0741 (N)	0.3081 (S)	0.2405 (S)
	300	9.0	50	60		0.0817	0.4183	0.1953
	95% Confidence Interval L.S.D. (P = 0.05)					±0.0138 0.0195	±0.0623 0.0894	±0.017 0.024
Variable-Frequency A-C	205	3.5	50	60		0.0575 (N)	0.3287 (S)	0.1749 (N)
	205	3.5	50	200		0.0448	0.2619	0.1711
	205	10.5	50	60		0.0163 (N)	0.1505 (S)	0.1083 (N)
	205	10.5	50	200		0.0237	0.1866	0.1270
	252	7.0	50	130		0.0585	0.3181	0.1839
	300	3.5	50	60		0.1954 (N)	0.6022 (S)	0.3245 (N)
	300	3.5	50	200		0.1661	0.4867	0.3413
	300	10.5	50	60		0.0676 (N)	0.3709 (N)	0.1823 (N)
	300	10.5	50	200		0.0792	0.3445	0.2298
	95% Confidence Interval L.S.D. (P = 0.05)					±0.0268 0.0380	±0.0216 0.0306	±0.070 0.098

(contd.)

Table 15. SUMMARY of BEAD DIMENSION RESULTS for PHASE IIA WELDS DEPOSITED on SCRAPED PLATE (contd.)

Power Supply	Current (amp.)	Speed (i.p.m.)	R.P. (%)	Frequency (c.p.s.)	Peak-Base Current (ratio)	Av. Depth (in.)	Av. Width (in.)	Depth-Width (ratio)
Pulsed A-C	180	8	50	60	1.5	0.1134 (S)	0.3651 (S)	0.3106 (N)
	180	8	50	60	2.5	0.1055	0.3346	0.3153
	180	24	50	60	1.5	0.0540 (N)	0.2596 (S)	0.2163 (N)
	180	24	50	60	2.5	0.0505	0.2485	0.2032
	240	16	50	60	2.0	0.1801	0.4189	0.2581
	300	8	50	60	1.5	0.3425 (S)	0.6739 (S)	0.5082 (S)
	300	8	50	60	2.5	0.3216	0.6594	0.4877
	300	24	50	60	1.5	0.1352 (S)	0.4171 (N)	0.3241 (S)
	300	24	50	60	2.5	0.1460	0.4173	0.3498
	95% Confidence Interval L.S.D. (P = 0.05)					±0.0045 0.0064	±0.0048 0.0068	±0.010 0.014

* (S) = Statistically significant at the 95% confidence level.
(N) = Not statistically significant at the 95% confidence level.

Table 16. SUMMARY of BEAD DIMENSION RESULTS for PHASE IIA WELDS DEPOSITED on AS-RECEIVED PLATE

Power Supply	Current (amp.)	Speed (i.p.m.)	R.P. (%)	Frequency (c.p.s.)	Av. Depth (in.)	Av. Width (in.)	Depth-Width (ratio)
Asymmetric A-C	220	3.0	10	60	0.0476 (S)	0.2552 (S)	0.1862 (N)
	220	3.0	50	60	0.0751	0.3876	0.1953
	220	9.0	10	60	0.0351 (N)	0.2184 (N)	0.1597 (N)
	220	9.0	50	60	0.0266	0.1946	0.1368
	260	6.0	30	60	0.0573	0.3415	0.1676
	300	3.0	10	60	0.1649 (S)	0.4689 (S)	0.3519 (S)
	300	3.0	50	60	0.2662	0.6179	0.4244
	300	9.0	10	60	0.0660 (N)	0.3134 (N)	0.2107 (N)
	300	9.0	50	60	0.0727	0.3300	0.2197
	95% Confidence Interval				±0.0098	±0.0288	±0.0222
	L.S.D. (P = 0.05)				0.0139	0.0407	0.0314
Variable-frequency A-C	205	3.5	50	60	0.0552 (S)	0.3736 (S)	0.1475 (S)
	205	3.5	50	200	0.0468	0.2759	0.1697
	205	10.5	50	60	0.0125 (S)	0.1560 (S)	0.0825 (S)
	205	10.5	50	200	0.0009	0.1037	0.0087
	252	7.0	50	130	0.0572	0.3314	0.1738
	300	3.5	50	60	0.2292 (S)	0.5908 (N)	0.3878 (S)
	300	3.5	50	200	0.1980	0.5644	0.3508
	300	10.5	50	60	0.0850 (S)	0.3794 (S)	0.2249 (S)
	300	10.5	50	200	0.0658	0.3201	0.2055
	95% Confidence Interval				±0.0058	±0.0198	±0.0108
	L.S.D. (P = 0.05)				0.0082	0.0280	0.0153

Table 17. MECHANICAL PROPERTIES of PHASE IIB WELDS

Power Supply	Current (amp.)	Speed (i.p.m.)	Yield Strength (p.s.i.)	Tensile Strength (p.s.i.)	Elongation in 1/2 in. (%)	Elongation in 1 in. (%)
Asymmetric A-C 15% R.P.	300	8	27,706	47,400	18.2	11.2
Variable Freq. A-C 200 c.p.s.	300	10	28,806	47,600	17.8	10.6
Pulsed D-C 1.7 Peak-Base Ratio	240	16	29,125	46,869	16.2	10.5
Conventional A-C 60 c.p.s.	275	6	28,325	47,988	17.5	10.5
Conventional D-C	300	24	33,031	45,075	17.2	9.5
Conventional D-C	240	16	32,025	48,369	17.8	10.5

Table 18. CONFIDENCE INTERVALS and LEAST SIGNIFICANT DIFFERENCES for PHASE IIB WELDS

Power Supply	Yield Strength		Tensile Strength		Elong. in 1/2 in		Elong. in 1 in.	
	Conf.Int.	L.S.D.	Conf.Int.	L.S.D.	Conf.Int.	L.S.D.	Conf.Int.	L.S.D.
Asymmetric A-C 300 amp., 8 i.p.m.	± 440	620	± 760	1080	± 2.08	2.94	± 0.92	1.30
Variable Freq. A-C 300 amp., 10 i.p.m.	± 520	740	± 540	760	± 1.32	1.86	± 0.60	0.84
Conventional A-C 275 amp., 6 i.p.m.	± 740	1040	± 1160	1640	± 1.28	1.80	± 0.70	0.98
Pulsed D-C 240 amp., 16 i.p.m.	± 360	500	± 380	540	± 2.88	4.08	± 0.40	0.56
Conventional D-C 240 amp., 16 i.p.m.	± 500	700	± 600	840	± 1.00	1.42	± 0.94	1.32
Conventional D-C 300 amp., 24 i.p.m.	± 2000	2820	± 1320	3240	± 1.12	1.58	± 1.08	1.52

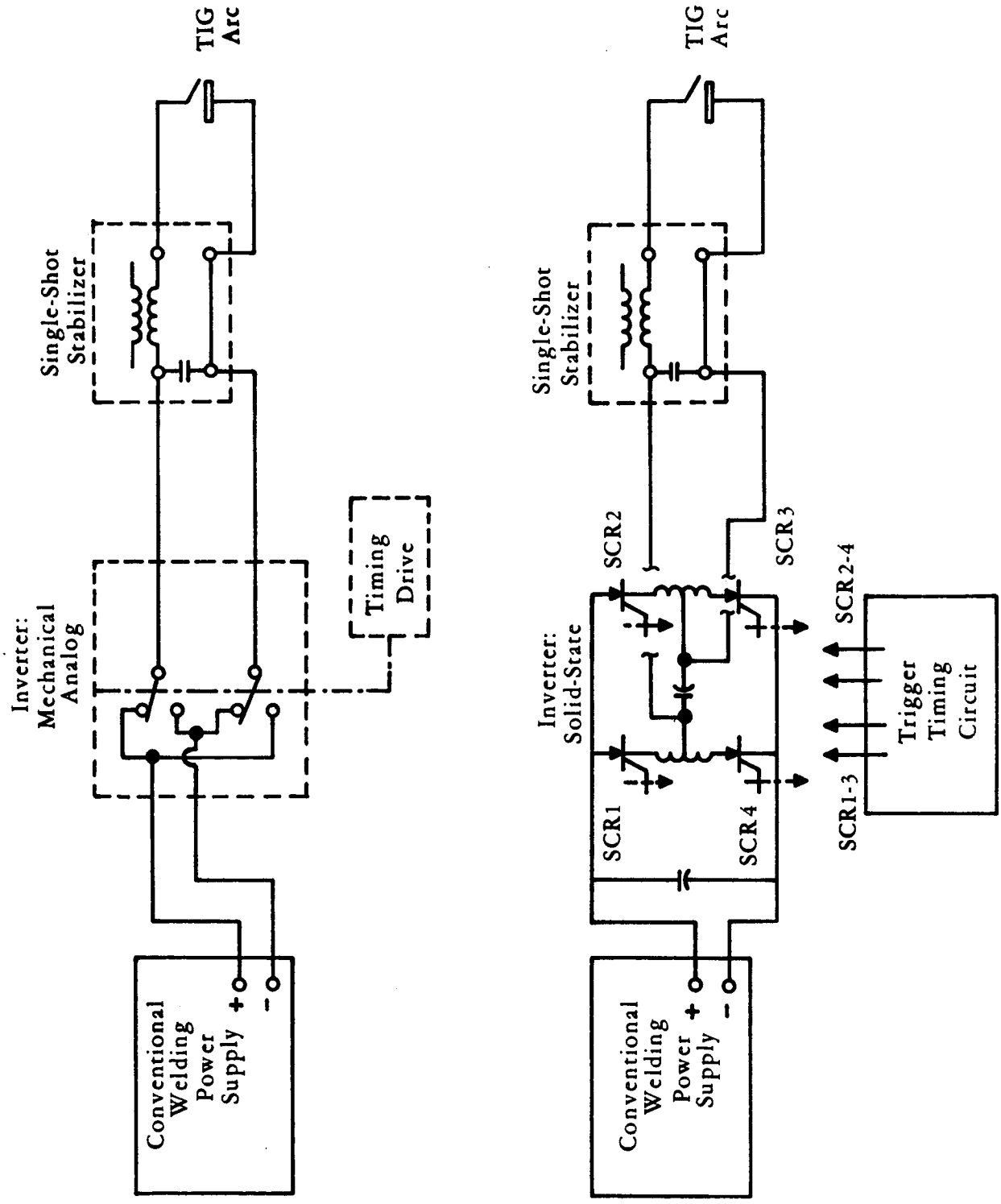

Fig. 1. COMPARISON of INVERTER and MECHANICAL COMMUTATOR

PRECEDING PAGE BLANK NOT FILMED.

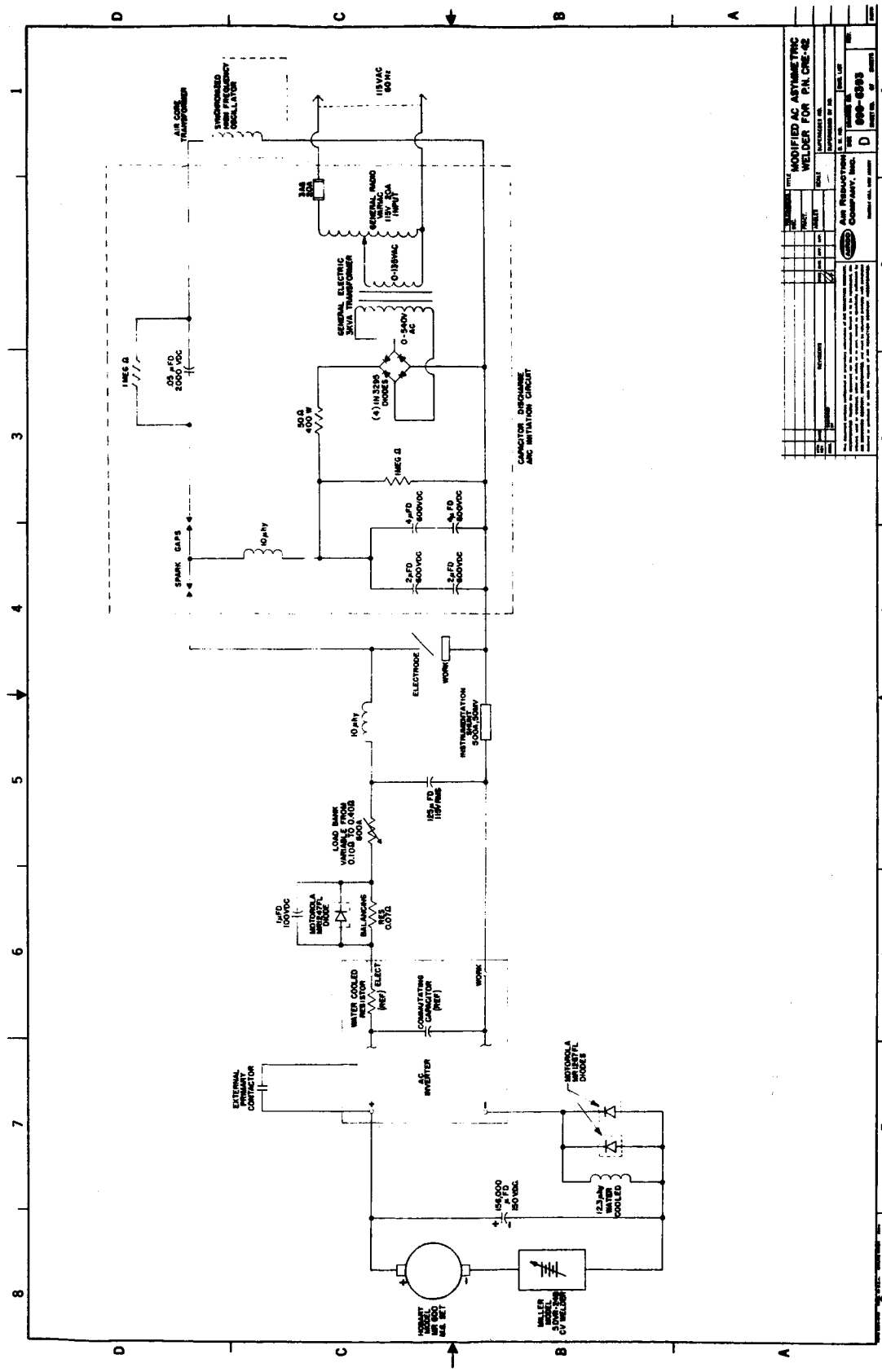

Fig. 2. MODIFIED CIRCUIT of INVERTER for WELDING on SCRAPED PLATE

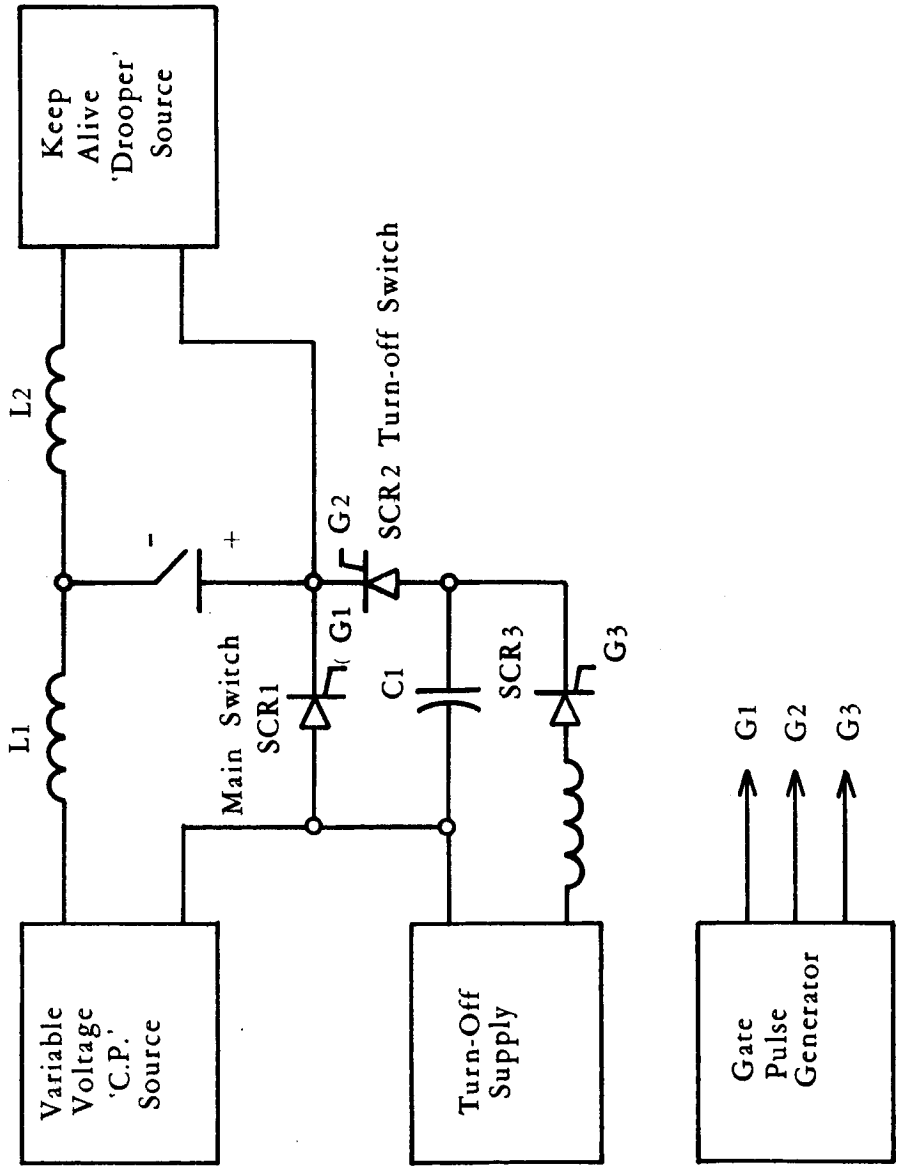

Fig. 3. PULSED POWER SUPPLY (Block Diagram)

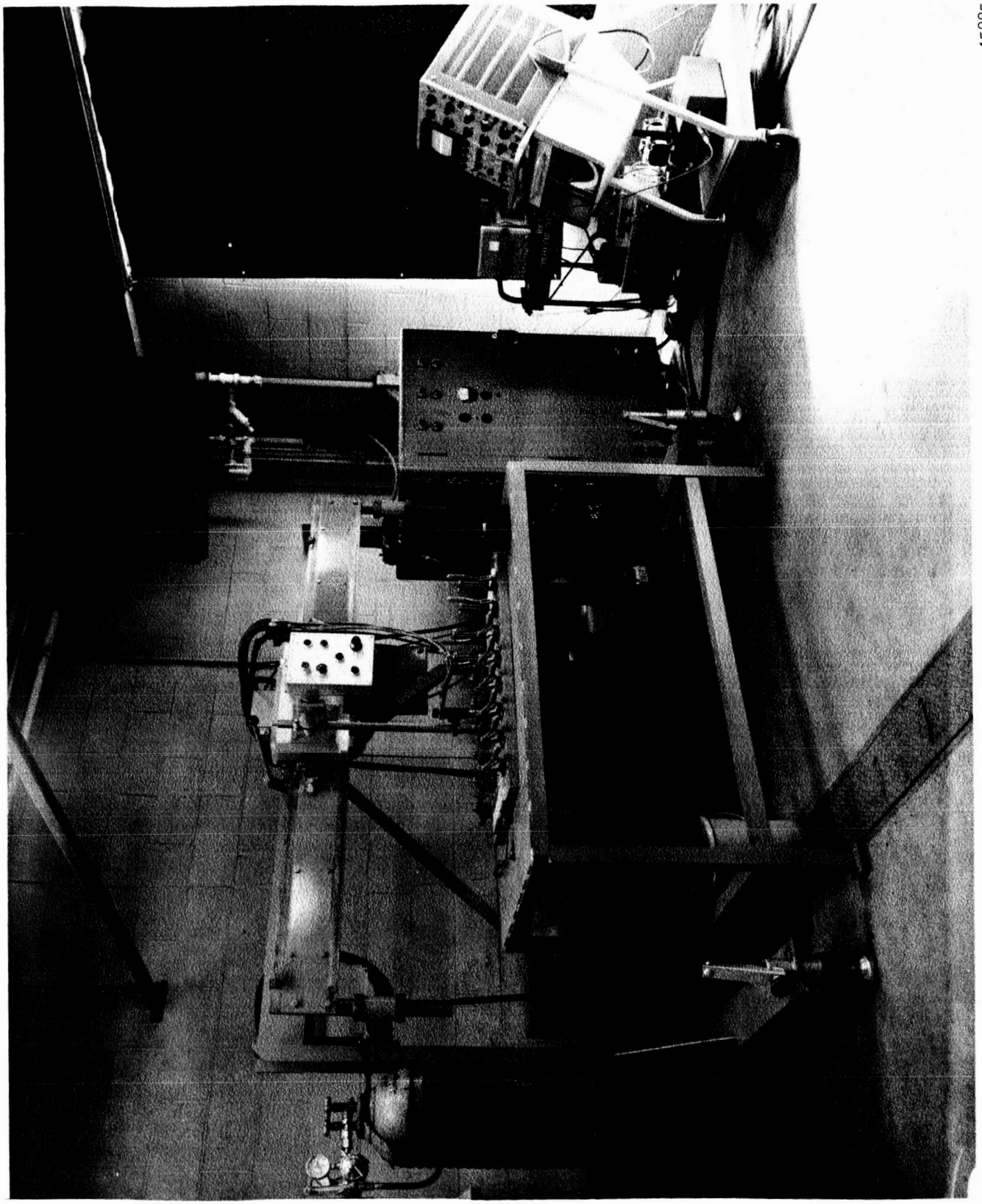

15885

Fig. 4. WELDING EQUIPMENT and INSTRUMENTATION

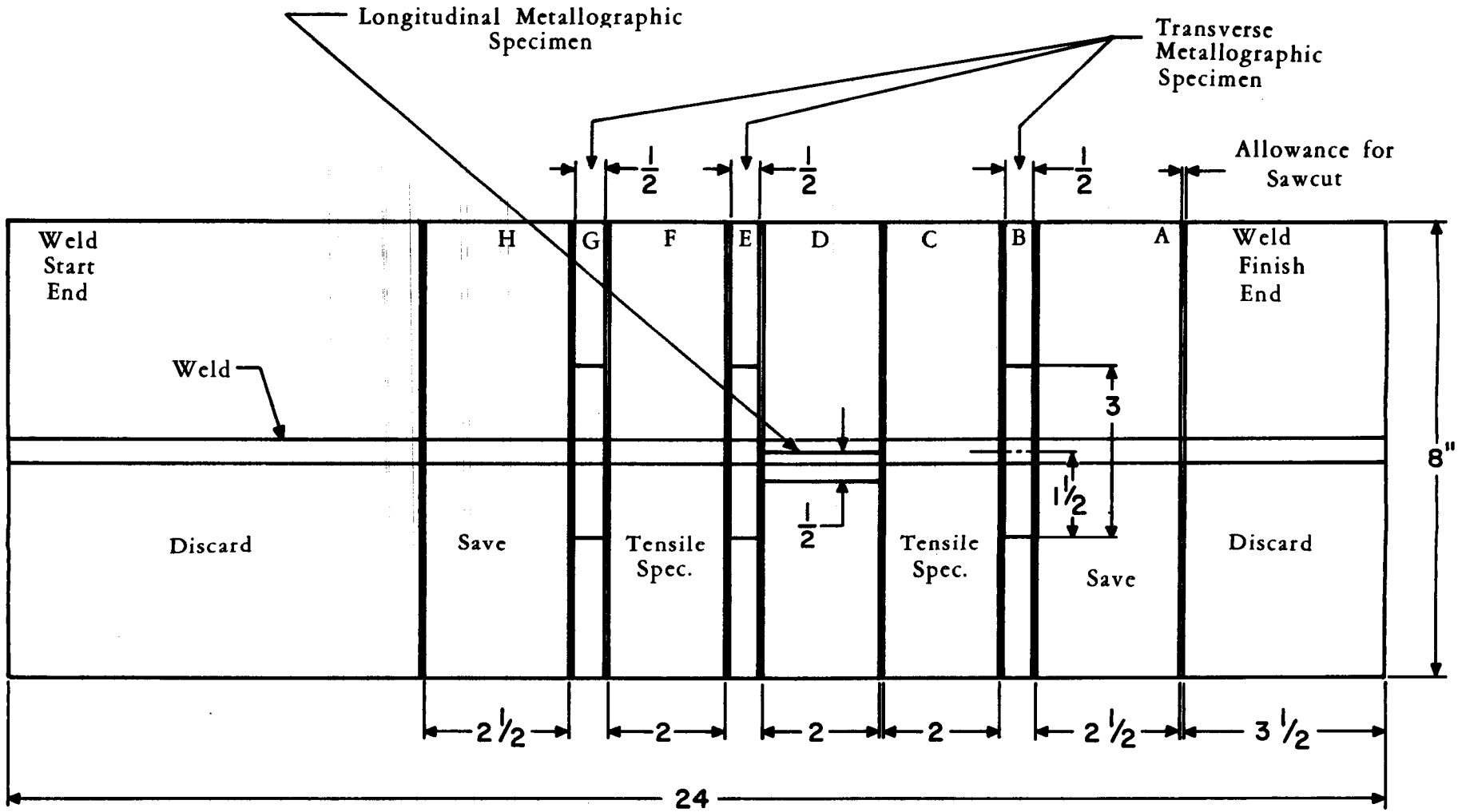

Fig. 5. LOCATION of TEST SPECIMENS in WELDED PLATE (all dimensions in inches)

Notes: 1) The longitudinal metallographic specimen should be machined such that the longitudinal section along the weld centerline is a plane surface suitable for metallographic examination.

2) Both transverse surfaces of each transverse metallographic specimen should be machined such that they are plane and suitable for metallographic examination.

PRECEDING PAGE BLANK NOT FILMED.

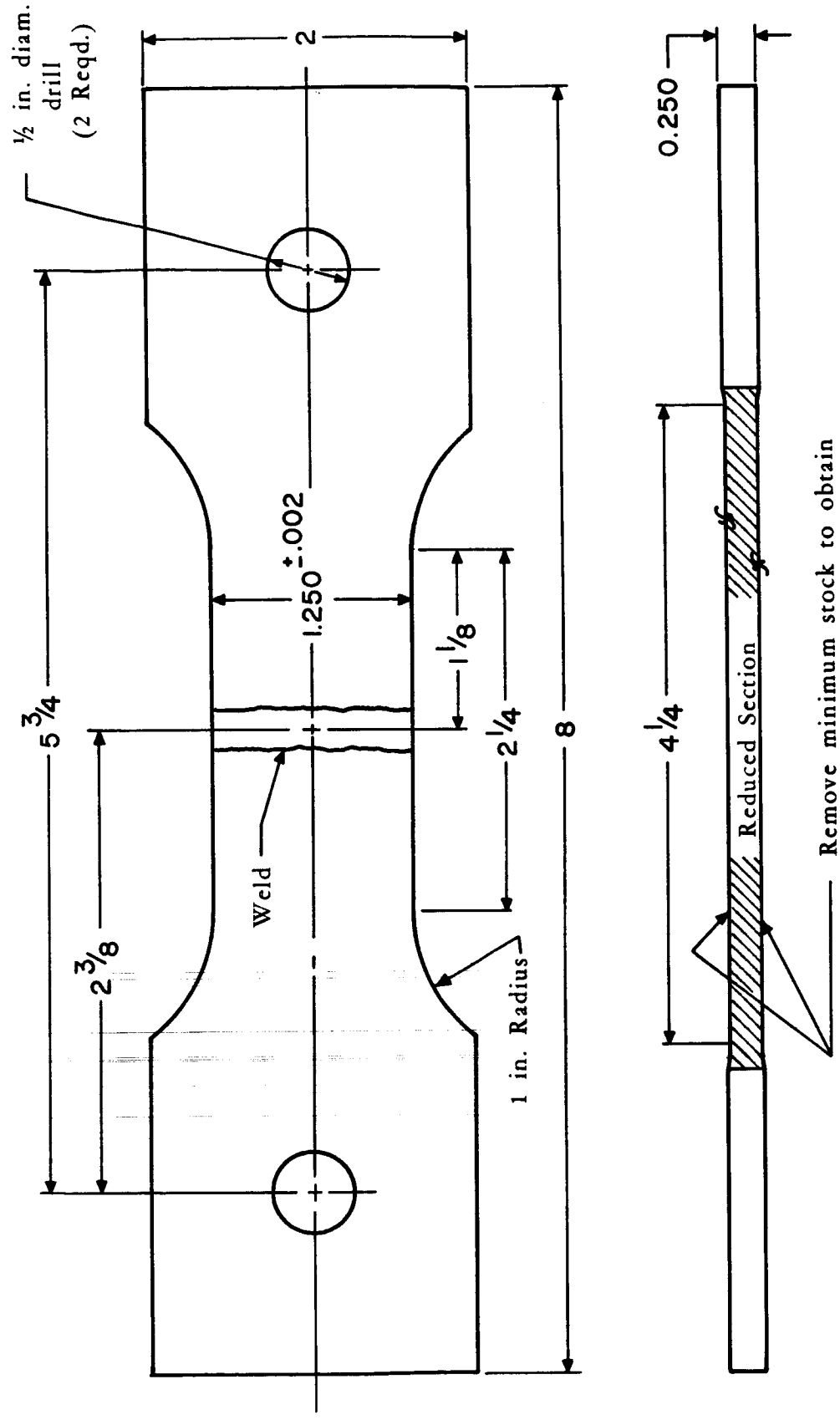

Fig. 6. TRANSVERSE TENSILE SPECIMEN (all dimensions in inches)

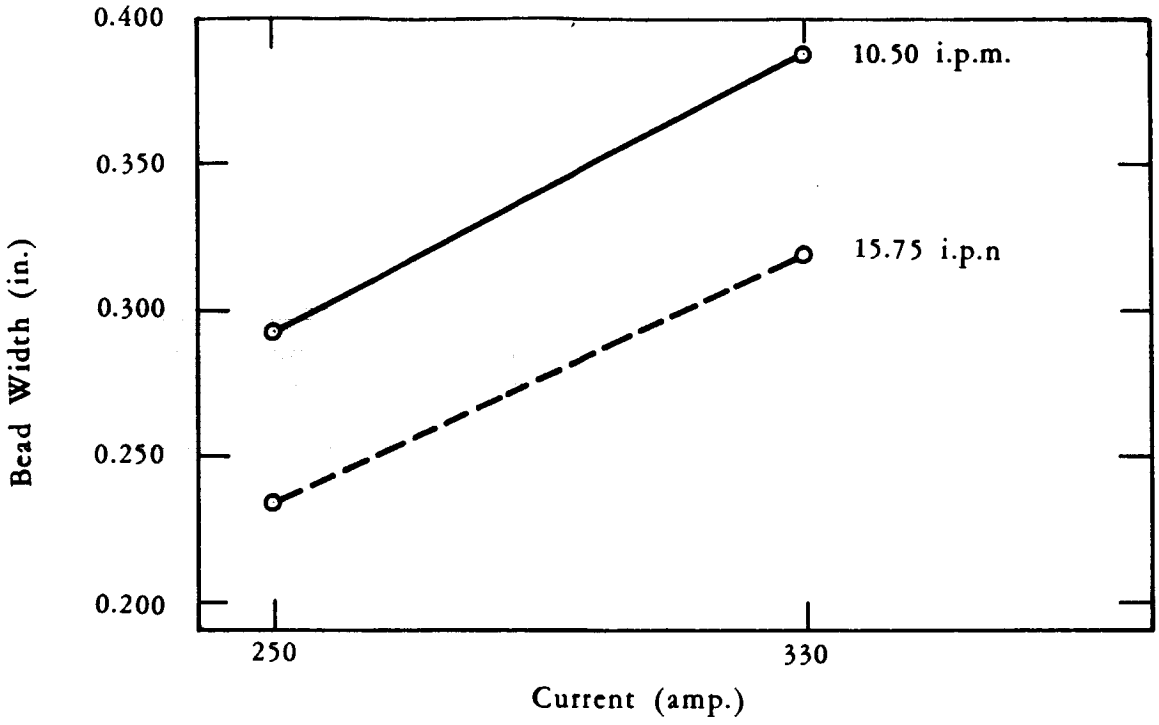

Fig. 7. EFFECT of CURRENT and SPEED on BEAD WIDTH of ASYMMETRIC A-C WELDS on EMISSIVE PLATE

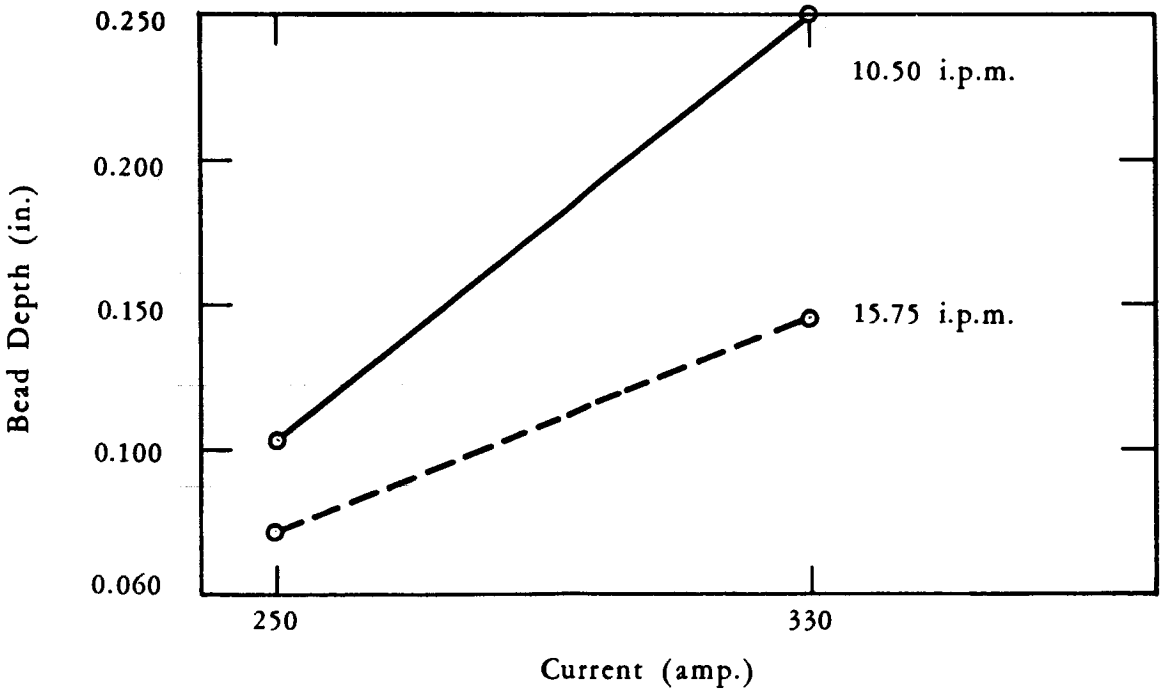

Fig. 8. EFFECT of CURRENT and SPEED on BEAD DEPTH of ASYMMETRIC A-C WELDS on EMISSIVE PLATE

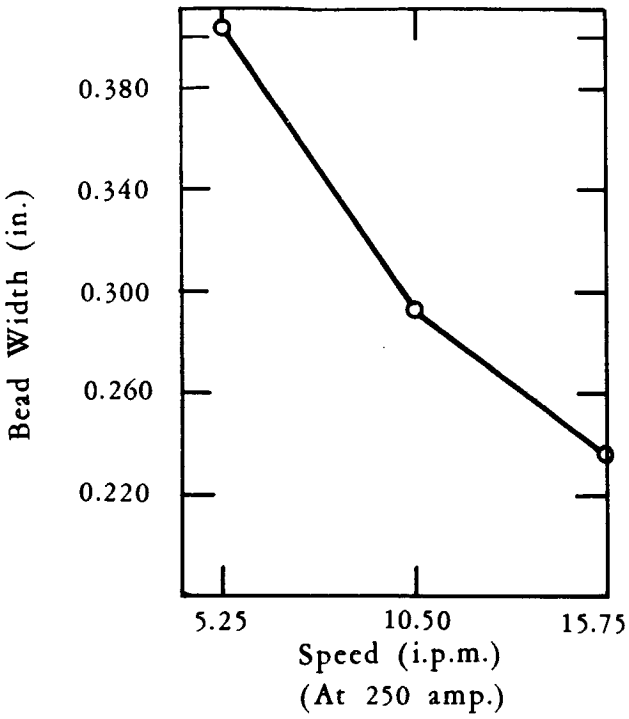

Fig. 9. EFFECT of SPEED on BEAD WIDTH (Asymmetric A-C, Emissive Plate)

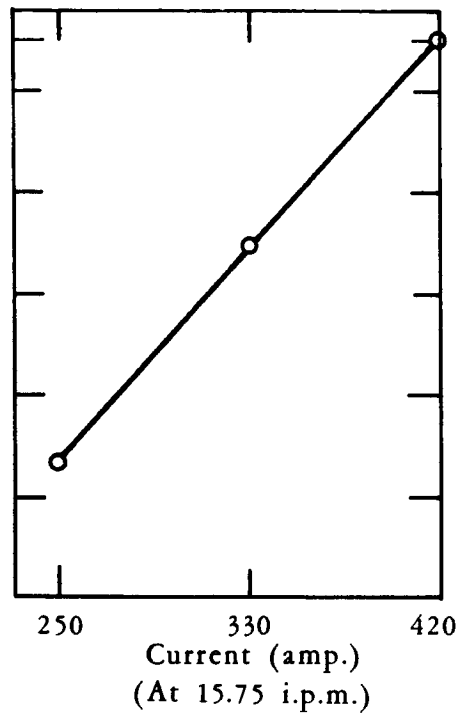

Fig. 10. EFFECT of CURRENT on BEAD WIDTH (Asymmetric A-C, Emissive Plate)

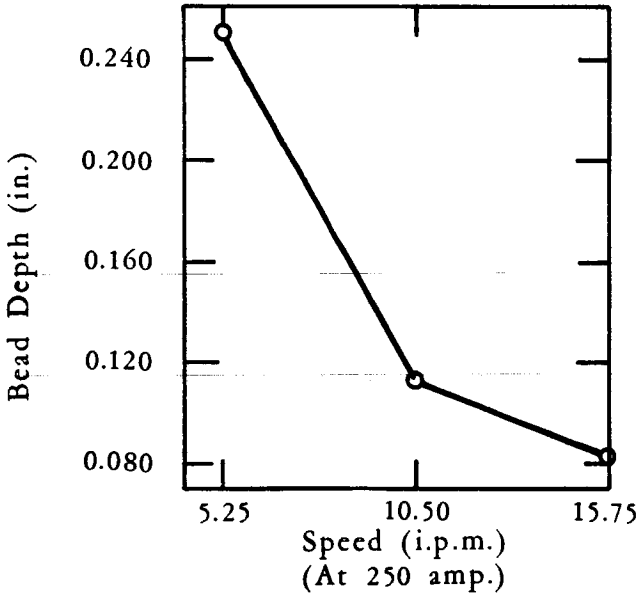

Fig. 11. EFFECT of SPEED on BEAD DEPTH (Asymmetric A-C, Emissive Plate)

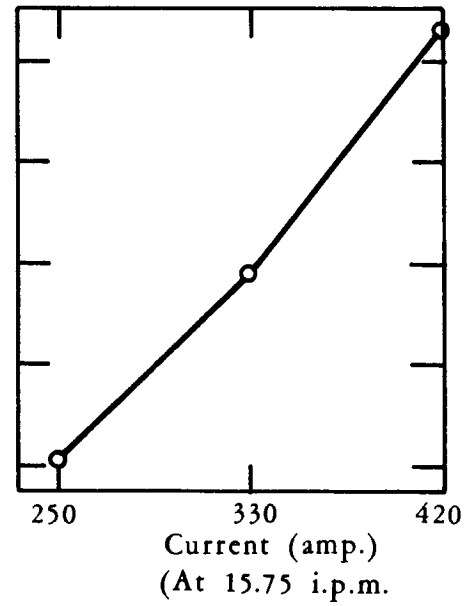

Fig. 12. EFFECT of CURRENT on BEAD DEPTH (Asymmetric A-C, Emissive Plate)

PRECEDING PAGE BLANK NOT FILMED.

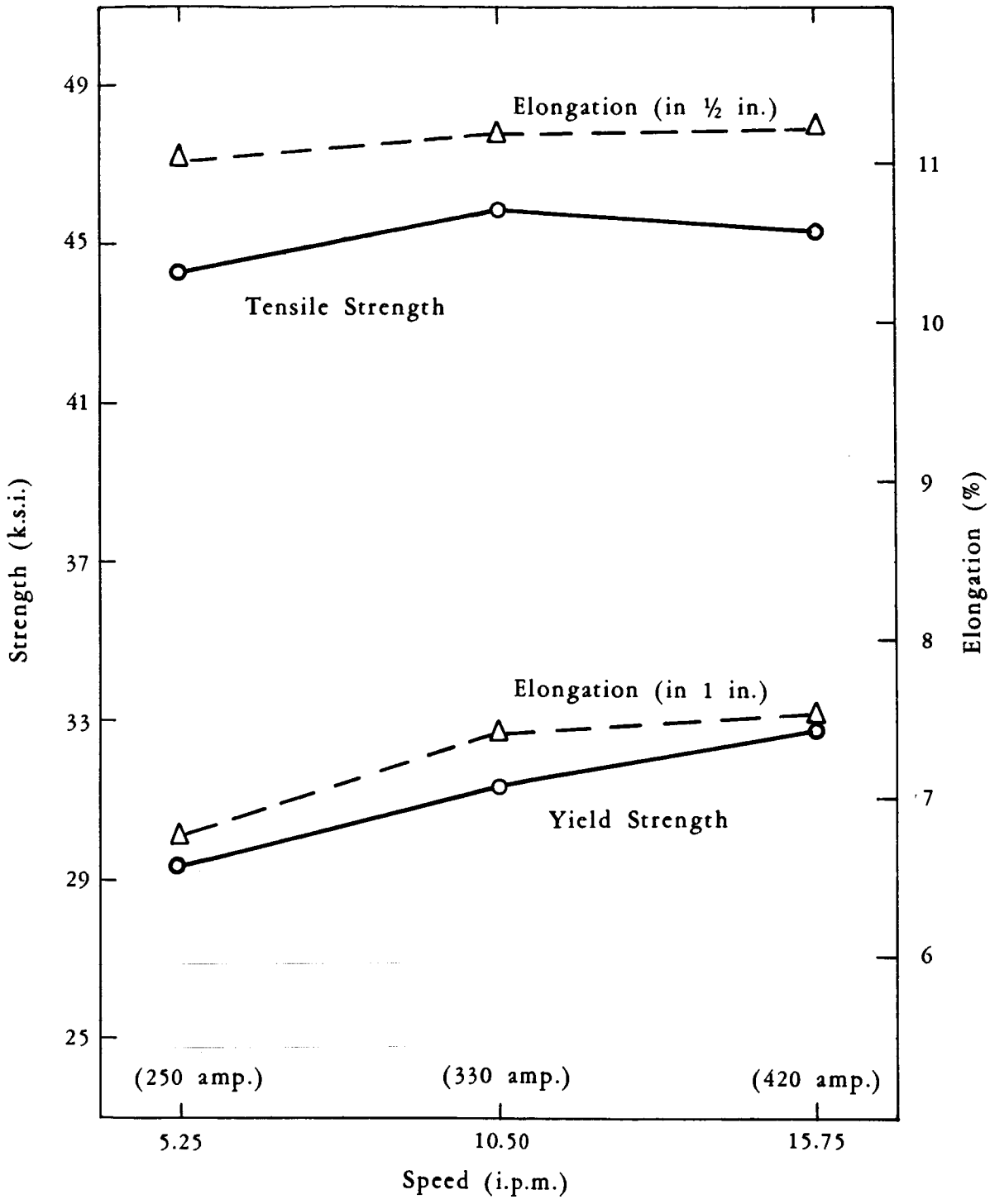

Fig. 13. EFFECT of SPEED on TENSILE PROPERTIES of ASYMMETRIC A-C WELDS (on emissive plate)

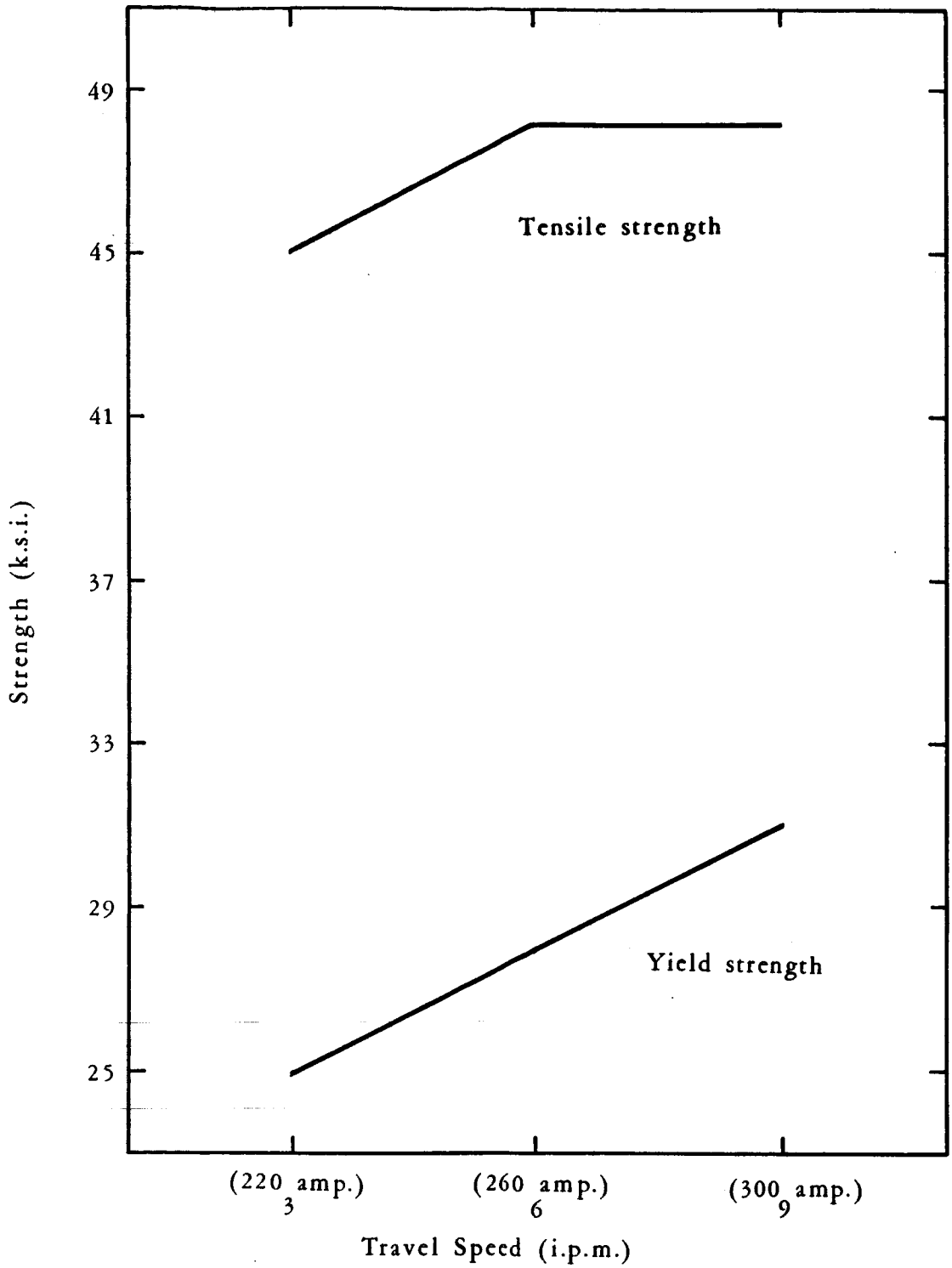

Fig. 14. EFFECT of SPEED on TENSILE PROPERTIES of ASYMMETRIC A-C WELDS (10% R.P.,60 c.p.s.) (on scraped plate)

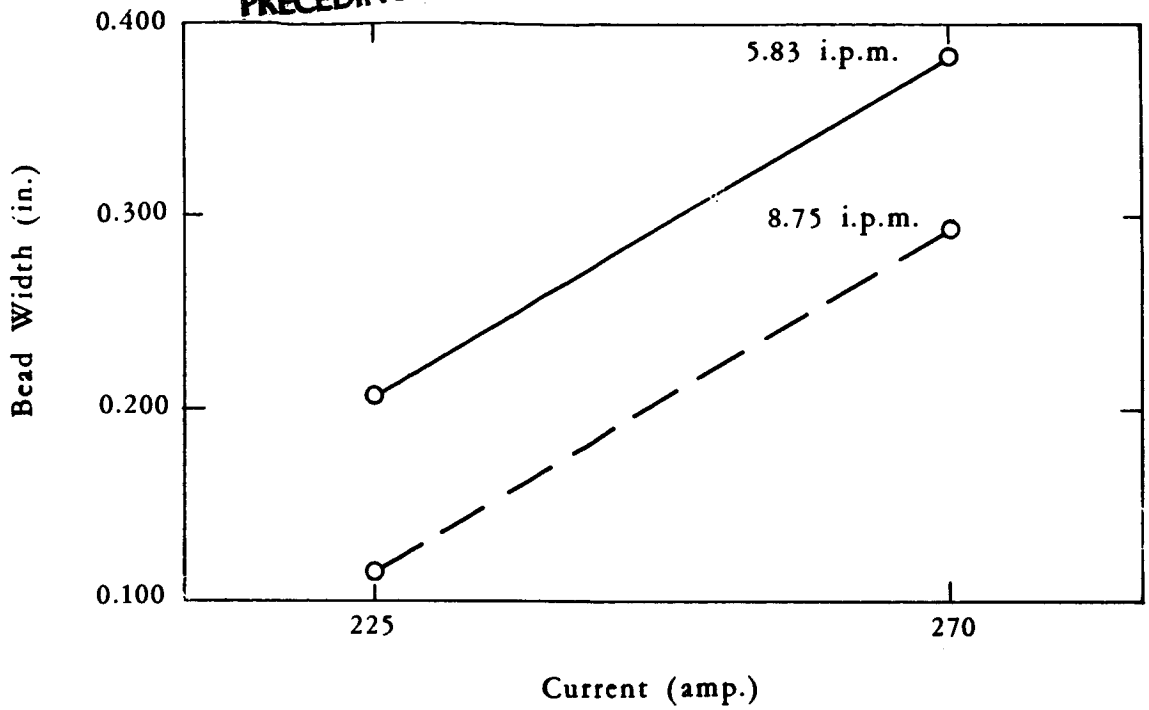

Fig. 15. EFFECT of CURRENT and SPEED on BEAD WIDTH of 300 c.p.s. A-C WELDS (on emissive plate)

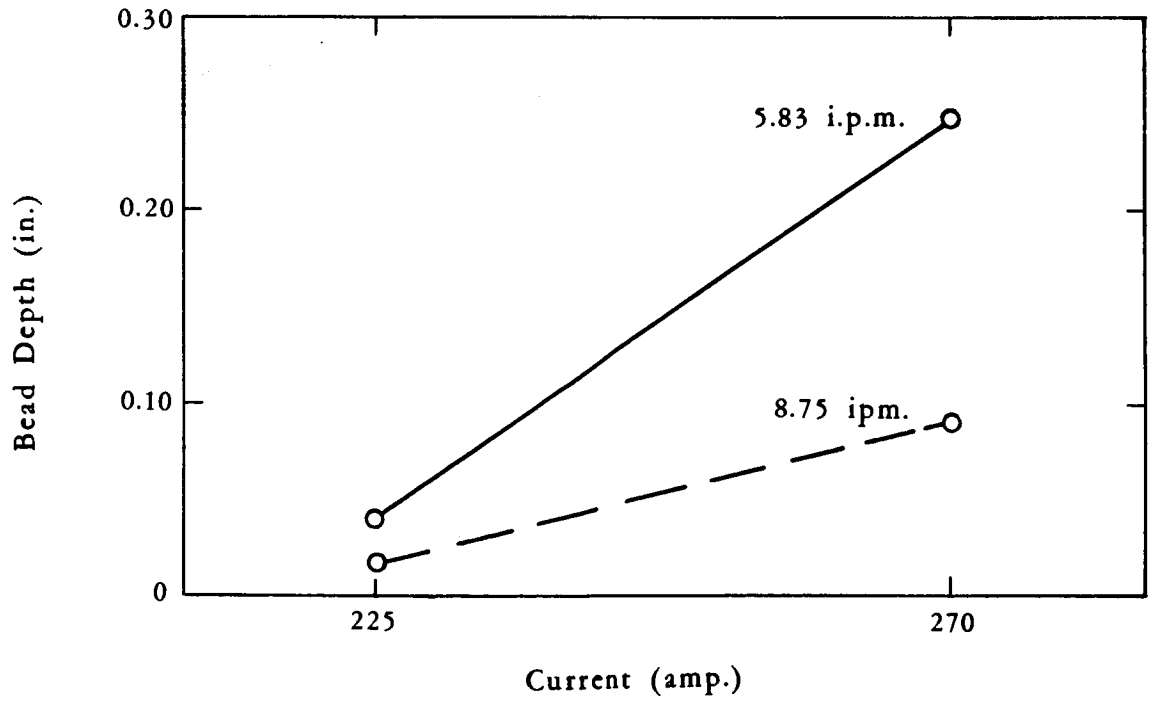

Fig. 16. EFFECT of CURRENT and SPEED on BEAD DEPTH of 300 c.p.s. A-C WELDS (on emissive plate)

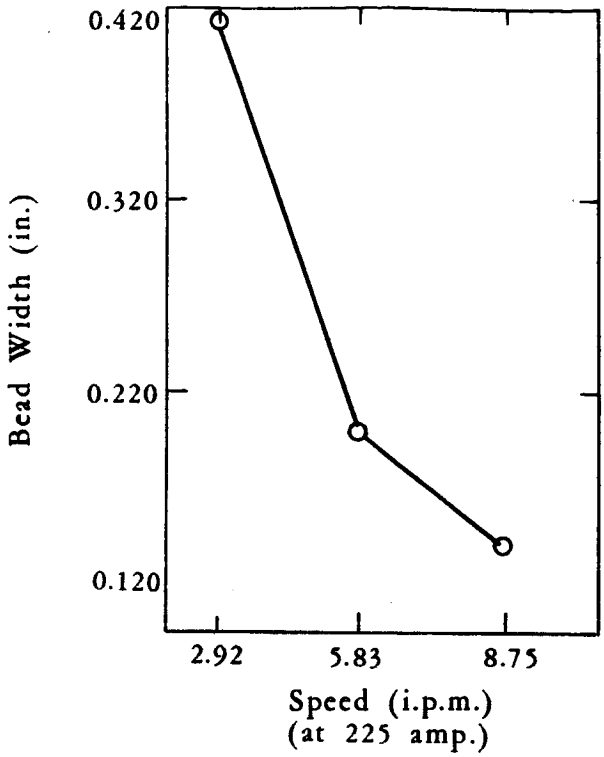

Fig. 17. EFFECT of SPEED on BEAD WIDTH of 300 c.p.s. A-C WELDS (emissive plate)

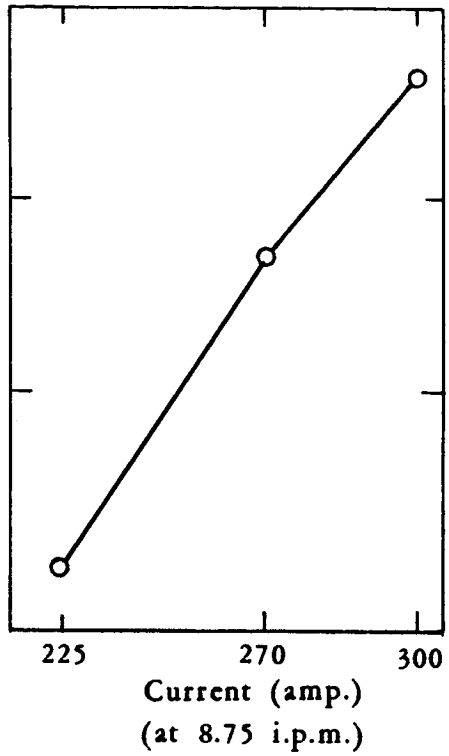

Fig. 18. EFFECT of CURRENT on BEAD WIDTH of 300 c.p.s. A-C WELDS (emissive plate)

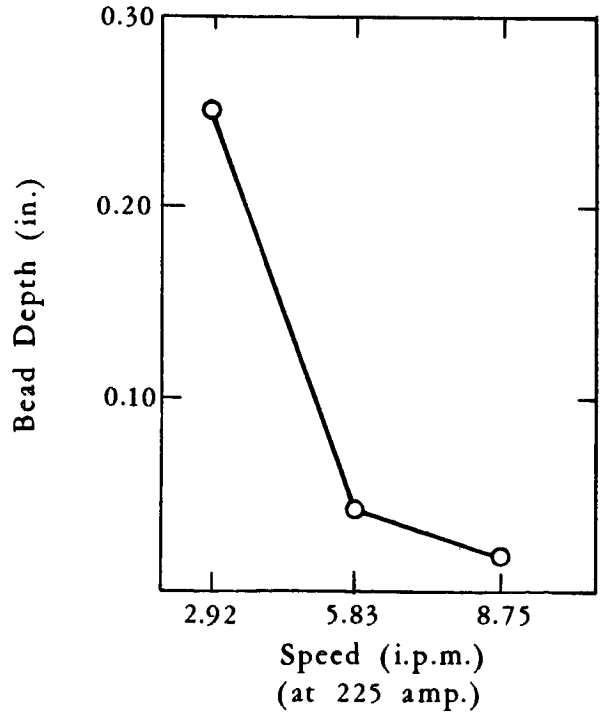

Fig. 19. EFFECT of SPEED on BEAD DEPTH of 300 c.p.s. A-C WELDS (emissive plate)

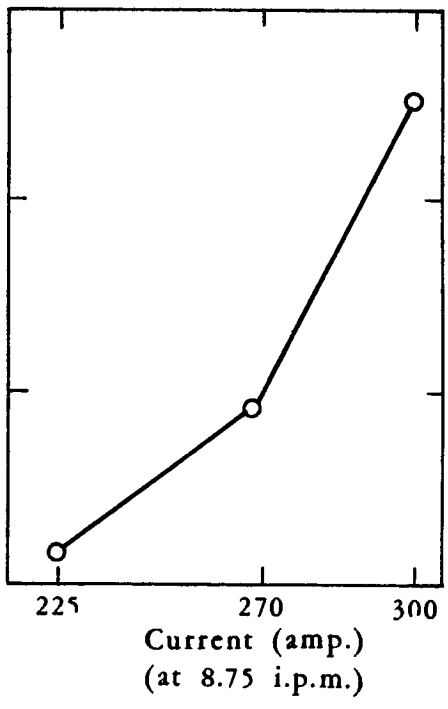

Fig. 20. EFFECT of CURRENT on BEAD DEPTH of 300 c.p.s. A-C WELDS (emissive plate)

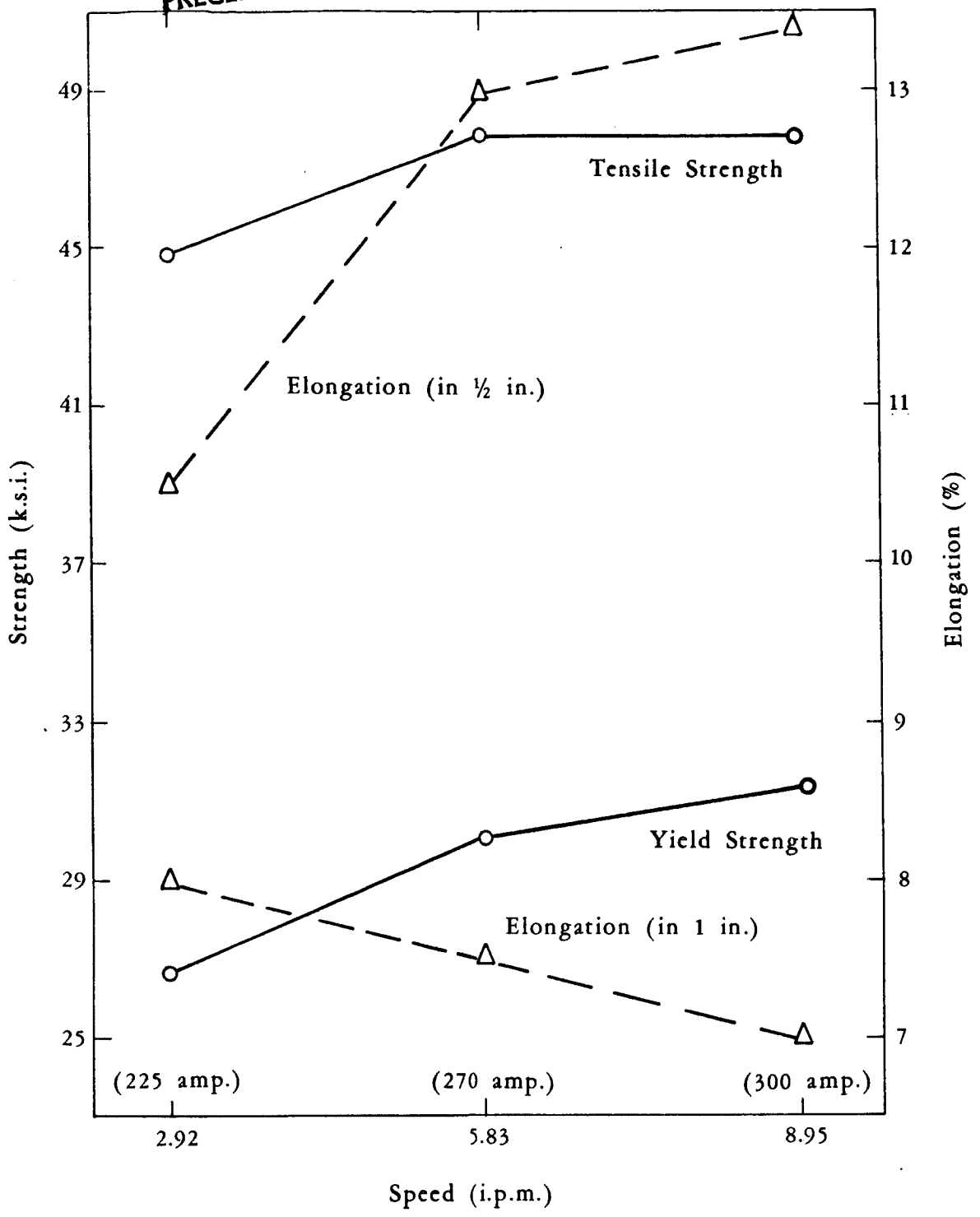

Fig. 21. EFFECT of SPEED on TENSILE PROPERTIES of 300 c.p.s. A-C WELDS (emissive plate)

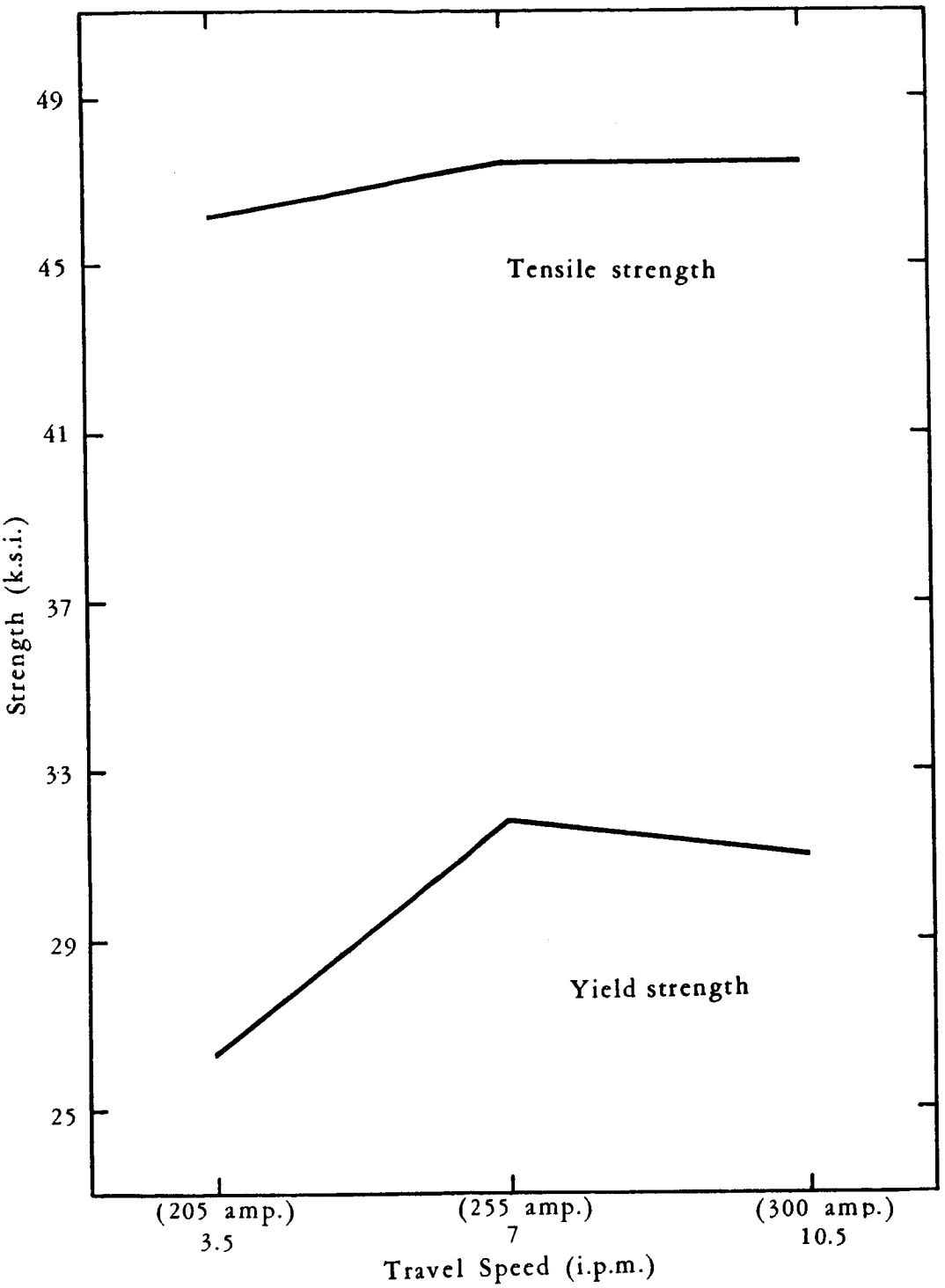

Fig. 22. EFFECT of SPEED on TENSILE PROPERTIES of 200 c.p.s. A-C WELDS (scraped plate)

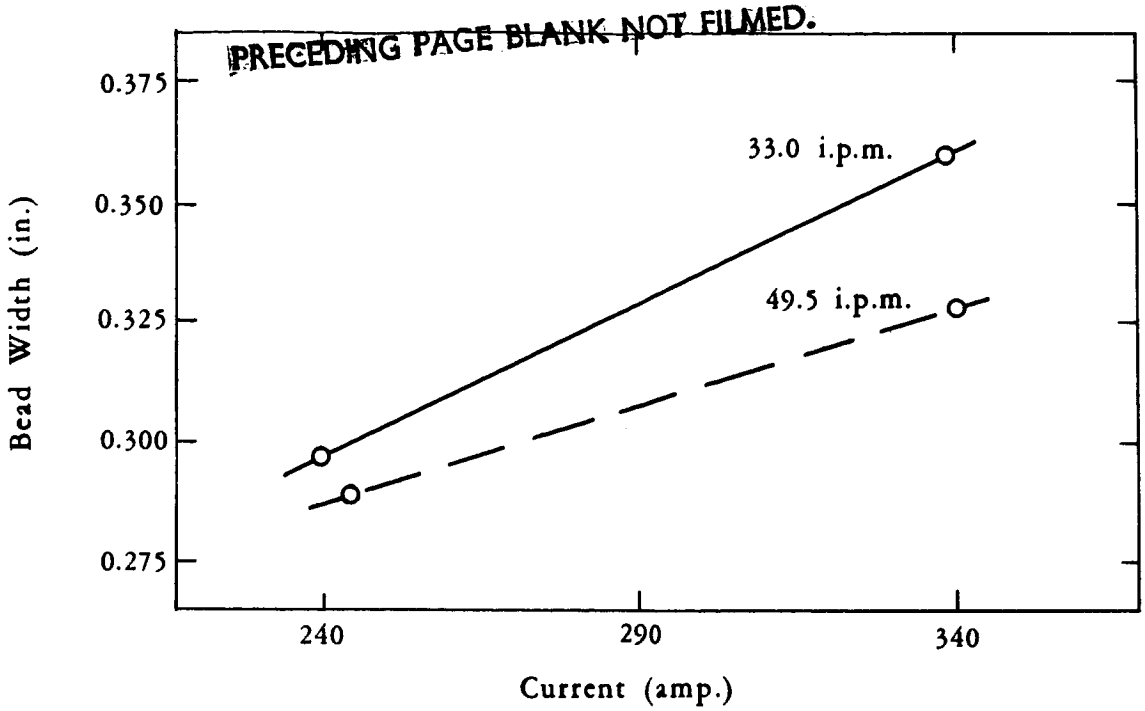

Fig. 23. EFFECT of CURRENT and SPEED on BEAD WIDTH of PULSED D-C WELDS (Phase I)

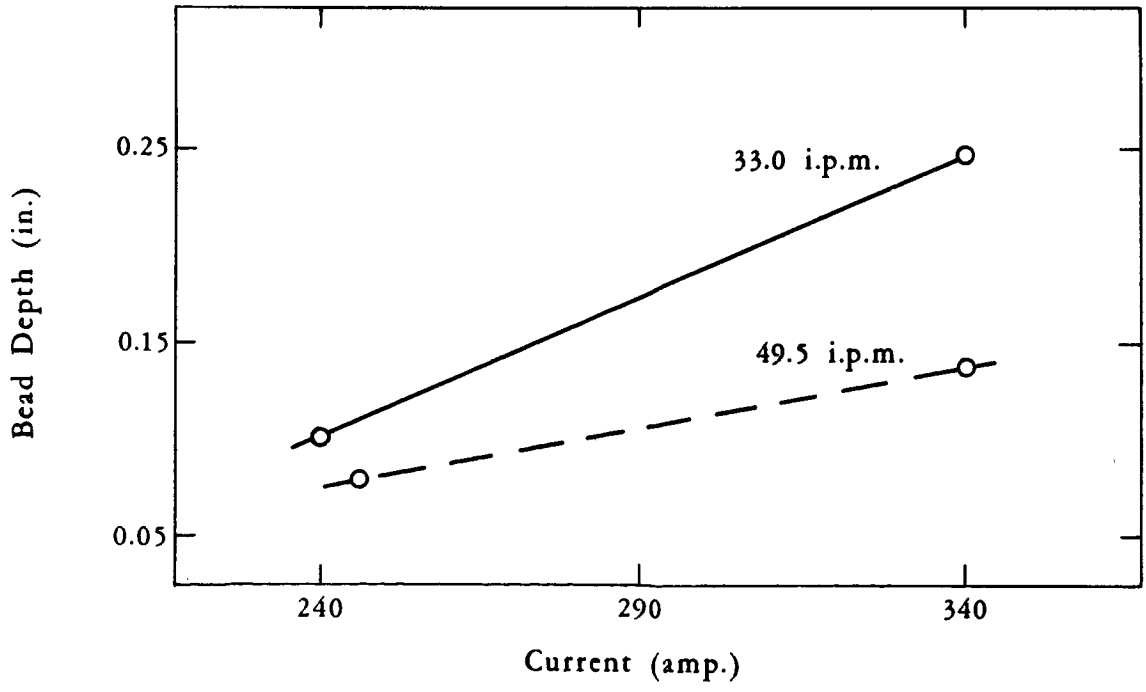

Fig. 24. EFFECT of CURRENT and SPEED on BEAD DEPTH of PULSED D-C WELDS (Phase I)

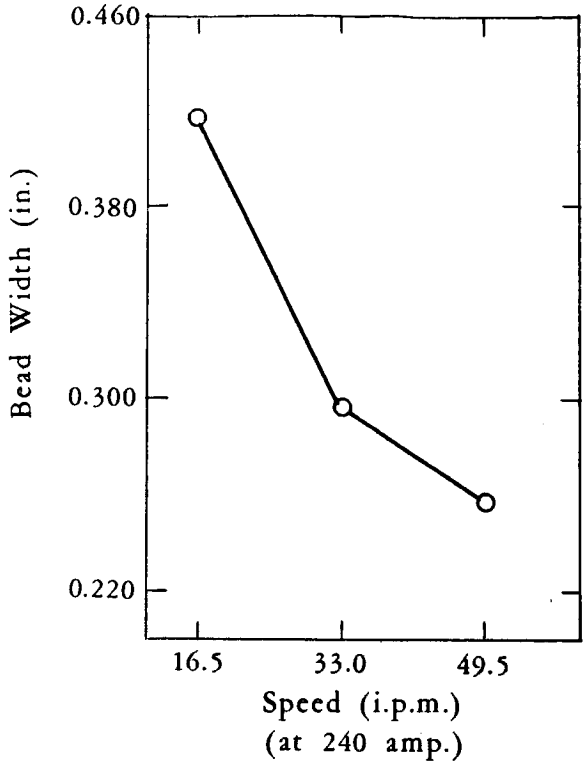

Fig. 25. EFFECT of SPEED on BEAD WIDTH of PULSED D-C WELDS (Phase I)

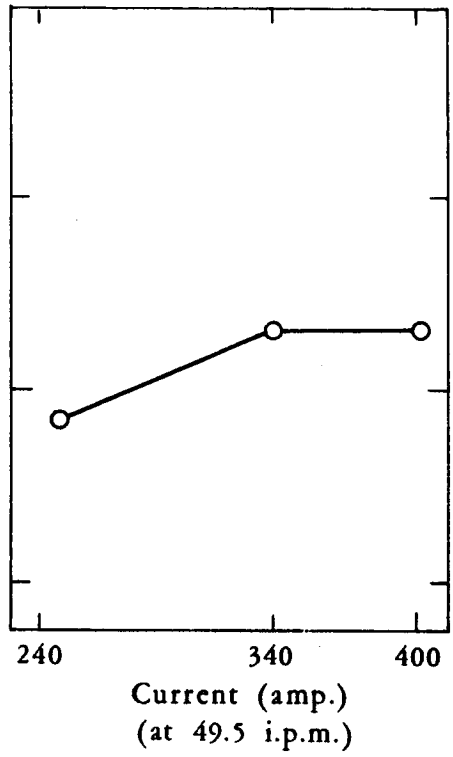

Fig. 26. EFFECT of CURRENT on BEAD WIDTH of PULSED D-C WELDS (Phase I)

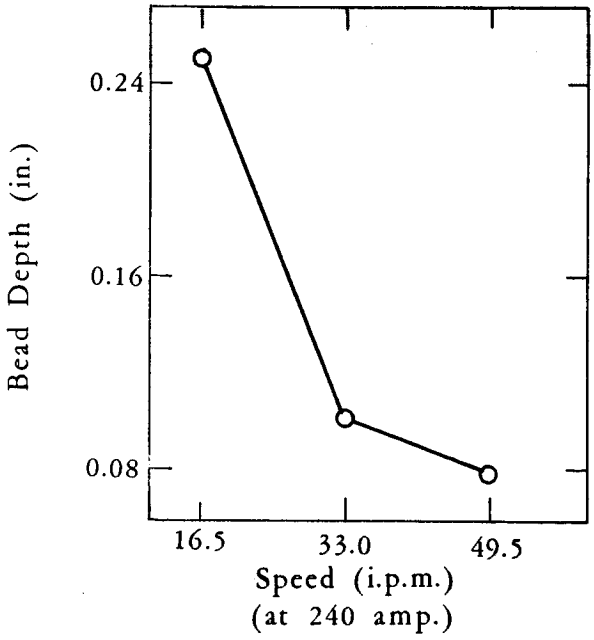

Fig. 27. EFFECT of SPEED on BEAD DEPTH of PULSED D-C WELDS (Phase I)

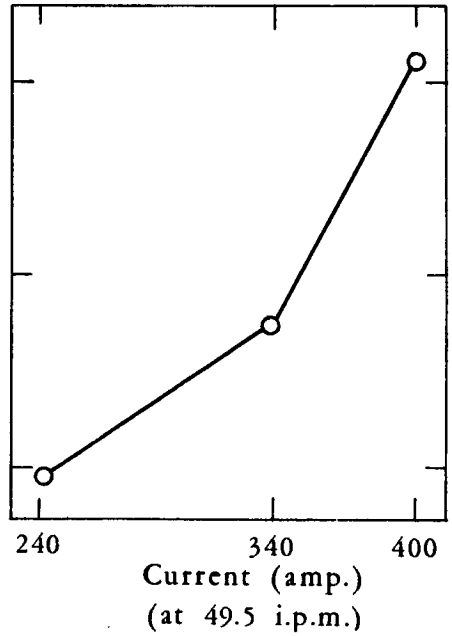

Fig. 28. EFFECT of CURRENT on BEAD DEPTH of PULSED D-C WELDS (Phase I)

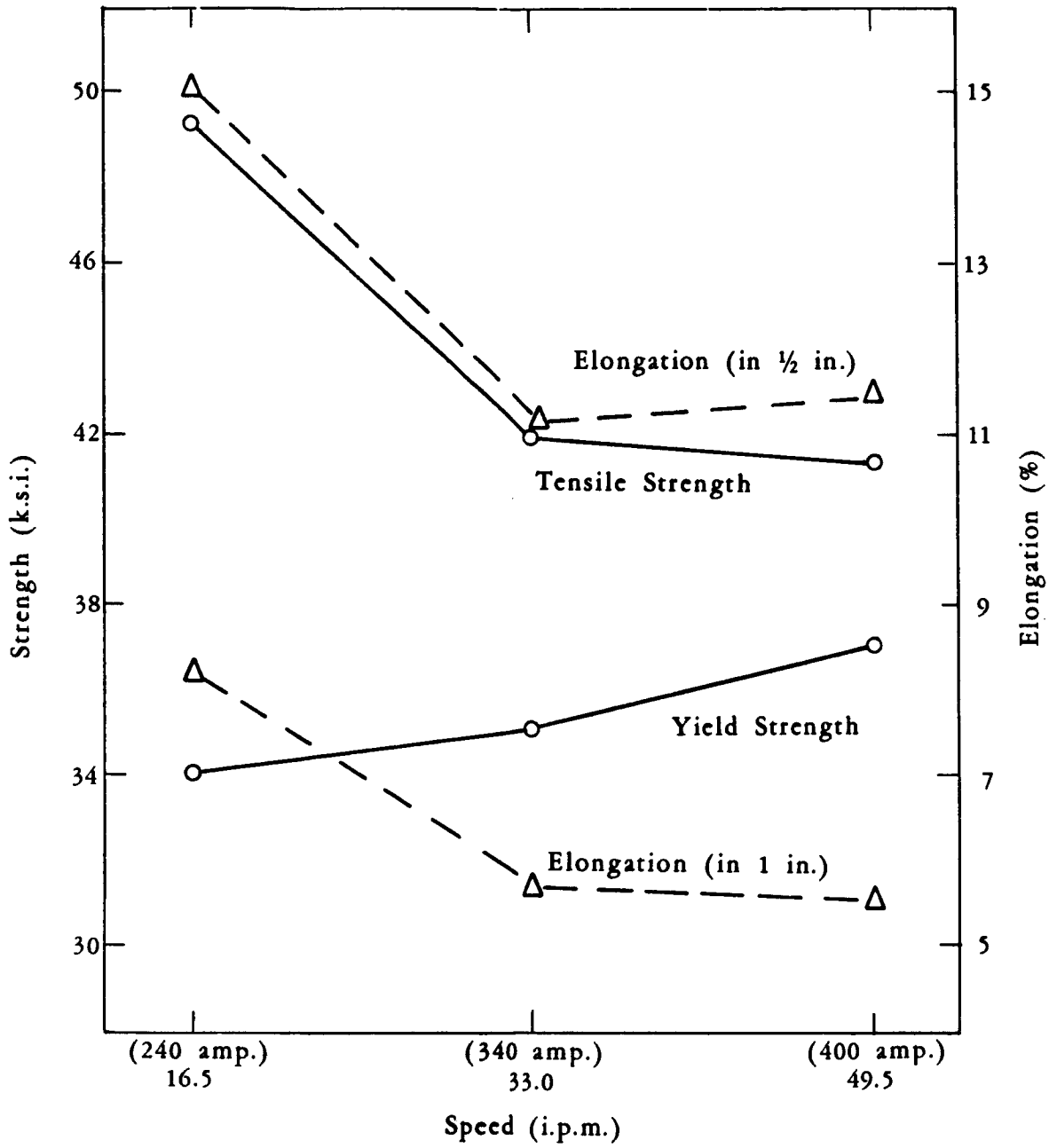

Fig. 29. EFFECT of SPEED on TENSILE PROPERTIES of PULSED D-C WELDS (First set of data, Phase I)

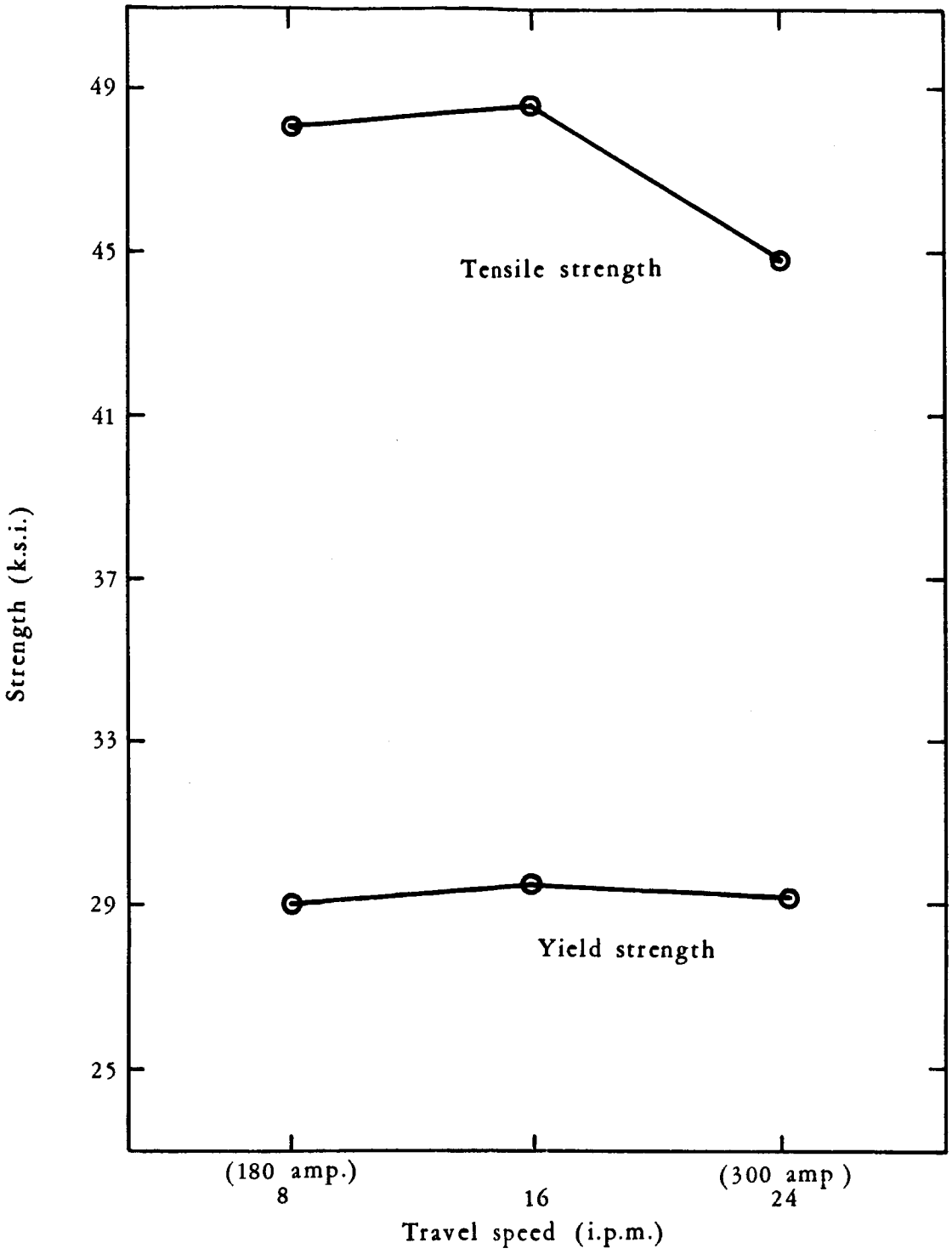

Fig. 30. EFFECT of SPEED on TENSILE PROPERTIES of PULSED D-C WELDS (Second set, Phase I)

M5651

300 amp. 24 i.p.m. 43,600 p.s.i. tensile strength

M5650

240 amp. 16 i.p.m. 47,600 p.s.i. tensile strength

Fig. 31. PHOTOMICROGRAPHS of 'STRONG' and 'WEAK' WELDS MADE with PULSED DIRECT CURRENT

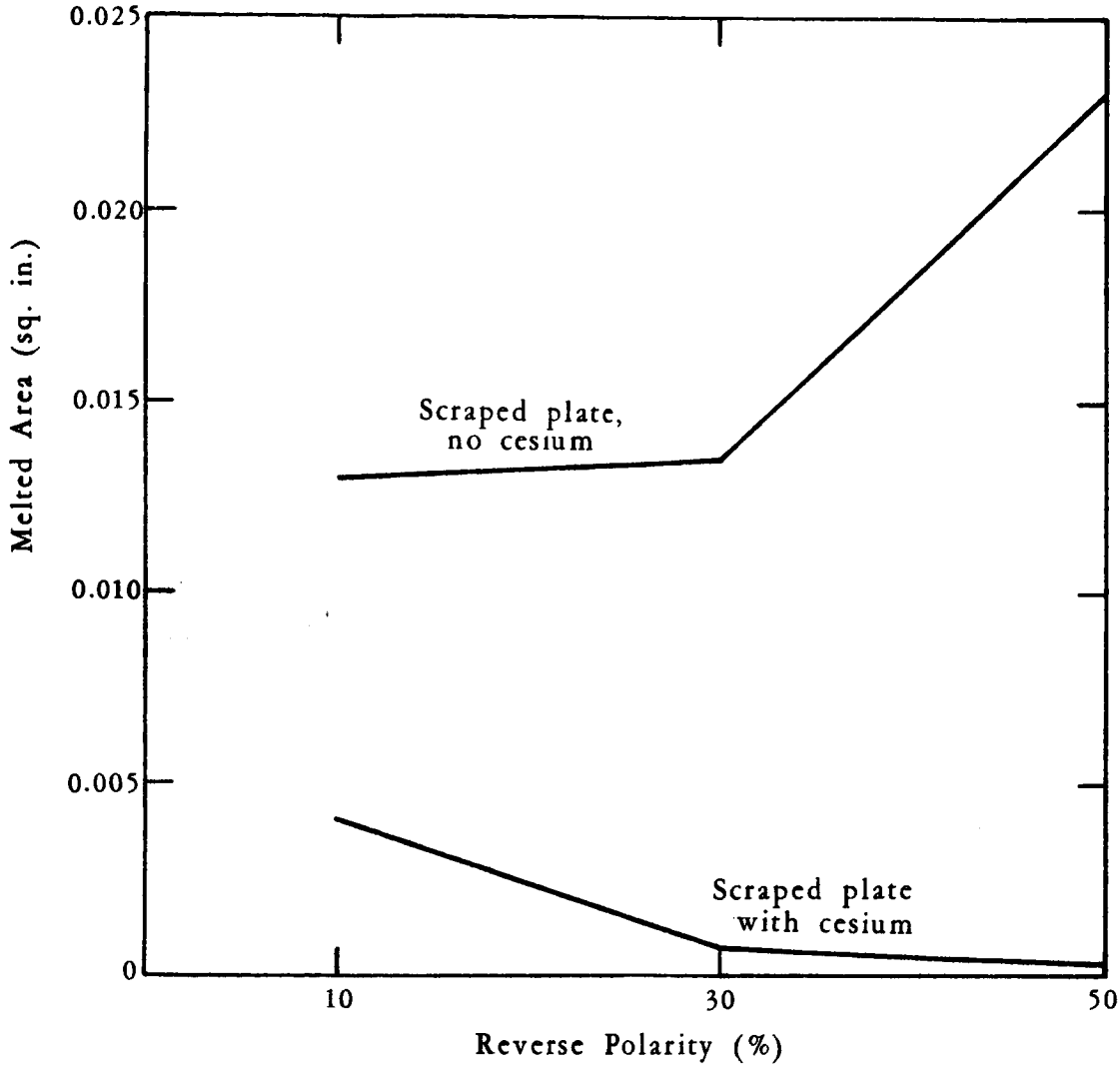

Fig. 32. THE STRONG INFLUENCE of CESIUM in CHANGING the EFFECT of R.P. % on MELTED AREA of WELD CROSS-SECTION (All welds at 250 amp. 5 i.p.m.)

PRECEDING PAGE BLANK NOT FILMED.

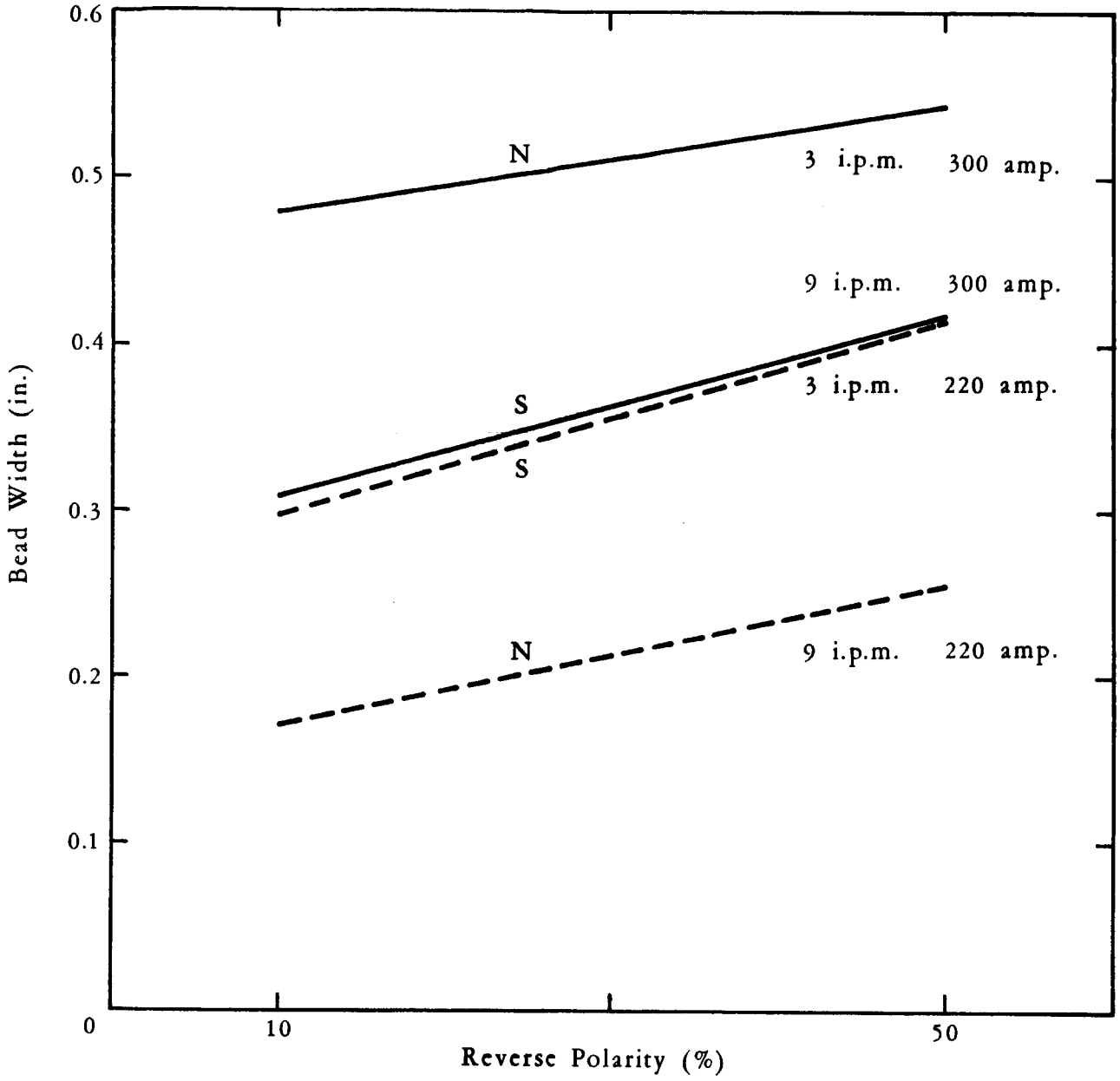

Fig. 33. EFFECT of REVERSE POLARITY PERCENTAGE on WIDTH of ASYMMETRIC A-C WELDS, PHASE IIA

PRECEDING PAGE BLANK NOT FILMED.

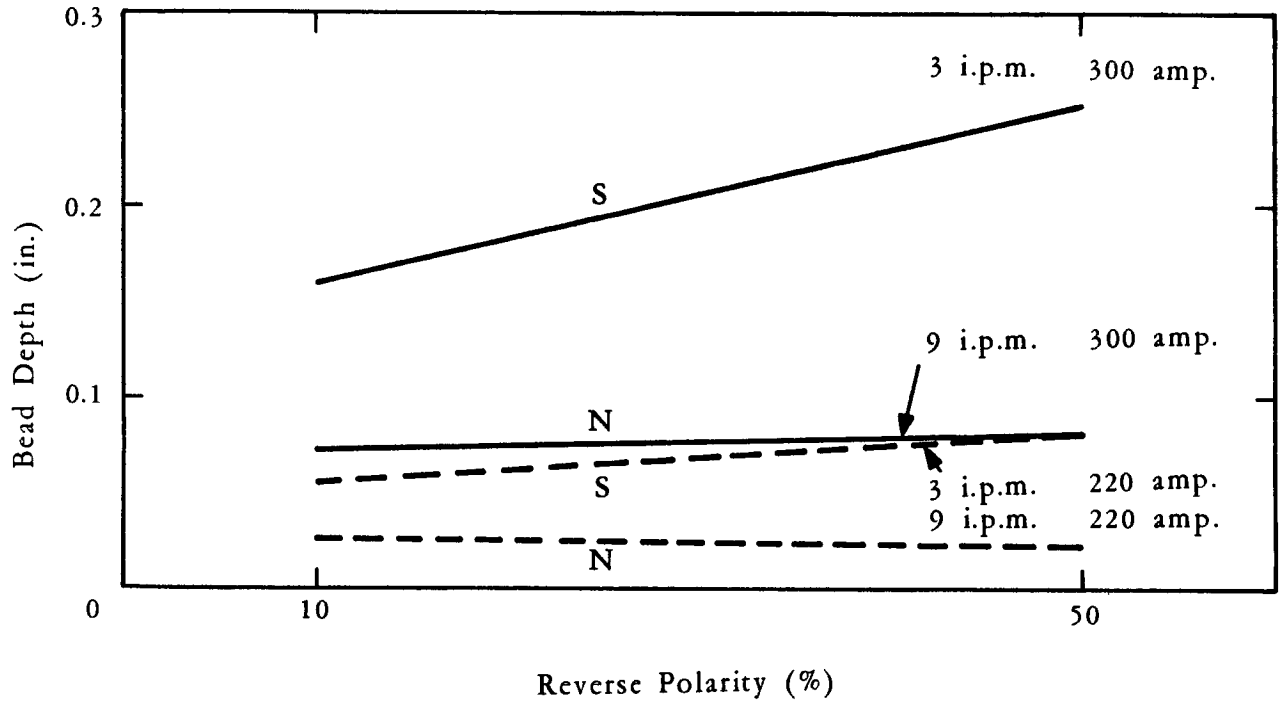

Fig. 34. EFFECT of REVERSE POLARITY PERCENTAGE on DEPTH of ASYMMETRIC A-C WELDS, PHASE IIA

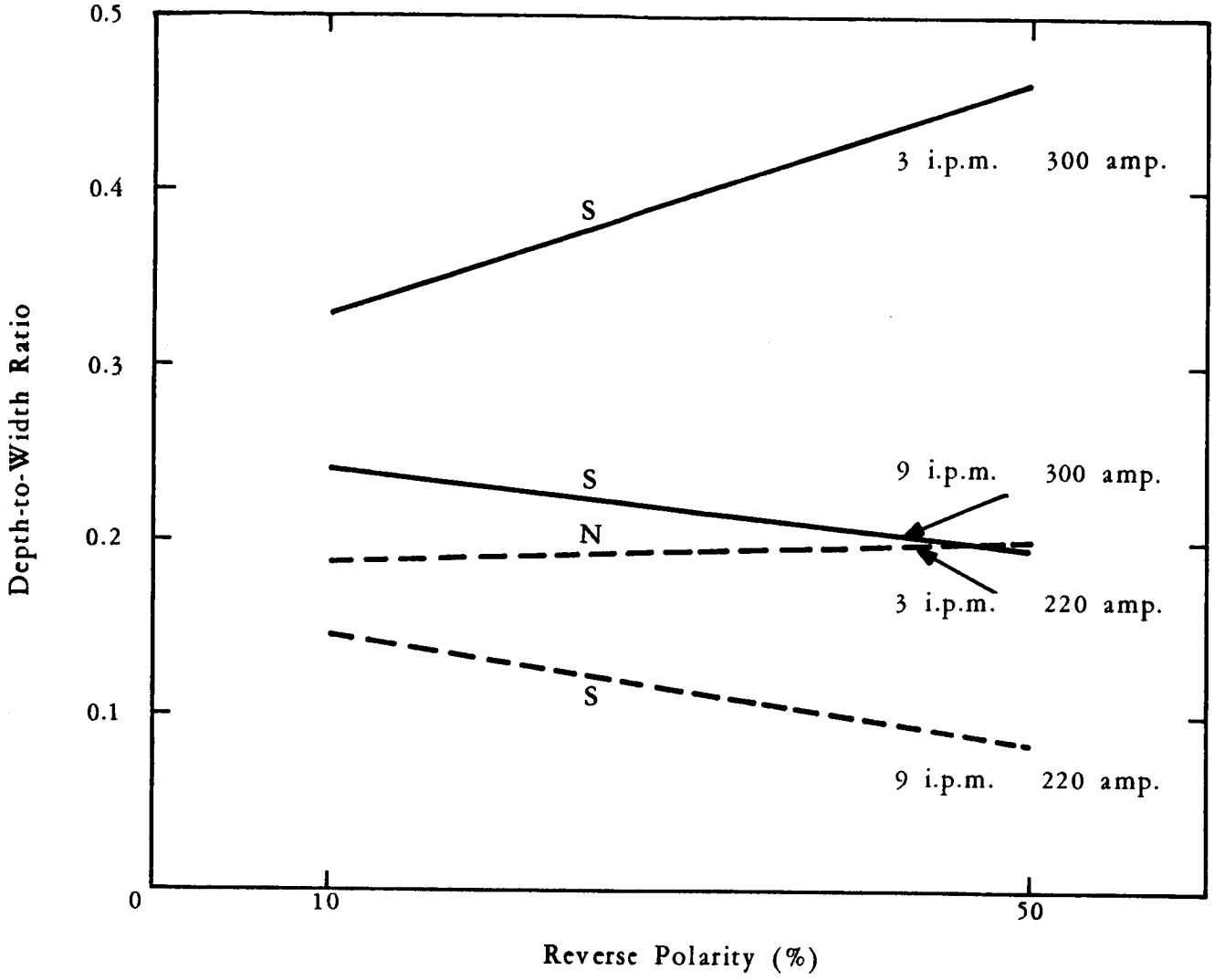

Fig. 35. EFFECT of REVERSE POLARITY PERCENTAGE on DEPTH-WIDTH RATIO of ASYMMETRIC A-C WELDS PHASE IIA

PRECEDING PAGE BLANK NOT FILMED.

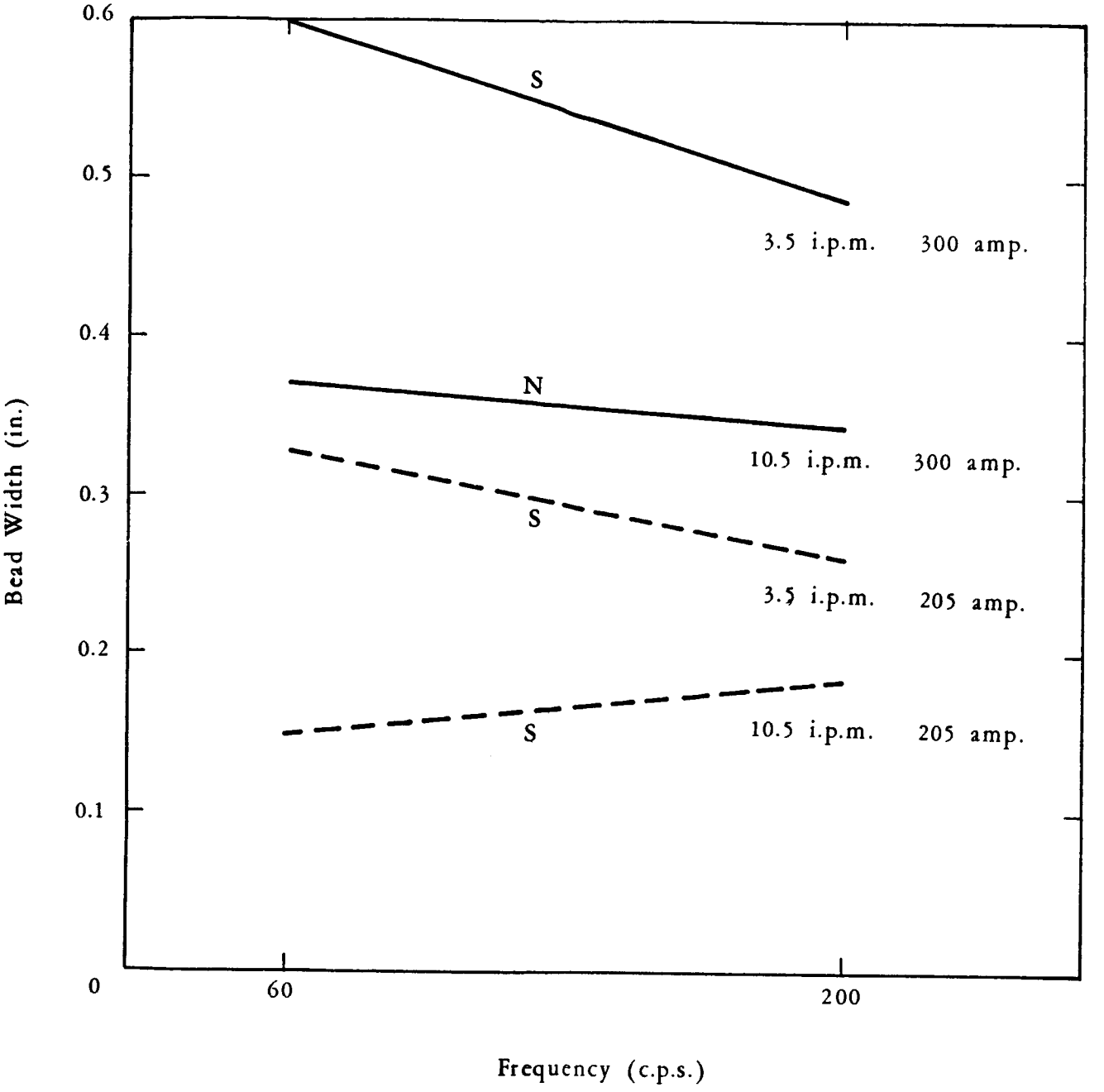

Fig. 36. EFFECT of FREQUENCY on WIDTH of VARIABLE FREQUENCY A-C WELDS, PHASE IIA

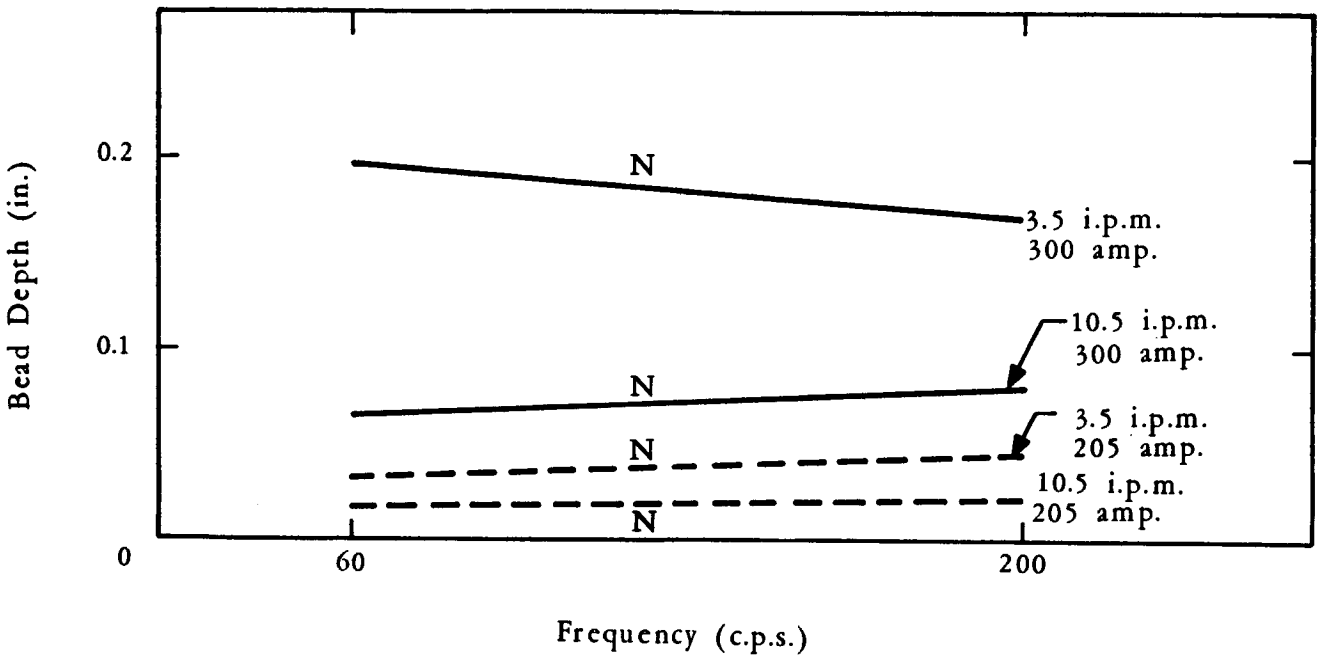

Fig. 37. EFFECT of FREQUENCY on DEPTH of VARIABLE FREQUENCY A-C WELDS, PHASE IIA

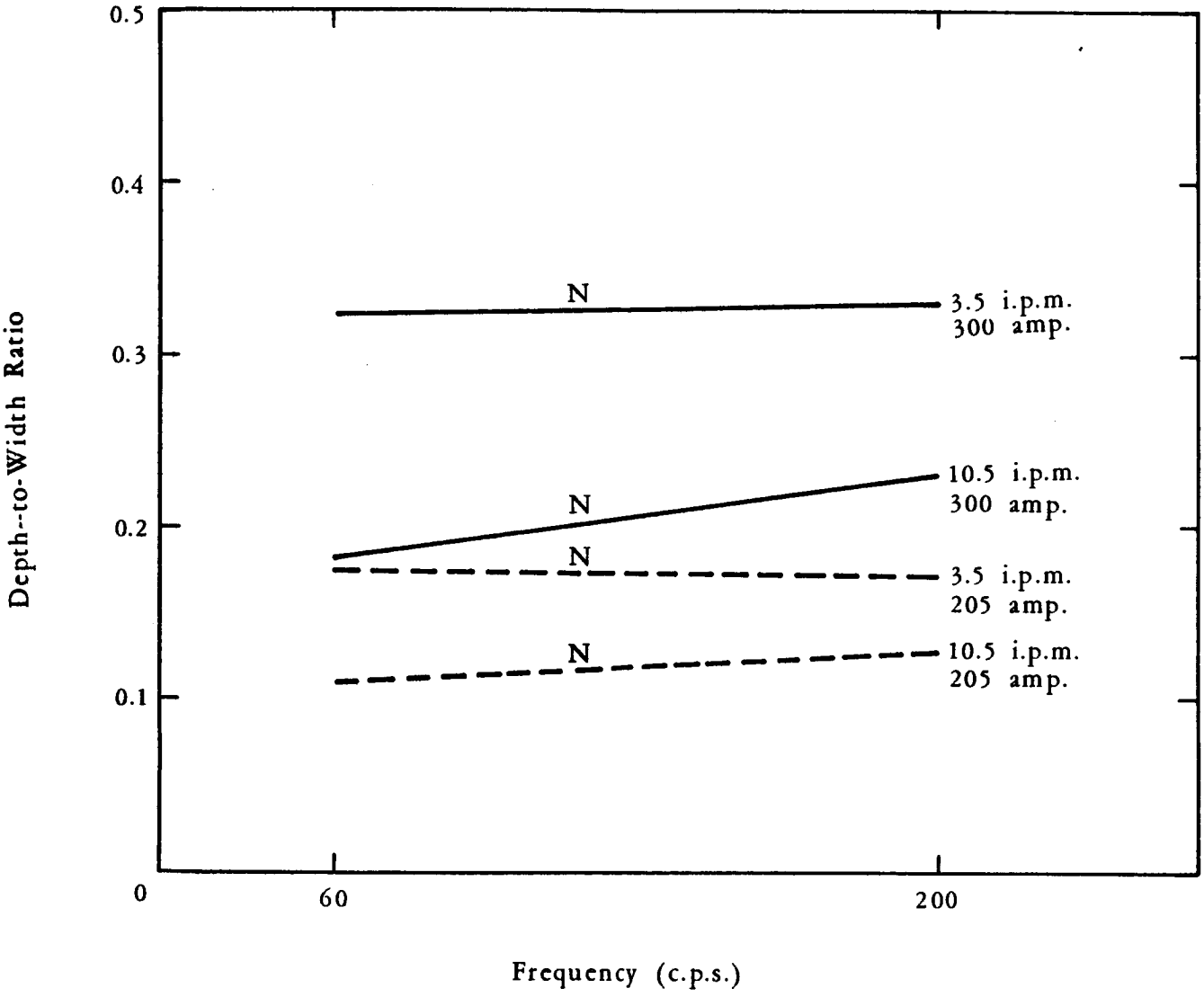

Fig. 38. EFFECT of FREQUENCY on DEPTH-WIDTH RATIO of VARIABLE FREQUENCY A-C WELDS, PHASE IIA

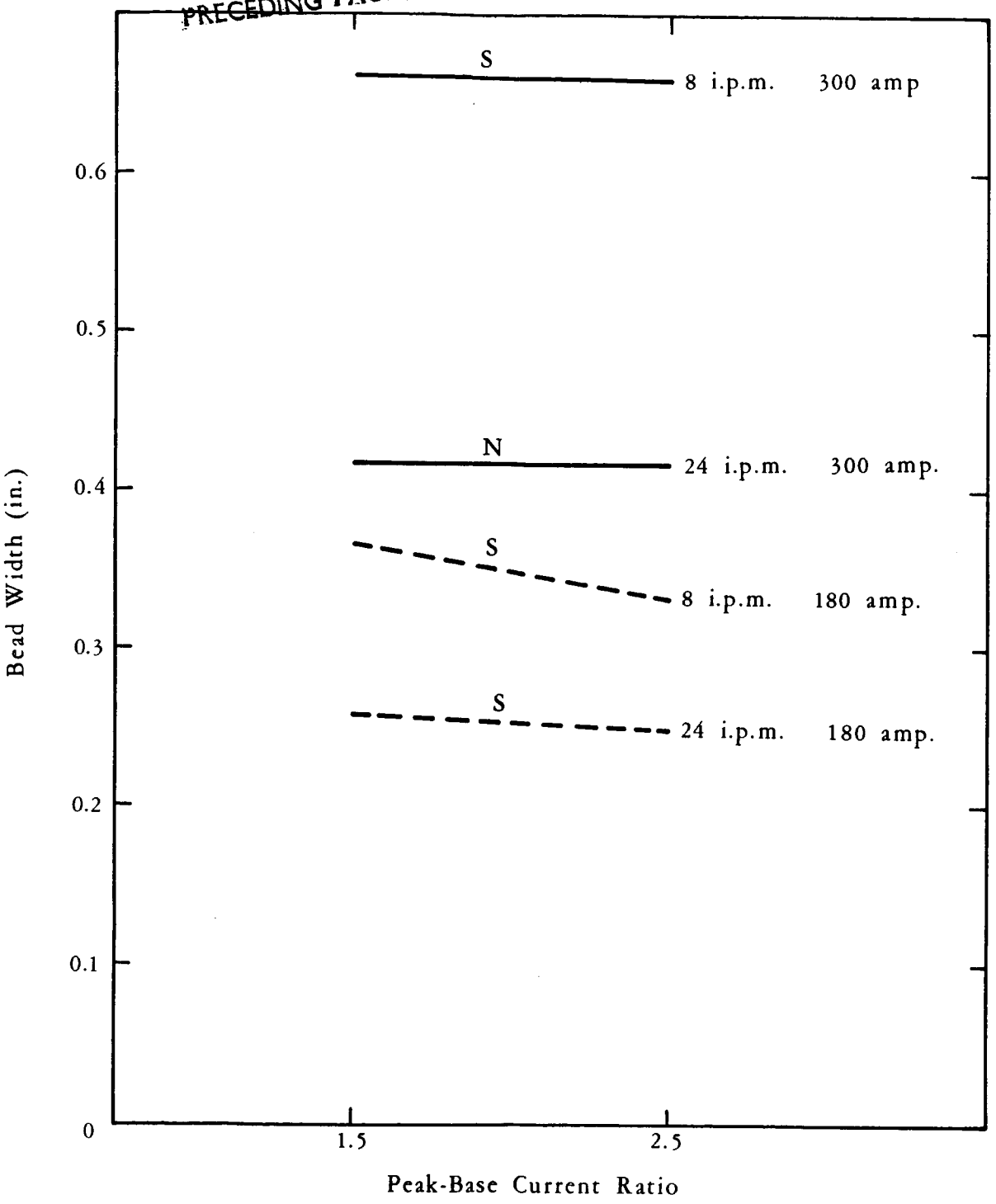

Fig. 39. EFFECT of PEAK-to-BASE RATIO on WIDTH of PULSED D-C WELDS, PHASE IIA

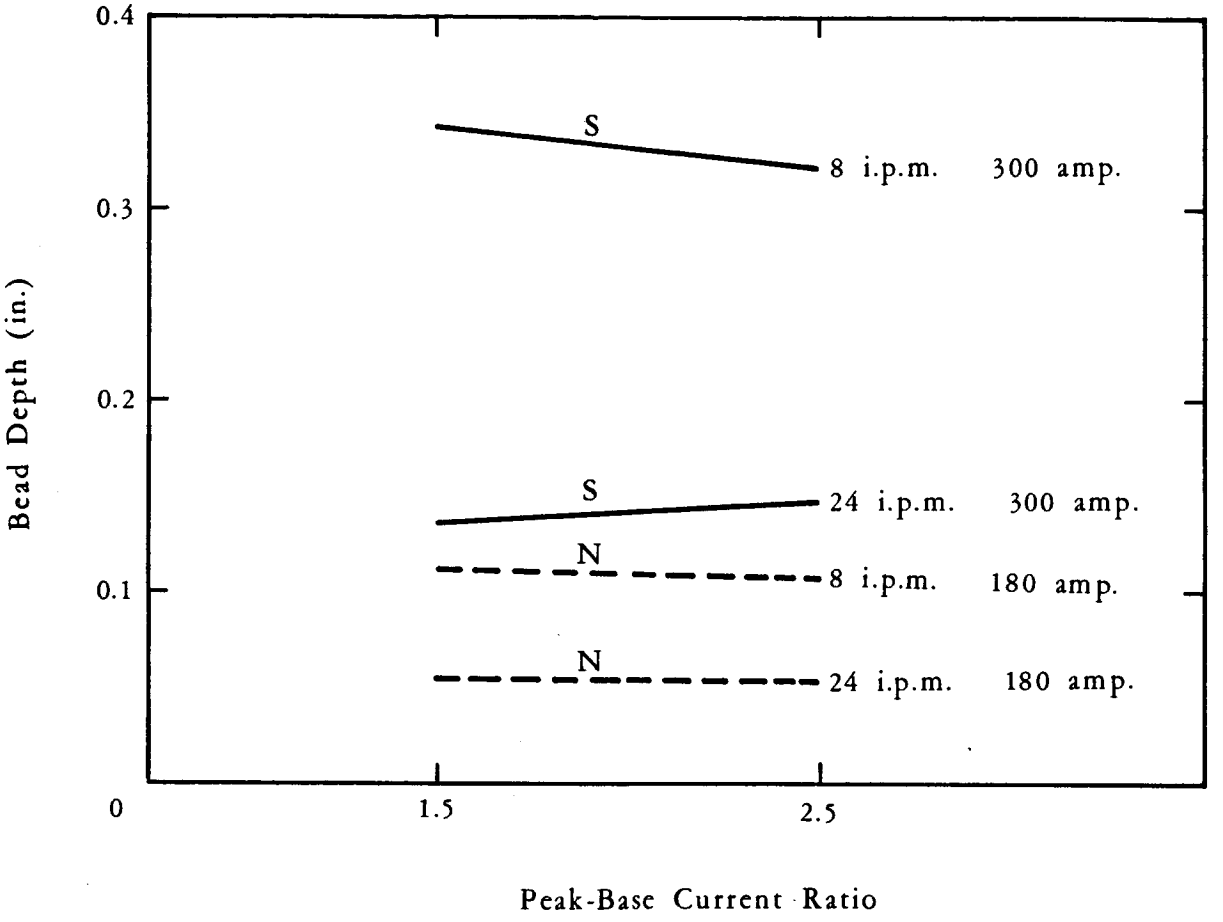

Fig. 40. EFFECT of PEAK-to-BASE RATIO on DEPTH of PULSED D-C WELDS, PHASE IIA

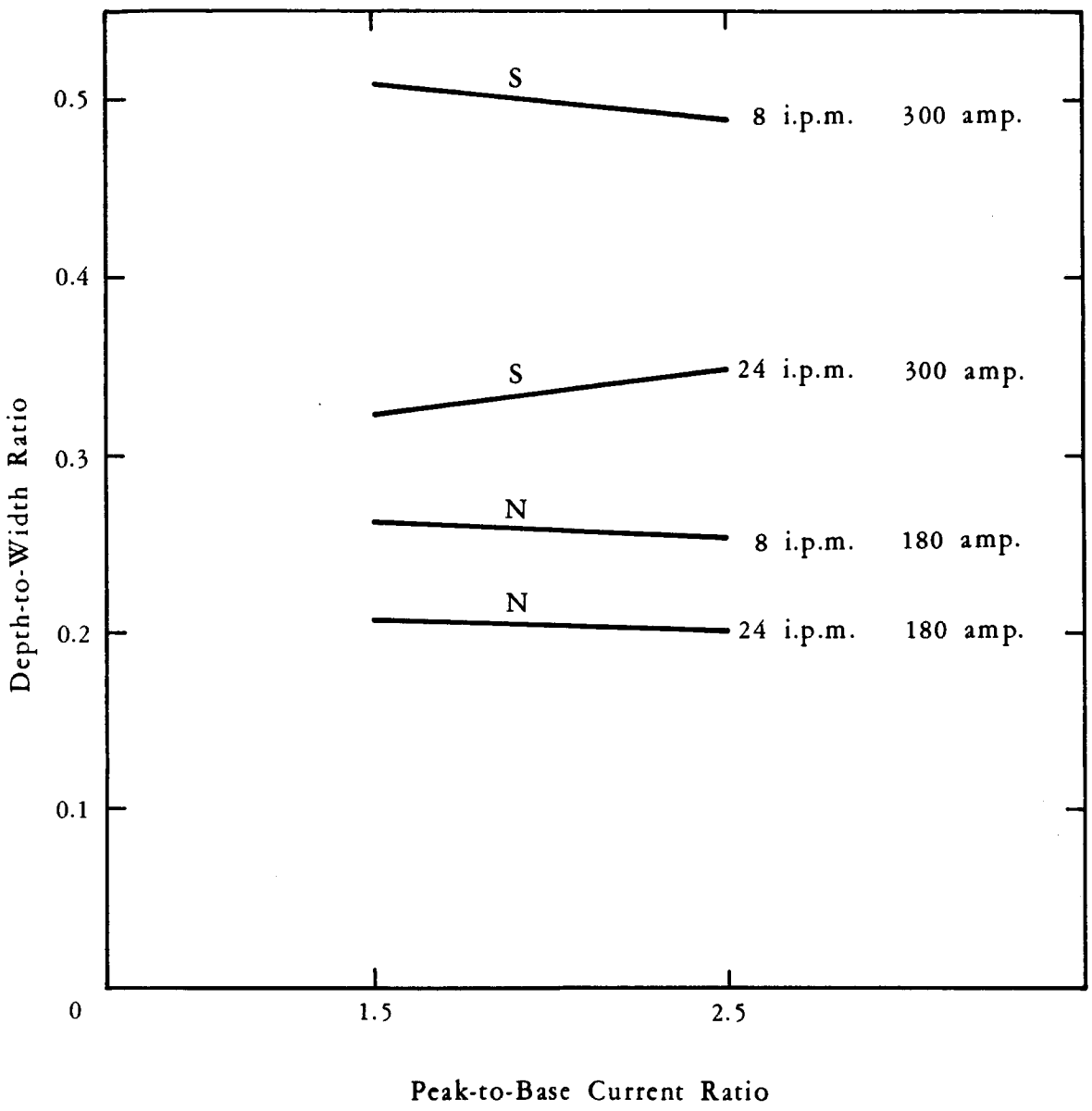

Fig. 41. EFFECT of PEAK-BASE RATIO on DEPTH-WIDTH RATIO of PULSED D-C WELDS, PHASE IIA

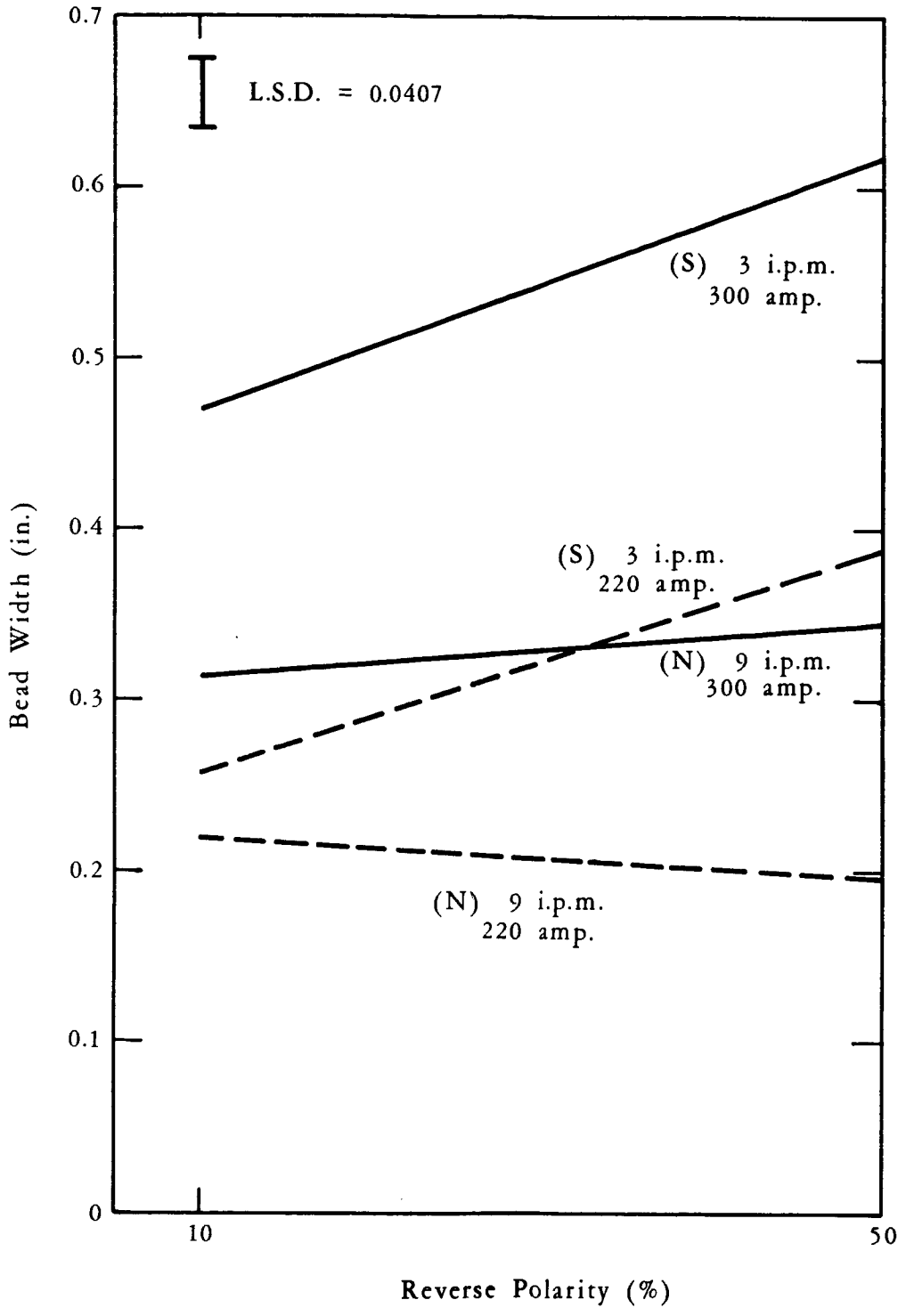

Fig. 42. EFFECT of REVERSE POLARITY PERCENTAGE on WIDTH of ASYMMETRIC A-C WELDS on AS-RECEIVED PLATE

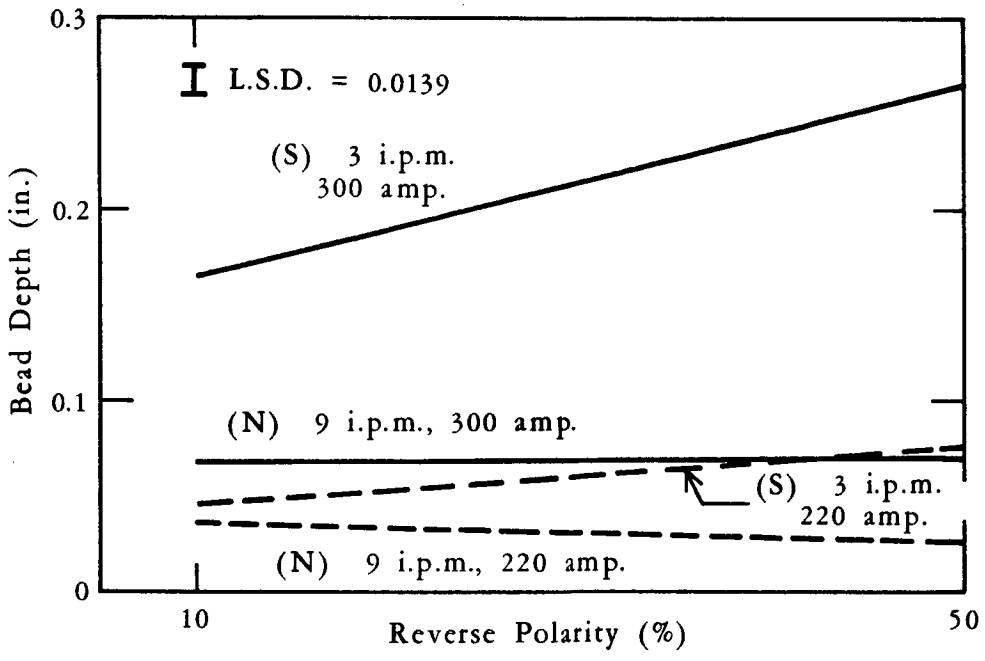

Fig. 43. EFFECT of REVERSE POLARITY PERCENTAGE on DEPTH of ASYMMETRIC A-C WELDS on AS-RECEIVED PLATE

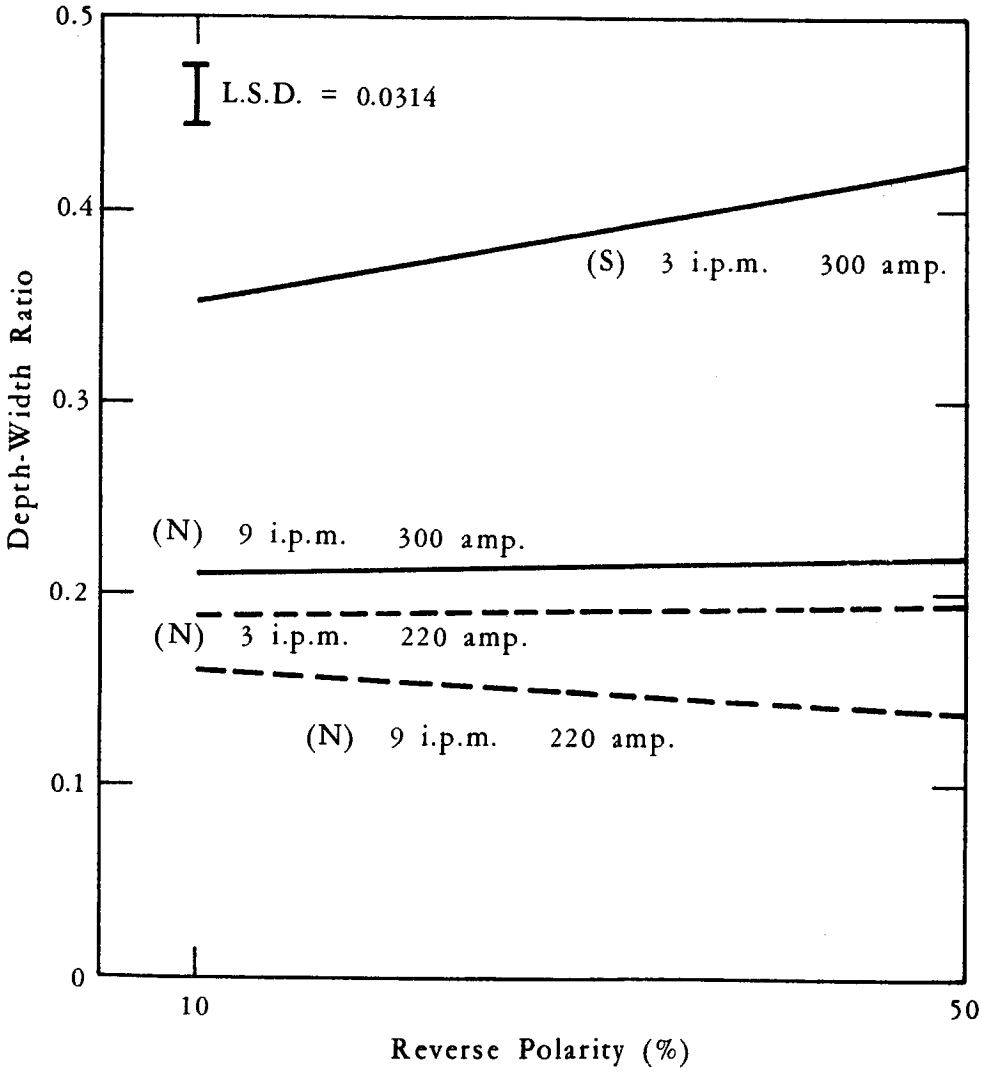

Fig. 44. EFFECT of REVERSE POLARITY PERCENTAGE on DEPTH-WIDTH RATIO of ASYMMETRIC A-C WELDS on AS-RECEIVED PLATE

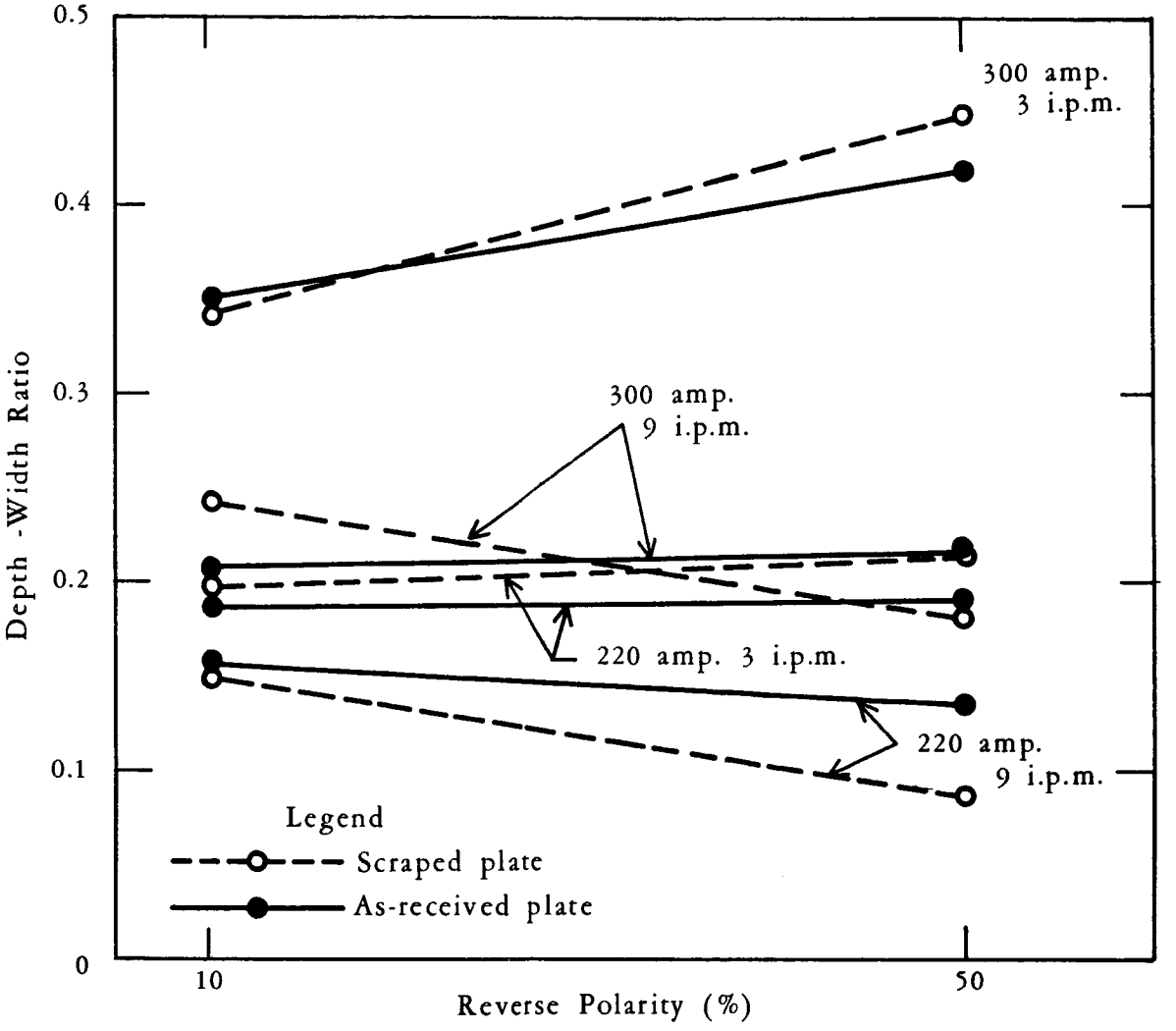

Fig. 45. EFFECT of REVERSE POLARITY PERCENTAGE on DEPTH-TO-WIDTH RATIO of ASYMMETRIC A-C WELDS on SCRAPED and AS-RECEIVED PLATE

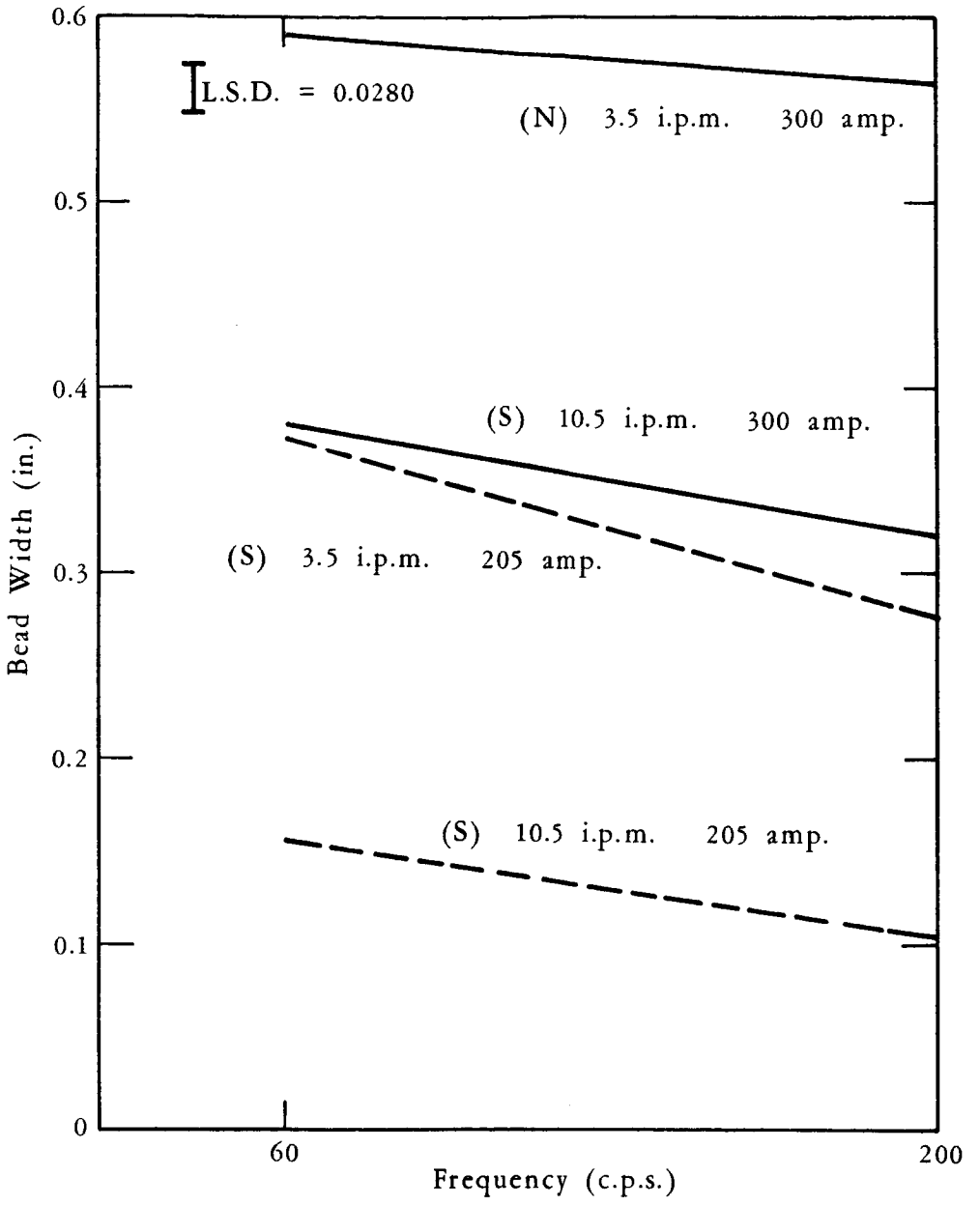

Fig. 46. EFFECT of FREQUENCY on WIDTH of VARIABLE FREQUENCY A-C WELDS on AS-RECEIVED PLATE

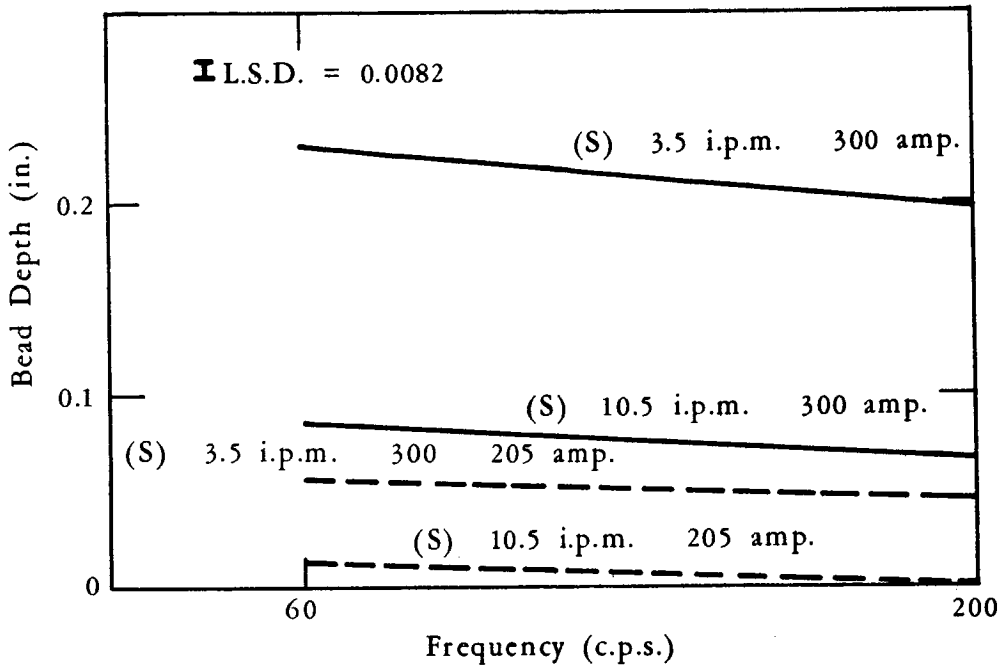

Fig. 47. EFFECT of FREQUENCY on DEPTH of VARIABLE FREQUENCY A-C WELDS on AS-RECEIVED PLATE

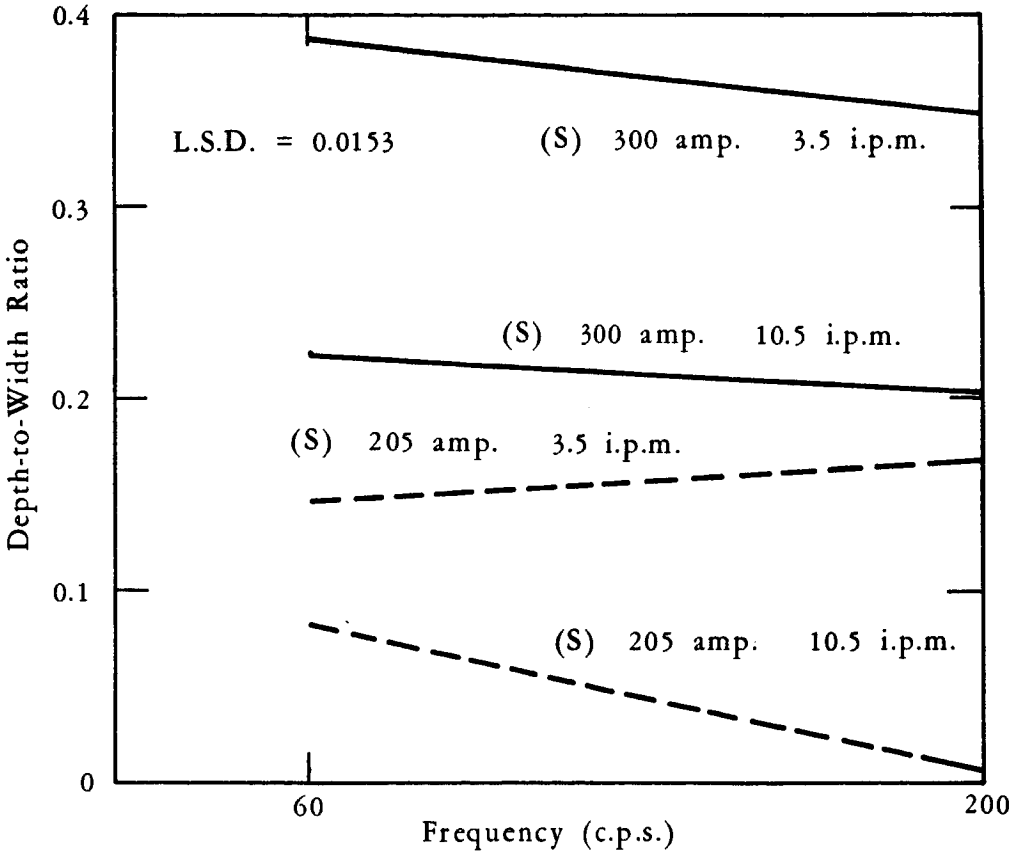

Fig. 48. EFFECT of FREQUENCY on DEPTH-to-WIDTH RATIO of VARIABLE FREQUENCY A-C WELDS on PLATE AS-RECEIVED

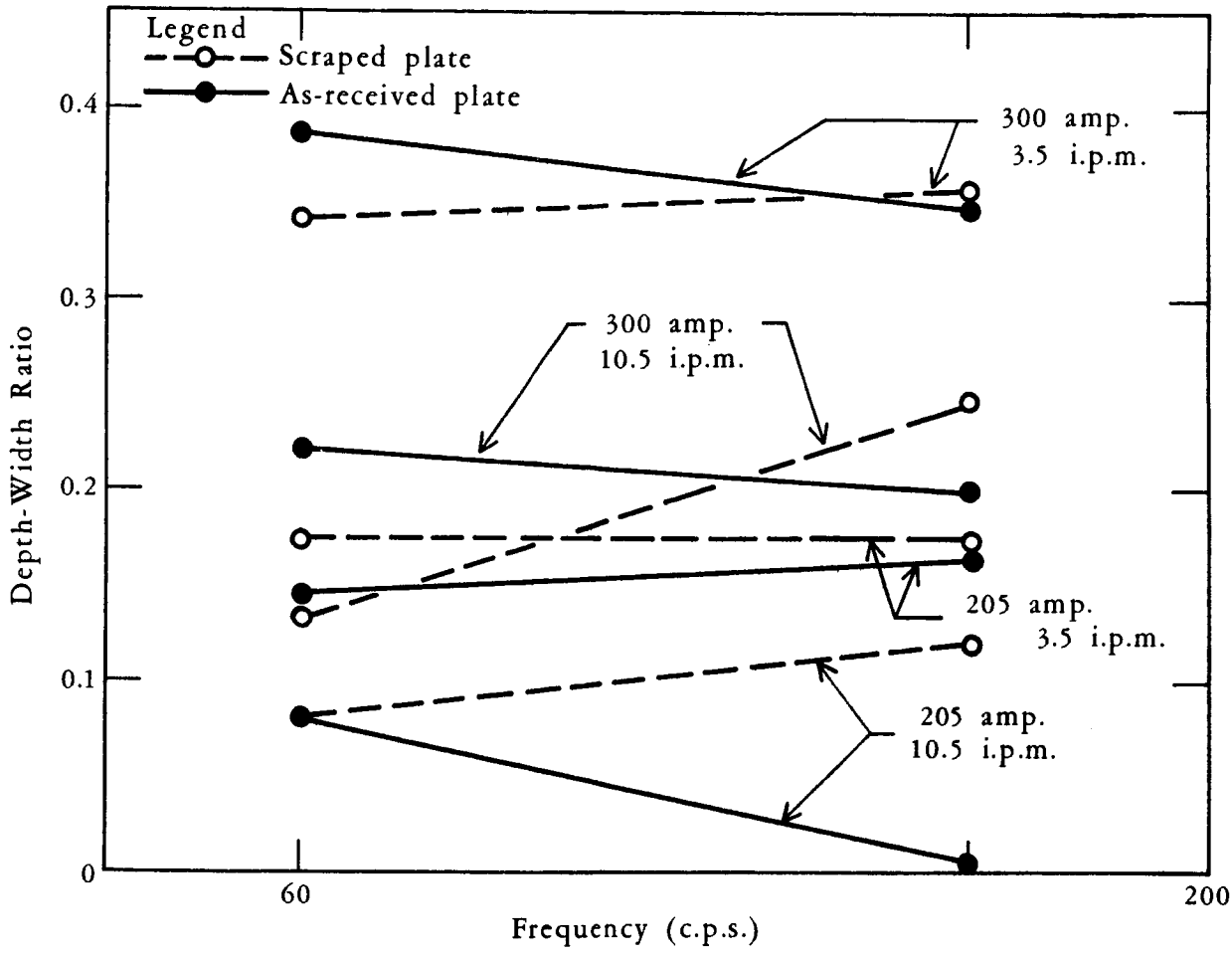

Fig. 49. EFFECT of FREQUENCY on DEPTH-to-WIDTH RATIO of VARIABLE FREQUENCY A-C WELDS on SCRAPED and AS-RECEIVED PLATE

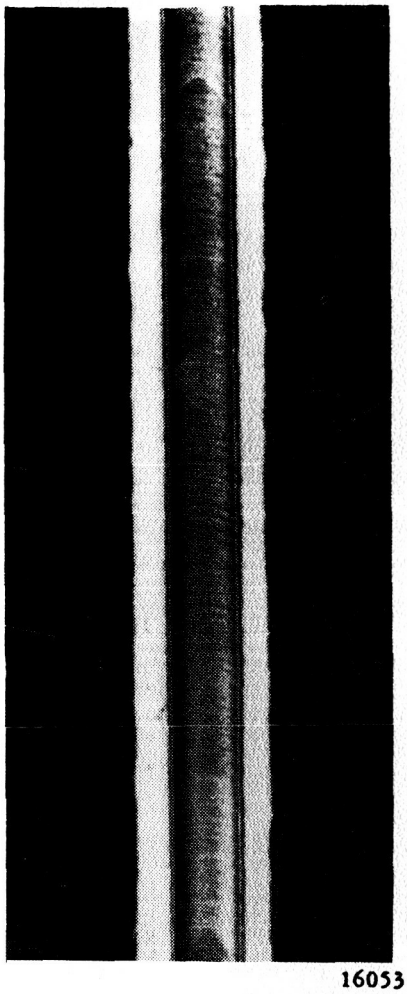

16053

Asymmetric A.C.
15% R.P., 60 c.p.s.
300 amps.

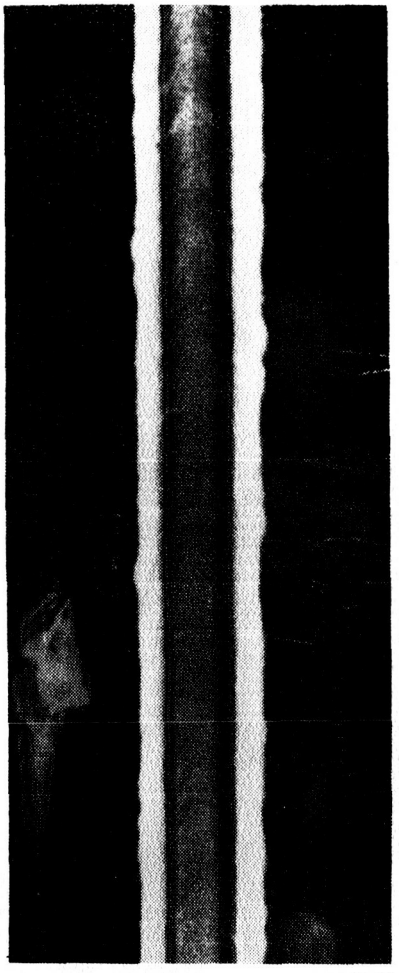

16055

High Frequency A.C.
50% R.P., 200 c.p.s.
300 amps.

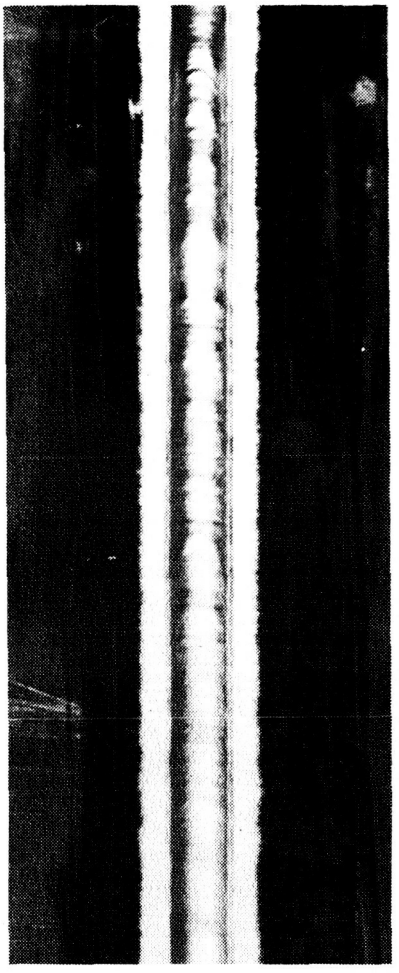

16063

Conventional A.C.
50% R.P., 60 c.p.s.
275 amps.

Fig. 50 PHOTOGRAPHS of PHASE IIB A.C. WELDS

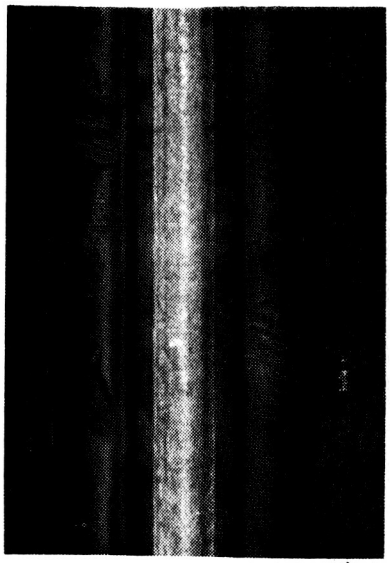

16057

top

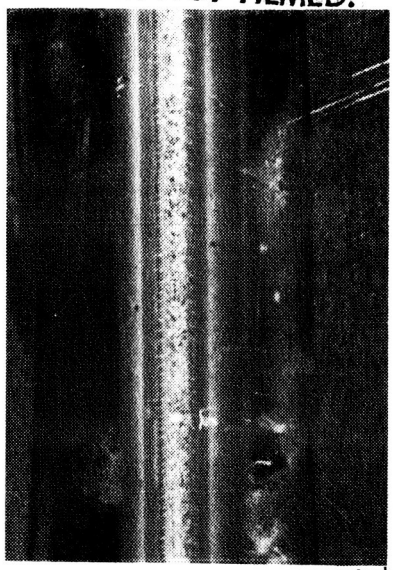

16061

top

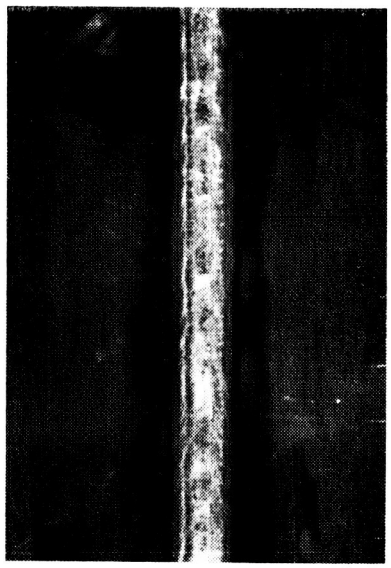

16059

top

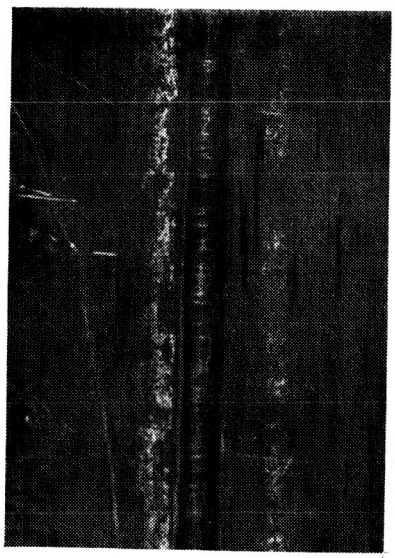

16058

underbead

Pulsed D.C.
240 amp.

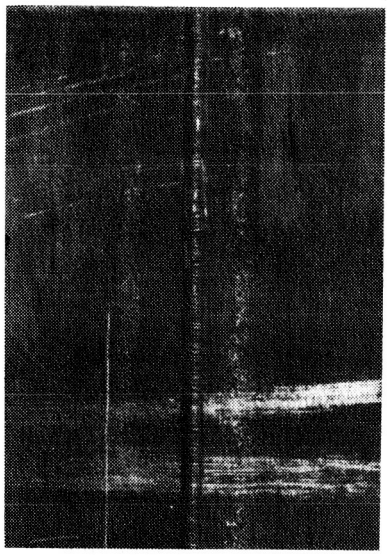

16062

underbead

Conventional D.C.
240 amp.

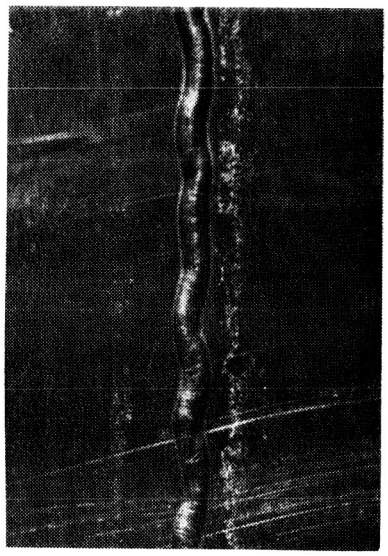

16060

underbead

Conventional D.C.
300 amp.

Fig. 51. PHOTOGRAPHS of PHASE IIB D.C. WELDS

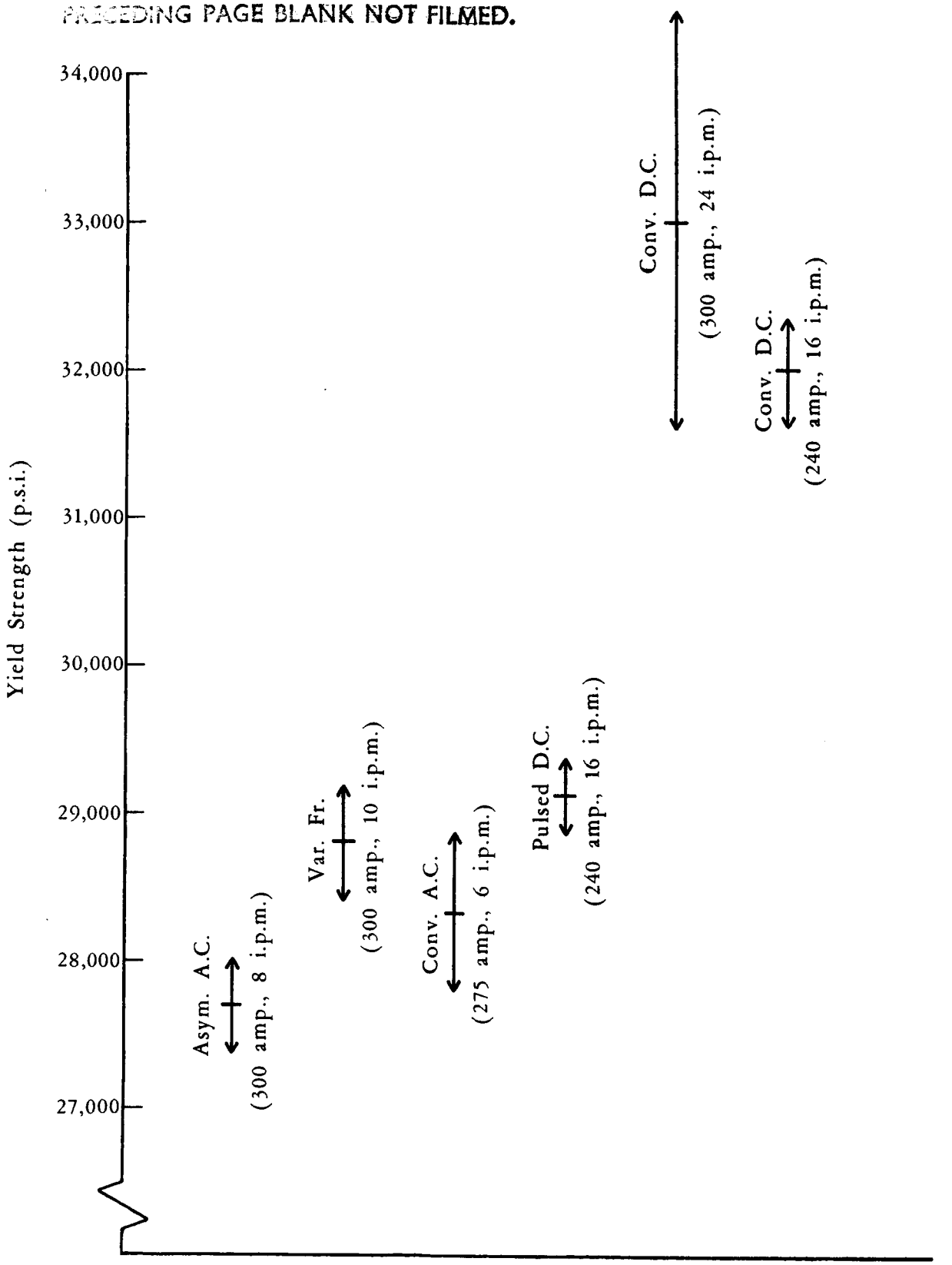

Fig. 52. LEAST SIGNIFICANT CONFIDENCE INTERVALS for YIELD STRENGTH of PHASE IIB WELDS

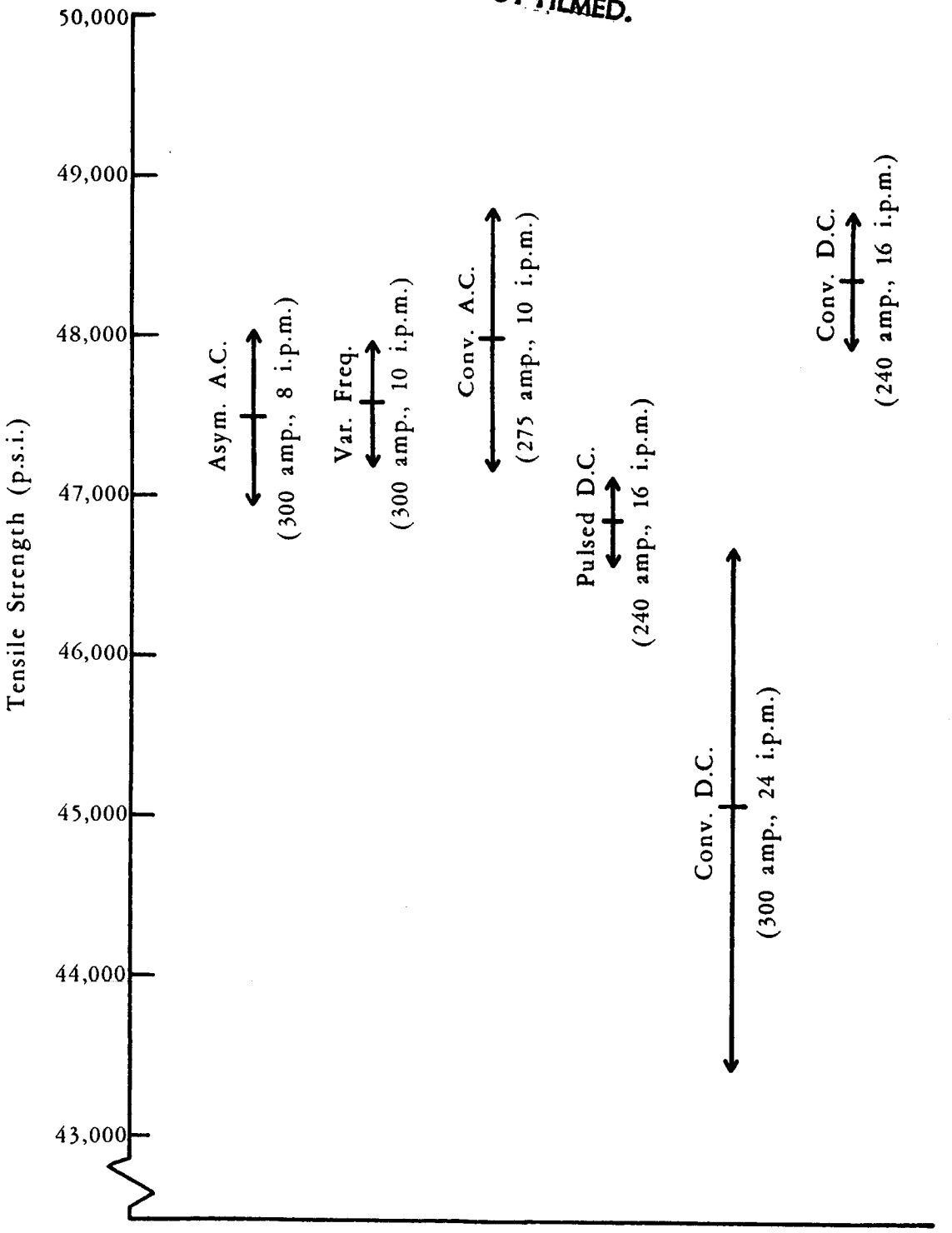

Fig. 53. LEAST SIGNIFICANT CONFIDENCE INTERVALS for TENSILE STRENGTH of PHASE IIB WELDS

Fig. 54. LEAST SIGNIFICANT CONFIDENCE INTERVALS for ELONGATION of PHASE IIB WELDS

DISTRIBUTION

Copies	
	National Aeronautics and Space Administration George C. Marshall Space Flight Center Huntsville, Alabama 35812
1	PR-SC
2	MS-IL
3	MS-T
4 - 20 plus Repro	R-ME-MW (Harry Lienau)
	Air Reduction Company, Inc.
	Murray Hill
21	E.H. Cushman
22	K.E. Dorschu
23	L.N. Faringhy
24	W.J. Greene
25	J.K. Hamilton
26	A. Lesnewich
27	N.W. Marinelli
28	H.H. Mathews
29	N.J. Normando
30	B.C. Redmon
	New York
31	A. Muller
	Union
32	J.W. Cunningham
33	G.R. Rothschild
34	R.W. Tuthill
35 - 40	Central Technical Records